The Relationship between Morphology and Ecological Performance in Malaysian Insectivorous Bats

by

Juliana Senawi

A Dissertation

In

Zoology

Submitted to the Graduate Faculty
of Texas Tech University in
Partial Fulfillment of
the Requirements for
the Degree of

DOCTOR OF PHILOSOPHY

Approved

Tigga Kingston
Chair of Committee

Dylan Schwilk

Nancy McIntyre

Richard Strauss

Elizabeth Dumont

Mark Sheridan
Dean of the Graduate School

May, 2015

ACKNOWLEDGEMENTS

First, I would like to thank Universiti Kebangsaan Malaysia and Ministry of Higher Education, Malaysia, for providing this academic advancement opportunity through a scholarship for my Ph.D. degree at Texas Tech University (TTU). I also would like to thank the Department of Biology at TTU for additional financial assistance and travel funds. Thank you to Earthwatch Institute – Neville Shulman Award, Bat Conservation International, American Society of Mammalogists, IDEA WILD, Long Term Research Scheme (LRGS/BU/2012/UKM/BS) and TTU Graduate School for research and travel funds.

I would like to gratefully and sincerely thank Dr. Tigga Kingston for her guidance, understanding, patience and most importantly, her friendship during my graduate studies at TTU. Her faith in me during the dissertation process enabled me to attend to life while also earning my Ph.D. She has been motivating, encouraging and enlightening. For everything you've done for me, Dr. Kingston, I thank you.

I am indebted to my committee members: Dr. Rich Strauss, Dr. Nancy McIntyre, Dr. Dylan Schwilk, Dr. Elizabeth Dumont and the late Dr. Björn Siemers. Their academic support and input are greatly appreciated. Thank you.

I would also like to thank all of the members of the Kingston Lab: Nurul Ain Elias, Kendra Phelps, Joe Chun-Chia Huang, Marina Fisher-Phelps, Iroro Tanshi and Macy Madden. You've always kept things light and me smiling. We have laughed and cried, traveled and played, and planned and discussed our graduate lives together. I could not have completed this journey without you guys.

My gratitude is also extended to Zamiza Zainal, Ahmad Degu, Sadri Ahmad, Zainuddin Ahmad, Aman Enya, Amri Aman, Bayek Naza, Pak Cik, Tacok and Bulat for their endless support in the field. Their kind assistance and patience while setting-up harp-traps and mistnets and staying-up all night testing the bats will always be cherished.

Recognition also goes to all the volunteers: Fauziah Syamsi, Jovic Fabello, Benjamin Logan, Ith Saveng, Kate Chamberlain, Christopher Blackburn, Ryan Healy, Dan Matthew, Fatim Akira Mustafa, Amira Rahman, Naziha Kamsol, Diah Syafiqa, Nor Atiqa Abdul Rahman, Shamin Aizat Abdul Rashid, Nor Laily Ibrahim, Johana Johari, Ting Jin Sia and to all undergraduate research assistances; Shaiyad Shabbi, Lucille Evans, Chelsea Truitt, Alexa Hand, Shelby Minchew, Holly Wilson, Narong Sok, Radhika Gandhi, Ivan Marsic, John Maneno and Tasnia Shawkat. My research would not have been possible without their help.

In addition, these acknowledgements would not be complete if I did not mention professors, staff and friends (graduates students) in the Department of Biology. No words could ever express my respect and appreciation for all the experiences and knowledge earned and shared here at TTU.

To my family especially my mom; Ruminah Mohd Ali, my dad; Senawi Johari, my siblings Jamaliah, Julian, Julia, Jamala and Junaina, my in-laws; Suhazliza Subdin, Mohd Qayum and Brian Miller my nieces and nephews, Azman Hakim, Anis Nurul Iman, Aliya Amani, Mohd Shamin, Mohd Aiman and Mohd Amar, thank you for your patience, unyielding support and your everlasting faith and belief in me. This dissertation is dedicated to all of you.

TABLE OF CONTENTS

LIST OF TABLES

LIST OF FIGURES

LIST OF EQUATIONS

CHAPTER I

INTRODUCTION

Bats comprise the second-largest order of mammal, with > 1,300 species recognized worldwide (Fenton & Simmons 2014) and they are extraordinarily diverse both taxonomically and ecologically (Kunz & Pierson 1994). A total of 298 species of terrestrial mammals have been recorded in Malaysia, of which more than 125 species are bats (Ministry of Natural Resources and Environment, Malaysia 2009). Bats can be found in almost every habitat in Malaysia, from rainforests to open habitats, montane forests to mangrove forests, and over 50% of Malaysia's rainforest mammal fauna comprise bat species. Not surprisingly, Malaysia's tropical rainforests are home to the greatest alpha diversity of bat species in the Old World. However, 38 species of Malaysian bats are red-listed by IUCN (2015) as being at some risk of extinction and populations of many other species are declining. One of the most significant threats to bat diversity is the change in forest ecology resulting from deforestation and degradation (Hansen et al. 2013).

The Southeast Asian region has the highest relative rate of deforestation among all tropical regions in the world, and could lose up to three quarters of its original forest by 2100 and about 42% of its biodiversity (Sodhi et al. 2004; Kingston 2010). Although Malaysia is reported to have 58.60% forest coverage from total land area, only 11.58% is primary forest, of which only 5.9% falls within protected areas (Food and Agriculture Organization of the United Nation - FAO 2010), the main hope for preserving forest

biodiversity. The rest of the forests are allocated for timber production (Kumari 1995) and are highly fragmented and embedded within a cultivated landscape.

Long-term monitoring of forest-dependent insectivorous bats has been conducted at Krau Wildlife Reserve (KWR), Pahang, from 2002 until today (Kingston et al. 2003; Kingston et al. 2006). One of the primary findings shows that KWR hosts local species assemblages exceeding 50 of the 95 insectivorous bat species recorded for Malaysia (Kingston et al. 2006). However, monitoring habitat alteration alone is not sufficient for understanding or managing the consequences of human activities on this complex insectivorous assemblage. This remarkably high species richness is most likely influenced by the differences in morphology and performance strategy that permit this coexistence. This is because morphological features of a species shape how bats can occupy and coexist in the same area and provide explanation of species ecological function (Kunz & Fenton 2003). This can be demonstrated through ecomorphological studies.

Ecomorphological Studies of Bats

Ecomorphology explores the underlying relationships among morphological structures, function and performance capability of the organism's life (Wainwright & Reilly 1994). Differences in phenotype (i.e. morphology) translate into differences in performance ability, which then result in differences in ecology or behavior that can ultimately facilitate resource partitioning (Losos 1990). In bats, the phenotypic correlates of resource partitioning have been widely studied through differences in skull

morphology (Freeman 1979, 1981, 1984; Dumont 1997), echolocation strategies (Schnitzler & Kalko 2001) and wing morphology (Norberg & Rayner 1987; Norberg 1994; Dietz et al. 2006). Within paleotropical insectivorous bats, several families have experienced a rapid radiation, but have retained their ancestral feeding specialization as insectivores and show minimal gross changes in morphology. These radiations generated species-rich assemblages made up of species that broadly occupy the same trophic niche. However, the role of ecomorphological differences among species in facilitating coexistence in these assemblages is poorly known (but see Heller & Von Helversen 1989; McKenzie et al. 1995; Kingston et al. 2000; Dumont & O'Neal 2004; Hodgkinson et al. 2004; Campbell et al. 2007), and is the guiding question for my research.

Recent advances in the ability to measure the performance of bats at ecologically relevant tasks provide an opportunity to quantify unexplored ecomorphological relationships. Several studies have quantified the interspecific relationship between morphology and bite performance (Aguirre et al. 2002; Nogueira et al. 2009; Santana et al. 2010; Dumont et al. 2012; Dumont et al. 2014) and between morphology and flight performance (Aldridge 1986; Aldridge & Rautenbach 1987; Jones 1993; Rhodes 1995; Stockwell 2001). However, just one "performance testing" study has been reported for paleotropical bats, investigating the sensory performance of vespertilionid bats (Schmieder et al. 2012).

Dissertation Overview

Despite being one of highest biodiversity countries in the world, Malaysia still lacks information on the ecomorphology of bats. Furthermore, the threat from habitat loss makes urgent improved understanding of resource partitioning among species. There were at least 50 insectivorous bats species can be found within my study site (Krau Wildlife Reserve; KWR). Understanding resources partitioning among these species may help us uncover the truth of how these species can coexist in the same habitat structure without one species pushing the other species to extinction through competition. With devastation rate of deforestation in Malaysia, information of resource partitioning within these species will ultimately help us to predict how ongoing species declines will impact the functioning of the forest ecosystem.

The goal of my research is to shed light on the relationship between morphology and performance of species belonging to species-rich insectivorous bats assemblages from undisturbed tropical rainforest of Malaysia. My investigations focused on morphological variation in the craniodental structure of bats and bite performance, and variation in wing morphology and flight performance. By studying the differences in their performance, I try to explain patterns in resources partitioning within this species-rich insectivorous bats assemblage.

Chapter II explores the relationship study between craniodental morphology and bite performance. This chapter was published in Journal of Functional Ecology (Juliana et al. 2015). Previous studies have demonstrated that bite force is strongly correlated with body and head size in bats (Aguirre et al. 2002; Santana et al. 2010). As a result, larger

bats will be able to take larger and harder prey compared to smaller bats (Aguirre et al. 2003). This correlation also holds in my study; however, size is not the only factor in determining the maximum bite force of a bat. In this chapter, I also investigate a factor other than size, the mechanical advantage of the lever mandible that may contribute to differences in bite force and may also facilitate resource partitioning within species-rich insectivorous bat assemblages. I found that size-independent mechanical advantage was positively and significantly correlated with size-independent bite force. Bats with shorter out-lever arms generate greater bite force, whereas bats with longer out-lever arms produce a lower bite force. However, following the law of equilibrium as applied to levers, the speed at which a load moves increases with the length of the out-lever arm. Although differences in size may explain differences in bite force capacity, the trade-offs between force and speed of the mandible lever further refined the explanation of separation among species in the assemblage.

In chapter III, I use a two-dimensional model of the skull to estimate masticatory muscle stress across species. One of the biggest constraints in determining the relationship between skull morphology and bite force using skull models has historically been the estimation of masticatory muscles stress values. Understanding the crucial functional features may improve our knowledge of the influence of functional morphology on the ecology of bite force in bats. In this chapter, I am using 2D skull models generated from digital images to estimate the masticatory muscle stress of the bats by rearranging the bite force estimation equation by Thomason (1990). The masticatory muscle stress within 29 insectivorous bats studied ranged from 71.38 kPa to 469.74 kPa. I found that measures of size did not fully explain the masticatory muscle

stress differences among species. However, the masticatory muscles stress is more linked to the mechanical advantage of the mandible lever. Because of the nature of the study (2D model), the size and volume of the masticatory muscles were not determine. For this reason, I think the typical constant muscles stress value for determining bite force in bats, which is 250 kPa and is derived from muscle stress tests of the soleus or calf muscle of cats and rats, may not an appropriate value for masticatory muscle stress in bat bite force models.

Chapter IV presents a study of the relationship between wing morphology and flight performance. In theory bats with low wing loading, low aspect ratio and broader wingtip, will be more maneuverable and, in contrast, bats with high wing loading, high aspect ratio and narrow wingtip, will be more agile (Norberg & Rayner 1987; Norberg 1990; Swartz et al. 2012). Flying within vegetation requires high maneuverability and there at least 30 species of insectivorous bats reported for Krau Wildlife Reserve (KWR) are forest interior species (Kingston et al. 2006), which means these bats forage within cluttered environments and at the same time must avoid competition with each other. Several studies have experimentally tested the relationship between wing morphology parameters and maneuverability through an obstacle course; however, the validity of such experiments has never been tested. In this chapter, I experimentally tested 15 syntopic insectivorous bats species that forage within forest interior of KWR through an obstacle course with 11 different inter-string distances. Instead of using inferential statistical analyses to quantify maneuverability, I used a statistical approach from the human sciences, item response theory (IRT), to assess the ability of bats to negotiate obstacle courses of differing difficulty. This approach enabled me to determine the validity and

reliability of the obstacle course experiment conducted. Furthermore, the bats ability and tasks difficulty can be evaluated simultaneously, thus more insights into the experimental design and the distribution of bats ability were gained. I found that flight ability correlated with body mass and all wing variables tested; however, body mass and wing loading were the only significant predictors of flight performance. Body mass was directly correlated with wing loading, and in this experiment I found differences in wing loading that may facilitate niche partitioning within these 15 highly maneuverable insectivorous bats species.

Literature Cited

Aguirre, L.F., Herrel, A., Van Damme, R. & Matthysen, E. (2002) Ecomorphological analysis of trophic niche partitioning in a tropical savannah bat community. *Proceeding of the Royal Society of London Series B-Biological Sciences*, **269**, 1271-1278.

Aguirre, L.F., Herrel, A., Van Damme, R. & Matthysen, E. (2003) The implications of food hardness for diet in bats. *Functional Ecology*, **17**, 201-212.

Aldridge, H. (1986) Manoeuvrability and ecological segregation in the little brown (*Myotis lucifugus*) and Yuma (*M. yumanensis*) bats (Chiroptera: Vespertilionidae). *Canadian Journal of Zoology*, **64**, 1878-1882.

Aldridge, H.D.J.N. & Rautenbach, I.L. (1987) Morphology, echolocation and resource partitioning in insectivorous bats. *Journal of Animal Ecology*, **56**, 763-778

Campbell, P., Christopher, J., Zubaid, A. Adura, M.A. & Kunz, T.H. (2007) Morphological and ecological correlates of coexistence in Malaysian fruit bats. *Journal of Mammalogy*, **88**, 105-118.

Dietz, C., Dietz, I. & Siemers (2006) Wing measurement variations in the five European horseshoe bat species (Chiroptera: Rhinolophidae). *Journal of Mammalogy*, **87**, 1241-1251.

Dumont, E.R. (1997) Cranial shape in fruit, nectar and exudate feeders: implications for interpreting the fossil record. *American Journal of Physical Anthropology*, **102**, 187-202.

Dumont, E.R., Dávalos, L.M., Goldberg, A., Santana, S.E., Rex, K. & Voigt, C.C. (2012) Morphological innovation, diversification and invasion of a new adaptive zone. *Proceedings of the Royal Society*, **279**, 1797-1805.

Dumont, E.R. & O'Neal, R. (2004) Food hardness and feeding behavior in Old World bats (Pteropodidae). *Journal of Mammalogy*, **85**, 8-14.

Dumont, E.R., Samadevam, K., Grosse, I. Warsi, O.M., Baird, B. & Davalos, L.M. (2014) Selection for mechanical advantage underline multiple cranial optima in New World leaf-nosed bats. *Evolution*, **68**, 1436-1449.

FAO. 2010. *Global forest resources assessment 2010: country report; Malaysi*a. Food and Agriculture Organization of the United Nations, Rome.

Fenton, M.B. & Simmons, N.B. (2014) *A world of science and mystery: Bats*. The University of Chicago Press, Chicago.

Freeman, P.W. (1979) Specialized insectivory: beetle-eating and moth-eating molossid bats. *Journal of Mammalogy*, **60**, 467-479.

Freeman, P.W. (1981) A multivariate study to a family Molossidae (Mammalia, Chiroptera): morphology, ecology, evolution. *Fieldiana (Zoology)* **7**, 1-173.

Freeman, P.W. (1984) Functional cranial analysis of large animalivorous bats (Microchiroptera). *Biological Journal of the Linnean Society,* **21**, 387-408.

Hansen, M.C., Potapov, P.V., Moore, R., Hancher, M., Turubanova, S.A., Tyukarina, A., Thau, D., Stehman, S.V., Goetz, S.J., Loveland, T.R. Kommareddy, A., Egorov, A., Chini, L., Justice, C.O. & Townshend, J.R.G. (2013) High-resolution global maps of 21st – century forest cover change. *Science,* **342**, 850-853.

Heller, K-G. & Von Helversen, O. (1989) Resources partitioning of sonar frequency bands in rhinolophid bats. *Oecologia,* **80**, 178 - 186.

Hodgkison, R., Balding, B.T., Zubaid, A. & Kunz, T.H. (2004) Habitat structure, wing morphology, and the vertical stratification of Malaysian fruit bats (Megachiroptera: Pteropodidae). *Journal of Tropical Ecology*, **20**, 667-673.

IUCN (2015) IUCN Red List of Threatened Species. Version 2014.3. Available from: http://www.iucnredlist.org (accessed on March 2015). International Union for Conservation of Nature and Natural Resources (IUCN), Cambridge.

Jones, G., Morton, M., Hughes, P.M. & Budden, R.M. (1993) Echolocation, flight morphology and foraging strategies of some West African hipposiderid bats. *Journal of Zoology*, **230**, 385-400.

Juliana, S., Schimeder, D., Siemers, B. & Kingston, T. (2015) Beyond size – morphological predictors of bite force in a diverse insectivorous bats assemblage of Malaysia. *Functional Ecology,* http://doi:10.1111/1365-2435.12447.

Kingston, T. 2010. Research priorities for bat conservation in Southeast Asia: a consensus approach. *Biodiversity and Conservation*, **19**, 471-484.

Kingston, T. Lim, B.L. & Zubaid, A. (2006) *Bats of Krau*. Penerbit Universiti Kebangsaan Malaysia, Bangi.

Kingston, T., Francis, C.M., Zubaid, A. & Kunz, T.H. (2003) Species richness in an insectivorous bat assemblage from Malaysia. *Journal of Tropical Ecology*, **19**(1), 67-79.

Kingston, T., Jones, G., Zubaid, A. & Kunz, T.H. (2000) Resource partitioning in rhinolophoid bats revisited. *Oecologia*, **124**, 332-342.

Kumari, K. (1995) Is Malaysian forest policy and legislation conductive to multiple-use forest management? *Unasylva*, **46**, 183.

Kunz, T.H. & Fenton, M.B. (2003) *Bat ecology*. The University of Chicago Press, Chicago.

Kunz, T.H. & Pierson, E.D. (1994) *Bats of the world: an introduction*. Walker's bats of the world (eds R.W. Nowak). Johns Hopkin University Press, Baltimore.

Losos, J.B. (1990) Ecomorphology, performance capability and scaling of West India *Anolis* lizards. *Ecological monographs*, **60**, 369-388.

McKenzie, N.L., Gunnell, A.C., Yani, M. & Williams, M.R. (1995) Correspondence between flight morphology and foraging ecology in some Palaeotropical bats. *Australian Journal of Zoology*, 43, 241-257.

Ministry of Natural Resources and Environment. (2009) *4th national report to the convention on biological diversity*. Ministry of Natural Resources and Environment, Malaysia.

Nogueira, M.R., Peracchi, A.L. & Monteiro, L.R. (2009) Morphological correlates of bite force and diet in the skull and mandible of phylostomid bats. *Functional Ecology*, **23**, 715-723.

Norberg, U.M. & Rayner, J.M.V. (1987) Ecological morphology and flight in bats (Mammalia; Chiroptera): wing adaptations, flight performance, foraging strategy and echolocation. *Philosophical Transactions of the Royal Society of London. Series B, Biological Sciences*, **316**, 335-427.

Norberg, U.M. (1990) *Vertebrate flight: flight mechanics, physiology, morphology, ecology and evolution*. Springer-Verlag, Berlin.

Norberg, U.M. (1994) Wing design, flight performance and habitat use in bats. *Ecological morphology: integrative organismal biology* (eds P.C. Wainright and M Reilly) pp. 205 – 239. University of Chicago Press, Chicago, Illinois.

Rhodes, M.P. 1995. Wing morphology and flight behaviour of the golden-tipped bat, Phoniscus papuensis (Dobson) (Chiroptera: Vespertilionidae). *Australian Journal of Zoology*, **43**: 657-663.

Santana, S.E., Dumont, E.R & Davis, J.L. (2010) Mechanics of bite force production and its relationship to diet in bats. *Functional Ecology*, **24**, 776-784.

Schmieder, D.A., Kingston, T., Hashim, R. & Siemers, B.M. (2012) Sensory constraints on prey detection performance in an ensemble of vespertilionid understorey rain forest bats. *Functional Ecology*, **26**, 1043-1053.

Schnitzler, H.U. & Kalko, E.K.V. (2001) Echolocation by insect-eating bats. *Bioscience*, **51**, 557 - 569.

Sodhi, N.S., Koh, L. P., Brook, B.W. & Ng, P. K.L. (2004) Southeast Asian biodiversity: an impending disaster. *Trends in Ecology and Evolution*, **19**, 654-660.

Stockwell, E.F. (2001) Morphology and flight manoeuvrability in New World leaf-nosed bats (Chiroptera: Phyllostomidae). *The Zoological Society of London*, **254**, 505-514.

Swartz, S.M, Iriarte-Díaz, J., Riskin, D.K. & Breuer, K.S. (2012) A bird? A plane? No, it's a bat: an introduction to the biomechanics of bat flight. *Evolutionary history of bats: fossils, molecules and morphology* (eds. G.F. Gunnell & N.B. Simmons) pp. 317-352. Cambridge University Press.

Thomason, J.J. (1990) Cranial strength in relation to estimated bite forces in some mammals. *Canadian Journal of Zoology*, **69**, 2326-2333.

Wainwright, P.C. & Reilly, S.M. (1994) *Ecological morphology: integrative organismal biology.* The University of Chicago Press, Chicago.

CHAPTER II

BEYOND SIZE – MORPHOLOGICAL PREDICTORS OF BITE FORCE IN A DIVERSE INSECTIVOROUS BAT ASSEMBLAGE FROM MALAYSIA

Abstract

Bite force is used to investigate feeding performance in a variety of vertebrates. In all taxa studied, bite force is strongly correlated with body and head size. Studies of bite force in bats have largely centred on neotropical species, with a particular focus on species that maximize dietary differences. Little is known about the bite force of bats from the Old World tropics, nor of variation in bite force within diverse assemblages of obligate insectivores. Moreover, factors other than size are poorly known but may be important in driving interspecific differences in bite force, and thereby diet. Here, we examine the correlation between morphological variation and bite force of 35 species of insectivorous bats from a single palaeotropical assemblage. We confirmed the overall relationship between size and bite force across species, but found that bite force is predicted more strongly by head length than body mass or forearm length. From the combined action of jaw muscles and muscle-bone mechanisms, bats generate a mechanical advantage that creates pressure during biting. We calculated the size-independent mechanical advantage for each of five mandible lever systems (three delineated by the temporalis muscle and two delineated by the masseter muscle)

operating through three function points (molar, canine and incisor). Size-independent mechanical advantage of the suprazygomatic portion of the temporalis muscle at the molar function point was the only significant predictor of size-independent maximum bite force across all species. Within families, the size-independent mechanical advantage of the superficial portion of the masseter muscle plays a significant role in predicting size-independent maximum bite force in both the Rhinolophidae and Vespertilionidae. For the family Hipposideridae; however, size-independent mechanical advantage showed no role in predicting size-independent maximum bite force, suggesting that size really matters in predicting the maximum bite force capacity for this family.

Key-words: mandible lever, masseter muscle, mechanical advantage, palaeotropical bats, temporalis muscle.

Introduction

Performance studies measure an organism's ability to carry out specific behaviours or tasks (Wainwright & Reilly 1994). Many studies focus on the relationship between morphological traits and performance (e.g. Losos 1990; Zani 2000; Berwaerts et al. 2002) to elucidate the relationship between an organism's phenotype and the environment. In some cases, small morphological differences are associated with differences in performance, whereas in others, differences in morphology can occur without having any effect on function (Koehl 1996). Moreover, the relationship between biological structure and function may be non-linear, context-dependent or unpredictable (Koehl 1996),

particularly if function is mediated by complex biomechanical processes involving multiple structures (Currey 1984; Dumont & Swartz 2009; Swartz et al. 2003).

Bite force is an important performance trait linking diet to feeding mechanisms that determine the ability to process food, a factor shaping the niche of many species (Aguirre et al. 2002; Nogueira et al. 2009; Davis et al. 2010; Santana et al. 2010). It is therefore viewed as a performance measure at the whole-organism level and is expressed as the pressure or force per unit area when the mouth encloses on an object. Bite force is determined by behavioural, physiological and morphological features (Anderson et al. 2008) but is strongly correlated with body and head size in turtles (Herrel & O'Reilly 2006), lizards (Verwaijen et al. 2002; Husak et al. 2006), alligators (Erickson et al. 2003) and mammals (Davis et al. 2010). Consequently, larger animals not only broaden the diversity of their diet by taking larger prey than smaller counterparts, but also by taking harder prey (Aguirre et al. 2003).

Beyond size, mechanical advantage may also explain bite force differences between species. In mammals, biting is achieved through a lever system consisting of a fulcrum, in-lever arm, out-lever arm, input force and output force. The mechanical advantage of the lever is the ratio of the length of the lever on the input force side of the fulcrum to the length of the lever on the output force side of the fulcrum. In mammals, the fulcrum is the jaw articulation or temporomandibular joint which in this paper is defined as the midpoint of the articular condyle of the mandible. The in-lever arm connects the fulcrum to the point where an input force is applied by a muscle (e.g. for the input force given by the zygomaticomandibularis portion of the masseter muscle, the in-lever arm is measured from the midpoint of the articular condyle to the anterior-most

edge of the mandibular fossa). The out-lever arm connects the fulcrum to the point where an output force is applied by particular teeth to the food, in this paper referred to as the function point. The higher the mechanical advantage value, the greater the bite force capacity produced (Greaves 2012).

Bats comprise the second largest order of mammals, with > 1,300 species recognized worldwide (N. Simmons pers. comm.). Differences in bat diets correlate with differences in cranial structure (Freeman 2000; Cakenberghe et al. 2002). Furthermore, differences in size explain much of the variation in bite force among bats (Aguirre et al. 2002). However, most bite force studies on bats have focused on the neotropical family Phyllostomidae. This family experienced the most radical adaptive radiation of feeding strategies within any group of mammals, diverging from a single insectivorous ancestor to c. 200 species occupying highly specialized feeding niches (sanguinivory, insectivory, carnivory, omnivory, nectarivory, palynivory and frugivory) in just over 28.5 myr (Cakenberghe et al. 2002; Agnarsson et al. 2011; Dumont et al. 2012). This dramatic trophic diversification likely originated with innovative changes in skull morphology that improved biting performance and gave access to new food sources, e.g. hard canopy fruits, creating a new adaptive zone that accelerated diversification still further (Dumont et al. 2012; Dumont et al. 2014).

Bite force in Old World bats remains relatively unstudied, but rapid radiation also occurred within several palaeotropical families, particularly the Rhinolophidae (c. 89 species in about 37 myr), Hipposideridae (c. 99 species in 37 myr) and Vespertilionidae subfamilies Kerivoulinae (c. 26 species in c. 30 myr) and Murininae (c. 37 species in c. 30 myr) (Anwarali Khan et al. 2010; Agnarsson et al. 2011). However, these were

radiations of insectivorous species, and lacked the extreme changes in craniodental morphology that facilitated exploitation of new diets in the Phyllostomidae. The role of bite force in originating or maintaining insectivorous bat diversity is unknown, yet palaeotropical bat assemblages can comprise > 50 syntopic insectivorous species (Kingston et al. 2003; Kingston, Lim & Zubaid 2006; Struebig et al. 2008). Here we ask how species within such diverse assemblages differ in bite force and, given the morphological conservatism of skull morphology within families (relative to the Phyllostomidae), whether differences are primarily driven by differences in size or mechanical advantage of the mandibular lever system. We hypothesized that bite force production capacity will increase with body size and the mechanical advantage ratio of the bats. We also hypothesized that size and mechanical advantage relationships with bite force would be influenced by phylogeny, differing among the families. As a result, species of similar size or similar size-independent mechanical advantage from different families would differ in bite force, facilitating resource partitioning in species-rich assemblages.

Materials and Methods

Study Site and Species

The study was conducted in Krau Wildlife Reserve (KWR), an area of 62,395 ha of continuous old-growth forest, located in the state of Pahang, Malaysia (DWNP-DANCED 2001). The reserve was selected because it supports the greatest diversity of bats in the Old World tropics, with at least 55 insectivorous bat species of seven families

(Kingston et al. 2006). Sampling was confined to approximately 300 ha around Kuala Lompat Research Station (KLRS) (3°43'N, 102°17'E) on the eastern edge of the reserve and nearby caves. The elevation at KLRS is approximately 50 m a.s.l with vegetation classified as lowland evergreen mixed dipterocarp forest (Hodgkison et al. 2004). Bats were captured in the forest understory using four-bank harp traps (Francis 1989) positioned across trails. Four-shelf mist-nets of 6 m, 9 m, 12 m, or 16 m (where appropriate) were used to capture bats at the forest edge, in forest gaps, in open areas, and over rivers. All species were captured at KLRS; however, trapping at nearby caves increased bite performance test sample sizes for some of the rarely-captured species. The Samad Cave (3°76'N, 102°25'E), containing *Hipposideros bicolour* 142 kHz and *H. cervinus*, is approximately 2 km from the reserve border, and the cave system of Gua Kota Gelanggi (3°89'N, 102°47'E), that houses *H. diadema*, *H. lylei*, *Miniopterus medius*, *Rhinolophus affinis* and *Taphozous melanopogon* is approximately 30 km away. All captured individuals were banded and released at the point of capture within 12 hours after all essential measurements were recorded. Trapping and bite force recording were conducted between February and June 2009 and May and July 2010.

Jaw structure and muscle location for species studied were determined from ethanol-preserved specimens collected within KWR by the Malaysian Bat Conservation Research Unit and deposited at the Museum of Zoology, Universiti Kebangsaan Malaysia (UKM). Skulls were extracted and cleaned using a colony of dermestid beetles (*Dermestes maculatus*). Extraction, cleaning and measurement of skulls were conducted between August and December 2011 and between June and August 2012. All procedures

were approved by Department of Wildlife and National Park Peninsular Malaysia, UKM and Texas Tech University (IACUC 10014-04).

Morphometrics and Bite Force Measurements

For each captured individual we measured to the nearest 0.1 mm with a dial calliper: length of the forearm (FA) – from the extremity of the elbow to the extremity of the carpus with the wings folded; head length (HL) – from the tip of rostrum to the back of the skull; head width (HW) – the broadest part of the zygomatic arches; and head height (HH) – from the highest part of skull to the underside of mandible. Body mass (M) was measured using Pesola scales (Pesola AG, Baar, Switzerland) to the nearest 0.25 g.

Dentary bone characters of the lower jaw were measured from ethanol-preserved specimens. We calculated the mechanical advantage of five mandibular lever systems, each operating through three function points. Three lever systems were associated with portions of the temporalis muscle, and two with portions of the masseter muscle (Fig. 2.1), and function points were set to reflect output force at the molar, canine and incisor (Fig. 2.2). The mechanical advantage of each lever system at each function point was calculated by dividing the in-lever arm by each out-lever arm (Reduker 1983). For example, to calculate the mechanical advantage of the superficial portion of the masseter muscle at the molar function point we divided the in-lever arm of the masseter muscle, superficial portion (ILMSF) by the out-lever arm of the molar function point (OLAM). This generated 15 mechanical advantage ratios for each specimen studied.

In vivo bite force for captured insectivorous bats was measured using an isometric Kistler force transducer (type 9217, range ± 500N; Kistler Inc., Switzerland) connected to a Kistler charge amplifier (type 5995; Kistler Inc., Switzerland). The distance between the bite plates was adjusted to preserve a gape angle of 25^{o}, which maximizes bite force with minimum stress at the maximum bite point location in different sizes of bats (Dumont & Herrel 2003; Bourke et al. 2008). The distance between the bite plates was calculated as $2(\sin 12.5 \times CM^{3})$ where 12.5 is half of the 25^{o} gape angle and CM^{3} (mm) is the length of maxillary tooth row of live bats measured from the distal end of the third molar to the mesial surface of the canine. During measurements, bats were held in the "pinch" grip so that they could freely bite the transducer (Kunz et al. 2009).

Bite force was recorded at the molars and measurements were repeated six times for each individual. Following the mechanical principle of a mandible lever system, the largest bite force is exerted at the most posterior biting position (Greaves 2012); therefore, the bite force was recorded at the posterior tooth row (molars). The maximum value (in Newtons) of the six measures was considered to be the maximum bite force that the individual could produce. Aguirre et al. (2002) and Anderson et al. (2008) found that maximum bite force is repeatable among trials, and that the second strongest bites were always within 10 % of the strongest bite even in separate trials. Therefore, the maximum bite force measurements produced by individuals can be considered to be reliable measures of bite performance (Anderson et al. 2008).

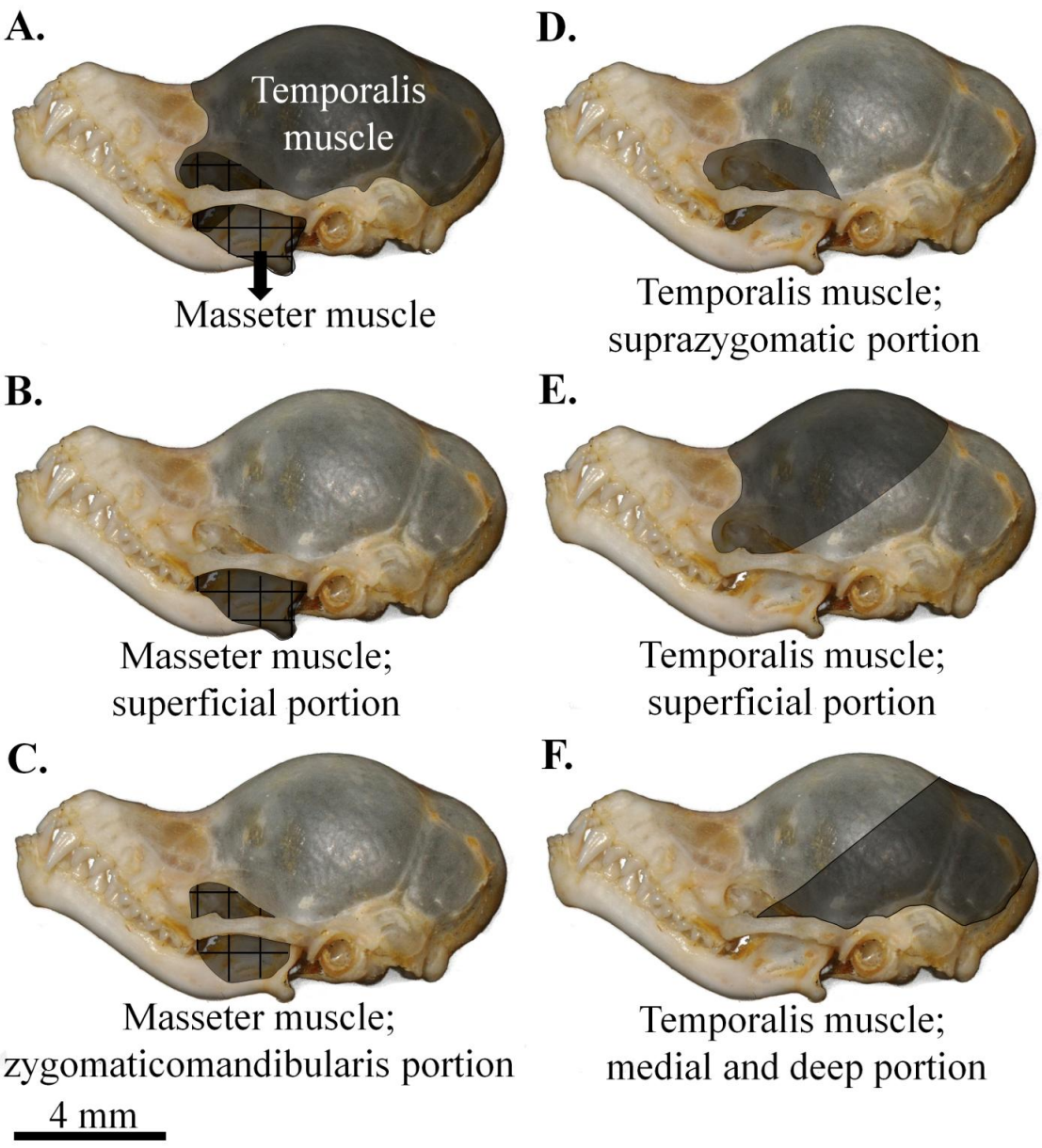

Figure 2.1. Estimated locations of the masseter (gridded) and temporalis (solid) muscles associated with the five mandibular lever systems thought to contribute to bite force in bats. Illustrated with reference to the skull of a *Kerivoula pellucida*.

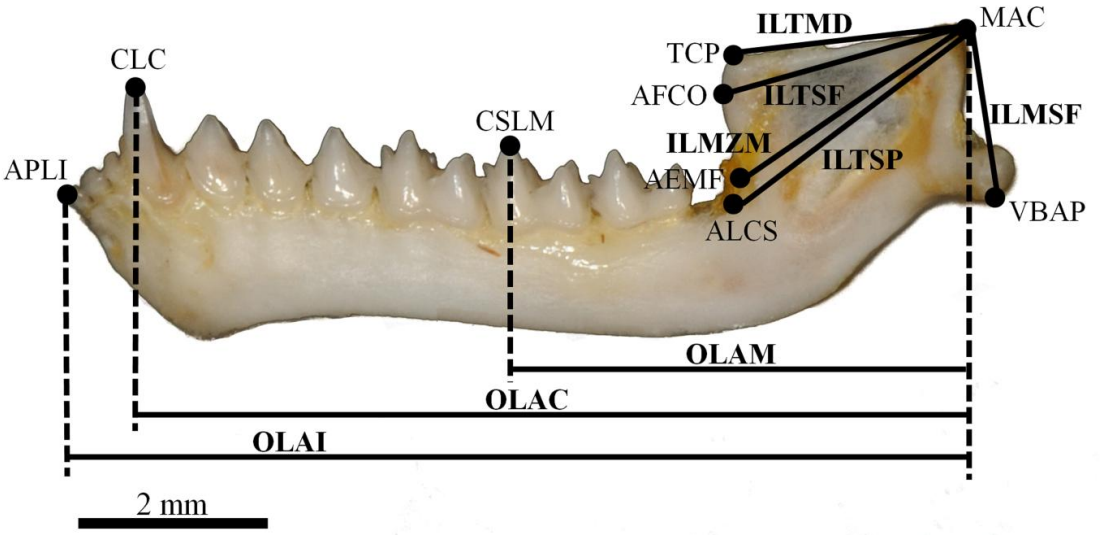

Figure 2.2. Dentary measurements used in mechanical advantage analysis. In levers denoted by IL, out levers by OL, function points given by APLI, CLC and CSLM. Full definitions of measurements given in Table 2.1.

Table 2.1. Description and details of variables used in calculation of mechanical advantage of five mandibular lever systems, each operating through three function points.

Abbreviation	Definition	Measurement
ILMSF	In-lever arm of the masseter muscle, superficial portion.	From the midpoint of the articular condyle (MAC) to the ventral border of the angular process (VBAP).
ILMZM	In-lever arm of the masseter muscle, zygomaticomandibularis portion.	From the midpoint of the articular condyle (MAC) to the anterior-most edge of the mandibular fossa (AEMF).
ILTSP	In-lever arm of the temporalis muscle, suprazygomatic portion.	From the midpoint of the articular condyle (MAC) to the anterio-lateral basal surface of the coronoid spine (ALCS).
ILTSF	In-lever arm of the temporalis muscle, superficial portion	From the midpoint of the articular condyle (MAC) to the anterior face of coronoid directly opposite (AFCO).
ILTMD	In-lever arm of the temporalis muscle, medial and deep portion.	From the midpoint of the articular condyle (MAC) to the tip of coronoid process (TCP).

Table 2.1. Continued.

Abbreviation	Definition	Measurement
OLAM	Out-lever arm to molar function point.	From the midpoint of the articular condyle (MAC) to the centre of protoconid on the second lower molar (CSLM).
OLAC	Out-lever arm to canine function point.	From the midpoint of articular condyle (MAC) to the centre of the lower canine (CLC).
OLAI	Out-lever arm to incisor function point.	From the midpoint of the articular condyle (MAC) to the anterior-most point of the lower incisors (APLI).

Statistical Analyses

Sexual dimorphism can confound interpretation of interspecific differences in morphology so we used two-tailed t-tests to check for sexual differences in body size, head dimensions and maximum bite force within all species represented by at least two individuals of each sex (Student 1908; De Winter 2013). We excluded species if the variance of male and female measures were not homogeneous (Levene's test for equality of variance). To determine the importance of any statistically significant differences between sexes, we estimated effect sizes following Hedges (1981). This estimation is based on differences between the standard deviations of the means of the sample tested. We interpreted Hedges's values; $g \geq 0.8$ as a large effect size. Only species with statistically significant differences between sexes and large effect sizes were considered dimorphic. Of the 35 species studied, 19 species had sufficient sample sizes for analysis. Only six species were dimorphic for forearm length, two for body mass, two for bite force, five for head length, four for head width and three for head height. However, when we ran analyses of covariance (ANCOVA) there was no effect of sex on the relationships between bite force and any of the size variables. Thus, subsequent analyses were based on pooled data.

We calculated species' means for maximum bite force and all morphological measures, giving assemblage-level data for the study area. To explore which variables best explained variation in maximum bite force among species in the assemblage, we tested the relationship between maximum bite force and all size variables (FA, HL, HW, HH and M) using simple linear regression analyses. We then ran stepwise multiple

regressions with maximum bite force as the dependent variable and morphological measures as independent variables. If a model included more than one significant size variable, the variable with the highest partial correlation with bite force was defined as the best size predictor. We used the most predictive size variables to scale maximum bite force using simple linear regression and obtained the residual measurement of size-independent maximum bite force. Analyses were conducted at the assemblage level, then repeated for families represented by more than two species. Families included in the final analyses were Hipposideridae, Vespertilionidae, Rhinolophidae and Molossidae, while Emballonuridae, Miniopteridae and Nycteridae were excluded.

To investigate the mechanistic link between biting levers and bite performance, we first calculated the mechanical advantage for each of the five mandible lever mechanisms for each individual, and then calculated the species' means. Next, we used species' mean values to scale mechanical advantage with the best size predictor variable of maximum bite force determined above. Simple linear regression analysis was thereby used to obtain a residual measurement of size-independent mechanical advantage. We then tested the relationship between residual (size-independent) mechanical advantage of each mechanism and residual (size-independent) maximum bite force using simple linear regression analyses. Finally, we ran stepwise multiple regressions with residual maximum bite force as the dependent variable and the residual mechanical advantages as the independent variables. Analyses were conducted at both assemblage and family level using SPSS version 17.0 statistical packages for Windows (SPSS Inc., Chicago, Illinois, USA) and all data were log transformed before analysis. The normality of the data was

tested using graphical and numerical methods to meet the assumptions of parametric statistical tests and skewness scores were within -1 to 1.

Results

Bite Force and Mechanical Advantage

Maximum bite force and morphometric measurements were recorded for 789 individuals of 35 species belonging to seven families (Table 2.2). The maximum bite force ranged from 0.91 ± 0.25 N (mean ± SD) in *Kerivoula intermedia* to 24.81 ± 3.37 N in *Hipposideros diadema*. These bats also represented the shortest and longest FA length across all species studied, with measurements of 28.69 ± 1.74 mm and 84.30 ± 2.29 mm respectively. Measurements of the mandible lever mechanisms were completed for 451 specimens of 29 species belonging to six families (Tables 2.3 and 2.4). *Cheiromeles torquatus* had the greatest mechanical advantage for the superficial portion of the masseter muscle at all three function points tested, while *Rhinolophus robinsoni* had the greatest mechanical advantage for the zygomaticomandibularis of the masseter muscles at all three function points (Table 2.3). For the temporalis muscle complexes, *Murina aenea* had the greatest mechanical advantage for all muscle portions at all three function points (Table 2.4).

Table 2.2. Summary of the sample sizes, maximum bite force, and morphological data collected for 35 bat species from Krau Wildlife Reserve, Malaysia (mean ±SD).

Species	***n***	**Maximum bite force (N)**	**Mass (g)**	**Forearm length (mm)**	**Head height (mm)**	**Head length (mm)**	**Head width (mm)**
Emballonuridae							
Emballonura monticola	6	1.06 ± 0.11	6.29 ± 0.56	44.48 ± 1.85	9.03 ± 0.49	16.52 ± 0.54	9.88 ± 0.64
Taphozous melanopogon	10	7.78 ± 0.91	24.33 ± 1.60	63.74 ± 1.60	11.98 ± 0.56	26.27 ± 0.59	13.95 ± 0.26
Hipposideridae							
Hipposideros bicolor 131 kHz*	16	3.35 ± 0.53	8.73 ± 0.84	45.23 ± 1.11	10.38 ± 0.71	19.39 ± 0.66	12.18 ± 0.76
Hipposideros bicolor 142 kHz*	59	3.63 ± 0.69	8.59 ± 0.71	43.14 ± 0.75	9.03 ± 0.71	18.74 ± 0.55	11.26 ± 0.84

Table 2.2. Continued

Species	***n***	**Maximum bite force (N)**	**Mass (g)**	**Forearm length (mm)**	**Head height (mm)**	**Head length (mm)**	**Head width (mm)**
Hipposideros cervinus	60	4.30 ± 0.55	10.00 ± 0.95	49.32 ± 1.02	10.39 ± 1.24	19.54 ± 0.68	11.78 ± 0.98
Hipposideros cineraceus	1	1.61	4.75	36.90	8.10	16.20	10.80
Hipposideros diadema	77	24.81 ± 3.37	47.68 ± 4.41	84.30 ± 2.29	18.11 ± 1.12	33.61 ± 0.91	20.80 ± 1.32
Hipposideros galeritus	2	1.13 ± 0.00	6.88 ± 0.18	46.40 ± 1.70	9.79 ± 0.01	18.10 ± 0.14	9.71 ± 0.01
Hipposideros larvatus	14	9.40 ± 1.73	17.66 ± 1.82	58.02 ± 1.27	11.35 ± 0.43	23.74 ± 0.86	13.51 ± 0.40
Hipposideros lylei	5	16.31 ± 1.95	38.30 ± 3.19	77.50 ± 1.62	17.62 ± 0.19	31.50 ± 0.58	17.68 ± 0.94
Hipposideros ridleyi	12	3.74 ± 0.49	9.60 ± 0.84	48.54 ± 0.54	10.33 ± 1.38	20.73 ± 0.95	11.83 ± 1.75
Molossidae							
Chaerephon johorensis	13	4.45 ± 1.18	19.77 ± 1.73	46.43 ± 1.09	12.82 ± 1.53	24.82 ± 1.15	14.82 ± 1.21

Table 2.2. Continued.

Species	***n***	**Maximum bite force (N)**	**Mass (g)**	**Forearm length (mm)**	**Head height (mm)**	**Head length (mm)**	**Head width (mm)**
Cheiromeles torquatus	4	16.41 ± 3.29	190.50 ± 36.93	82.58 ± 3.20	29.85 ± 0.10	44.30 ± 2.16	34.88 ± 0.67
Mops mops	29	7.06 ± 3.07	26.93 ± 2.41	43.71 ± 1.25	14.08 ± 0.93	26.78 ± 0.77	16.23 ± 1.24
Miniopteridae							
Miniopterus medius	49	1.32 ± 0.35	8.54 ± 0.65	42.48 ± 0.72	9.87 ± 0.51	16.26 ± 0.59	10.09 ± 0.98
Nycteridae							
Nycteris tragata	4	9.43 ± 1.48	19.94 ± 0.1.53	50.33 ± 1.30	11.98 ± 0.05	23.90 ± 0.14	15.70 ± 0.23

Table 2.2. Continued.

Species	***n***	**Maximum bite force (N)**	**Mass (g)**	**Forearm length (mm)**	**Head height (mm)**	**Head length (mm)**	**Head width (mm)**
Rhinolophidae							
Rhinolophus affinis	58	4.35 ± 0.75	13.95 ± 0.94	49.82 ± 0.78	11.96 ± 0.98	23.84 ± 0.47	13.39 ± 0.81
Rhinolophus lepidus	49	1.77 ± 0.52	6.36 ± 0.71	40.52 ± 1.56	8.93 ± 0.89	18.02 ± 0.53	10.35 ± 1.65
Rhinolophus luctus	2	18.19 ± 0.40	28.00 ± 1.41	63.35 ± 0.49	13.90 ± 0.85	30.25 ± 0.35	15.55 ± 0.78
Rhinolophus robinsoni	1	2.21	8.00	43.90	10.20	20.90	12.50
Rhinolophus sedulus	2	3.19 ± 0.67	7.63 ± 0.18	41.05 ± 0.21	9.15 ± 0.78	20.30 ± 0.28	11.05 ± 0.78
Rhinolophus stheno	66	2.85 ± 0.79	8.81 ± 1.11	45.74 ± 1.09	9.54 ± 0.62	20.99 ± 0.54	10.93 ± 0.55
Rhinolophus trifoliatus	48	6.66 ± 1.27	14.01 ± 1.98	51.08 ± 2.09	11.40 ± 0.99	23.68 ± 0.89	12.92 ± 1.37

Table 2.2. Continued.

Species	***n***	**Maximum bite force (N)**	**Mass (g)**	**Forearm length (mm)**	**Head height (mm)**	**Head length (mm)**	**Head width (mm)**
Vespertilionidae							
Kerivoulinae							
Kerivoula intermedia	71	0.91 ± 0.25	3.16 ± 0.52	28.69 ± 1.74	7.36 ± 0.71	13.54 ± 0.75	8.09 ± 0.57
Kerivoula krauensis	1	1.99	3.50	30.50	8.50	14.00	9.20
Kerivoula papillosa	41	7.38 ± 1.51	9.05 ± 1.23	41.64 ± 1.99	11.39 ± 1.04	19.29 ± 0.19	12.01 ± 1.05
Kerivoula pellucida	23	1.84 ± 0.51	4.73 ± 0.44	30.83 ± 0.92	9.02 ± 0.61	15.55 ± 0.51	9.50 ± 0.63
Phoniscus atrox	15	2.60 ± 0.53	4.87 ± 0.48	33.31 ± 1.08	9.91 ± 0.50	17.38 ± 0.20	9.79 ± 0.53
Phoniscus jagorii	1	6.42	9.50	37.60	10.80	19.80	13.20
Murininae							
Murina aenea	2	12.52 ± 0.25	7.75 ± 0.71	35.15 ± 0.21	10.85 ± 0.49	18.60 ± 0.85	10.85 ± 1.20

Table 2.2. Continued

Species	***n***	**Maximum bite force (N)**	**Mass (g)**	**Forearm length (mm)**	**Head height (mm)**	**Head length (mm)**	**Head width (mm)**
Murina cyclotis	11	11.90 ± 3.54	8.45 ± 0.51	35.85 ± 1.29	11.20 ± 0.71	19.56 ± 0.59	11.77 ± 1.14
Murina suilla	29	4.41 ± 0.65	3.99 ± 0.45	30.29 ± 2.11	8.80 ± 0.87	15.86 ± 2.13	8.90 ± 1.13
Vespertilioninae							
Myotis ater	2	2.44 ± 0.84	6.50 ± 2.12	35.95 ± 0.21	9.85 ± 0.07	17.60 ± 0.15	11.20 ± 0.00
Myotis ridleyi	1	1.38	5.50	29.80	7.20	13.60	8.90
Scotophilus kuhlii	5	9.18 ± 0.56	24.60 ± 0.89	51.18 ± 1.15	13.04 ± 0.15	23.44 ± 0.54	14.86 ± 0.36

*Cryptic species that were genetically and acoustically divergent and denoted as phonic types based on the mean frequency of their CF component of the call. Individual with 131 kHz was assigned as *Hipposideros bicolor* 131 kHz and individual with 142 kHz was assigned as *Hipposideros bicolor* 142 kHz.

Table 2.3. Mechanical advantage ratios calculated for the superficial and zygomaticomandibularis portions of the masseter muscle at molar, canine and incisor function points for 29 bat species from Krau Wildlife Reserve, Malaysia (mean ±SD). Mechanical advantage values in bold are the highest mean values for a particular muscle portion and function point.

Species	***n***	**Superficial portion of masseter muscle**			**Zygomaticomandibularis portion of masseter muscle**		
		Molar	**Canine**	**Incisor**	**Molar**	**Canine**	**Incisors**
Emballonuridae							
Taphozous melanopogon	6	0.32 ± 0.03	0.22 ± 0.01	0.21 ± 0.00	0.59 ± 0.20	0.40 ± 0.11	0.38 ± 0.11
Hipposideridae							
Hipposideros bicolor 131 kHz*	32	0.26 ± 0.02	0.19 ± 0.01	0.19 ± 0.01	0.50 ± 0.06	0.38 ± 0.03	0.36 ± 0.03
Hipposideros bicolor 142 kHz*	37	0.27 ± 0.04	0.20 ± 0.03	0.19 ± 0.03	0.49 ± 0.06	0.37 ± 0.03	0.34 ± 0.03
Hipposideros cervinus	67	0.28 ± 0.04	0.21 ± 0.02	0.20 ± 0.02	0.49 ± 0.08	0.37 ± 0.04	0.35 ± 0.04
Hipposideros cineraceus	2	0.24 ± 0.04	0.18 ± 0.03	0.17 ± 0.02	0.44 ± 0.01	0.34 ± 0.00	0.32 ± 0.00

Table 2.3. Continued

Species	***n***	**Superficial portion of masseter muscle**			**Zygomaticomandibularis portion of masseter muscle**		
		Molar	**Canine**	**Incisor**	**Molar**	**Canine**	**Incisors**
Hipposideros diadema	35	0.35 ± 0.05	0.25 ± 0.02	0.23 ± 0.04	0.42 ± 0.18	0.30 ± 0.13	0.29 ± 0.10
Hipposideros lylei	8	0.28 ± 0.01	0.21 ± 0.01	0.20 ± 0.01	0.45 ± 0.01	0.34 ± 0.01	0.32 ± 0.01
Hipposideros ridleyi	2	0.27 ± 0.04	0.20 ± 0.03	0.19 ± 0.03	0.51 ± 0.04	0.38 ± 0.03	0.37 ± 0.04
Miniopteridae							
Miniopterus medius	33	0.30 ± 0.03	0.22 ± 0.01	0.21 ± 0.01	0.52 ± 0.06	0.38 ± 0.03	0.37 ± 0.03
Molossidae							
Chaerephon johorensis	4	0.40 ± 0.04	0.31 ± 0.03	0.29 ± 0.02	0.55 ± 0.07	0.42 ± 0.04	0.40 ± 0.04
Cheiromeles torquatus	3	**0.49 ± 0.02**	**0.41 ± 0.01**	**0.38 ± 0.02**	0.51 ± 0.03	0.42 ± 0.03	0.40 ± 0.03

Table 2.3. Continued

Species	***n***	**Superficial portion of masseter muscle**			**Zygomaticomandibularis portion of masseter muscle**		
		Molar	**Canine**	**Incisor**	**Molar**	**Canine**	**Incisors**
Mops mops	6	0.40 ± 0.04	0.31 ± 0.02	0.29 ± 0.02	0.54 ± 0.08	0.42 ± 0.04	0.40 ± 0.04
Rhinolophidae							
Rhinolophus affinis	46	0.29 ± 0.04	0.21 ± 0.02	0.20 ± 0.02	0.49 ± 0.08	0.36 ± 0.05	0.34 ± 0.04
Rhinolophus Lepidus	40	0.28 ± 0.03	0.21 ± 0.02	0.20 ± 0.02	0.46 ± 0.06	0.34 ± 0.04	0.33 ± 0.04
Rhinolophus robinsoni	3	0.26 ± 0.02	0.18 ± 0.02	0.19 ± 0.02	**0.65 ± 0.06**	**0.44 ± 0.11**	**0.47 ± 0.18**
Rhinolophus sedulus	7	0.30 ± 0.04	0.23 ± 0.02	0.22 ± 0.02	0.50 ± 0.04	0.37 ± 0.02	0.35 ± 0.03
Rhinolophus stheno	9	0.28 ± 0.05	0.21 ± 0.03	0.20 ± 0.04	0.49 ± 0.08	0.35 ± 0.04	0.34 ± 0.05
Rhinolophus trifoliatus	18	0.32 ± 0.05	0.24 ± 0.03	0.23 ± 0.03	0.48 ± 0.04	0.37 ± 0.03	0.35 ± 0.04

Table 2.3. Continued

Species	***n***	**Superficial portion of masseter muscle**			**Zygomaticomandibularis portion of masseter muscle**		
		Molar	**Canine**	**Incisor**	**Molar**	**Canine**	**Incisors**
Vespertilionidae							
Kerivoulinae							
Kerivoula intermedia	18	0.30 ± 0.03	0.22 ± 0.02	0.21 ± 0.01	0.51 ± 0.06	0.36 ± 0.04	0.35 ± 0.05
Kerivoula papillosa	28	0.28 ± 0.02	0.20 ± 0.02	0.19 ± 0.02	0.51 ± 0.06	0.36 ± 0.04	0.34 ± 0.39
Kerivoula pelucida	17	0.30 ± 0.03	0.20 ± 0.01	0.19 ± 0.01	0.51 ± 0.08	0.36 ± 0.05	0.34 ± 0.05
Phoniscus atrox	6	0.28 ± 0.02	0.20 ± 0.02	0.19 ± 0.02	0.48 ± 0.10	0.34 ± 0.05	0.32 ± 0.05
Phoniscus jagorii	2	0.29 ± 0.02	0.20 ± 0.00	0.19 ± 0.01	0.48 ± 0.12	0.33 ± 0.07	0.31 ± 0.08
Murininae							
Murina aenea	3	0.38 ± 0.01	0.28 ± 0.01	0.27 ± 0.00	0.54 ± 0.03	0.40 ± 0.00	0.39 ± 0.01
Murina cyclotis	5	0.32 ± 0.02	0.24 ± 0.02	0.23 ± 0.02	0.59 ± 0.06	0.44 ± 0.04	0.42 ± 0.04

Table 2.3. Continued

Species	***n***	**Superficial portion of masseter muscle**			**Zygomaticomandibularis portion of masseter muscle**		
		Molar	**Canine**	**Incisor**	**Molar**	**Canine**	**Incisors**
Murina suilla	3	0.31 ± 0.01	0.24 ± 0.01	0.23 ± 0.01	0.49 ± 0.10	0.38 ± 0.05	0.37 ± 0.06
Vespertilioninae							
Myotis ater	2	0.28 ± 0.01	0.22 ± 0.02	0.21 ± 0.02	0.52 ± 0.03	0.40 ± 0.04	0.39 ± 0.05
Myotis ridleyi	5	0.33 ± 0.03	0.26 ± 0.02	0.25 ± 0.02	0.53 ± 0.02	0.42 ± 0.02	0.41 ± 0.02
Scotophilus kuhlii	4	0.34 ± 0.02	0.28 ± 0.01	0.27 ± 0.02	0.49 ± 0.08	0.40 ± 0.05	0.38 ± 0.08

*Cryptic species that were genetically and acoustically divergent and denoted as phonic types based on the mean frequency of their CF component of the call. Individual with 131 kHz was assigned as *Hipposideros bicolor* 131 kHz and individual with 142 kHz was assigned as *Hipposideros bicolor* 142 kHz.

Table 2.4. Mechanical advantage ratios calculated for the suprazygomatic, superficial, and medial and deep portions of the temporalis muscle at molar, canine and incisor function points for 29 bat species from Krau Wildlife Reserve, Malaysia (mean ±SD). Mechanical advantage values in bold are the highest mean values for a particular muscle portion and function point.

Species	***n***	**Suprazygomatic portion of temporalis muscle**			**Superficial portion of temporalis muscle**			**Medial and deep portion of temporalis muscle**		
		Molar	**Canine**	**Incisor**	**Molar**	**Canine**	**Incisors**	**Molar**	**Canine**	**Incisors**
Emballonuridae										
Taphozous melanopogon	6	0.41 ± 0.05	0.28 ± 0.03	0.27 ± 0.02	0.46 ± 0.05	0.32 ± 0.03	0.30 ± 0.02	0.88 ± 0.02	0.33 ± 0.01	0.31 ± 0.01
Hipposideridae										
Hipposideros bicolor 131 kHz*	32	0.38 ± 0.03	0.29 ± 0.01	0.27 ± 0.01	0.56 ± 0.03	0.33 ± 0.01	0.32 ± 0.01	0.41 ± 0.03	0.31 ± 0.01	0.30 ± 0.01
Hipposideros bicolor 142 kHz*	37	0.38 ± 0.05	0.29 ± 0.02	0.27 ± 0.02	0.45 ± 0.05	0.34 ± 0.02	0.32 ± 0.02	0.42 ± 0.04	0.32 ± 0.02	0.30 ± 0.01
Hipposideros cervinus	67	0.39 ± 0.04	0.29 ± 0.02	0.27 ± 0.02	0.45 ± 0.05	0.34 ± 0.02	0.32 ± 0.02	0.43 ± 0.04	0.32 ± 0.01	0.30 ± 0.01

Table 2.4. Continued

Species	*n*	Suprazygomatic portion of temporalis muscle			Superficial portion of temporalis muscle			Medial and deep portion of temporalis muscle		
		Molar	**Canine**	**Incisor**	**Molar**	**Canine**	**Incisors**	**Molar**	**Canine**	**Incisors**
Hipposideros cineraceus	2	0.33 ± 0.01	0.26 ± 0.01	0.24 ± 0.01	0.41 ± 0.01	0.32 ± 0.01	0.30 ± 0.01	0.41 ± 0.02	0.31 ± 0.02	0.29 ± 0.02
Hipposideros diadema	35	0.44 ± 0.08	0.32 ± 0.06	0.28 ± 0.02	0.48 ± 0.09	0.34 ± 0.06	0.31 ± 0.02	0.44 ± 0.02	0.32 ± 0.05	0.28 ± 0.01
Hipposideros lylei	8	0.42 ± 0.01	0.32 ± 0.01	0.30 ± 0.01	0.46 ± 0.01	0.34 ± 0.01	0.32 ± 0.01	0.41 ± 0.01	0.31 ± 0.01	0.29 ± 0.01
Hipposideros ridleyi	2	0.41 ± 0.02	0.31 ± 0.02	0.29 ± 0.01	0.41 ± 0.02	0.35 ± 0.02	0.33 ± 0.01	0.43 ± 0.00	0.32 ± 0.01	0.31 ± 0.00
Miniopteridae										
Miniopterus medius	33	0.31 ± 0.04	0.23 ± 0.02	0.22 ± 0.02	0.39 ± 0.04	0.29 ± 0.02	0.28 ± 0.02	0.34 ± 0.03	0.25 ± 0.02	0.24 ± 0.02
Molossidae										
Chaerephon johorensis	4	0.42 ± 0.05	0.32 ± 0.02	0.30 ± 0.02	0.47 ± 0.05	0.36 ± 0.02	0.34 ± 0.01	0.40 ± 0.04	0.31 ± 0.01	0.29 ± 0.01
Cheiromeles torquatus	3	0.45 ± 0.03	0.37 ± 0.03	0.35 ± 0.02	0.47 ± 0.03	0.39 ± 0.03	0.36 ± 0.02	0.43 ± 0.01	0.36 ± 0.01	0.33 ± 0.01

Table 2.4. Continued

Species	*n*	Suprazygomatic portion of temporalis muscle			Superficial portion of temporalis muscle			Medial and deep portion of temporalis muscle		
		Molar	**Canine**	**Incisor**	**Molar**	**Canine**	**Incisors**	**Molar**	**Canine**	**Incisors**
Mops mops	6	0.40 ± 0.05	0.32 ± 0.01	0.30 ± 0.01	0.45 ± 0.05	0.35 ± 0.01	0.33 ± 0.01	0.40 ± 0.05	0.31 ± 0.02	0.29 ± 0.02
Rhinolophidae										
Rhinolophus affinis	46	0.39 ± 0.04	0.28 ± 0.02	0.27 ± 0.01	0.44 ± 0.04	0.32 ± 0.02	0.30 ± 0.01	0.41 ± 0.03	0.30 ± 0.01	0.28 ± 0.01
Rhinolophus lepidus	40	0.35 ± 0.02	0.26 ± 0.02	0.25 ± 0.02	0.42 ± 0.03	0.31 ± 0.02	0.30 ± 0.01	0.39 ± 0.03	0.29 ± 0.02	0.27 ± 0.02
Rhinolophus robinsoni	3	0.37 ± 0.05	0.26 ± 0.02	0.27 ± 0.03	0.42 ± 0.05	0.30 ± 0.02	0.31 ± 0.03	0.40 ± 0.02	0.28 ± 0.04	0.29 ± 0.01
Rhinolophus sedulus	7	0.37 ± 0.03	0.28 ± 0.02	0.27 ± 0.02	0.43 ± 0.03	0.32 ± 0.03	0.31 ± 0.02	0.40 ± 0.02	0.30 ± 0.01	0.28 ± 0.01
Rhinolophus stheno	9	0.38 ± 0.04	0.28 ± 0.02	0.27 ± 0.02	0.44 ± 0.05	0.32 ± 0.02	0.31 ± 0.02	0.40 ± 0.03	0.29 ± 0.01	0.28 ± 0.01
Rhinolophus trifoliatus	18	0.40 ± 0.03	0.30 ± 0.02	0.29 ± 0.02	0.44 ± 0.03	0.34 ± 0.02	0.32 ± 0.02	0.41 ± 0.02	0.31 ± 0.01	0.30 ± 0.01
Vespertilionidae										
Kerivoulinae										
Kerivoula intermedia	18	0.36 ± 0.04	0.26 ± 0.02	0.25 ± 0.01	0.45 ± 0.05	0.33 ± 0.03	0.31 ± 0.02	0.38 ± 0.04	0.27 ± 0.02	0.26 ± 0.02

Table 2.4. Continued

Species	*n*	Suprazygomatic portion of temporalis muscle			Superficial portion of temporalis muscle			Medial and deep portion of temporalis muscle		
		Molar	**Canine**	**Incisor**	**Molar**	**Canine**	**Incisors**	**Molar**	**Canine**	**Incisors**
Kerivoula papillosa	28	0.39 ± 0.03	0.28 ± 0.02	0.27 ± 0.02	0.45 ± 0.03	0.33 ± 0.02	0.31 ± 0.02	0.42 ± 0.03	0.30 ± 0.02	0.29 ± 0.01
Kerivoula pelucida	17	0.38 ± 0.04	0.26 ± 0.02	0.25 ± 0.02	0.46 ± 0.04	0.32 ± 0.02	0.30 ± 0.02	0.40 ± 0.06	0.28 ± 0.03	0.26 ± 0.03
Phoniscus atrox	6	0.41 ± 0.03	0.29 ± 0.02	0.28 ± 0.02	0.49 ± 0.03	0.34 ± 0.03	0.33 ± 0.03	0.45 ± 0.03	0.32 ± 0.04	0.31 ± 0.04
Phoniscus jagorii	2	0.43 ± 0.01	0.29 ± 0.00	0.28 ± 0.01	0.49 ± 0.12	0.34 ± 0.01	0.32 ± 0.01	0.50 ± 0.00	0.34 ± 0.01	0.32 ± 0.00
Murininae										
Murina aenea	3	**0.51 ± 0.02**	**0.39 ± 0.02**	**0.36 ± 0.02**	**0.57 ± 0.02**	**0.43 ± 0.02**	**0.41 ± 0.02**	**0.53 ± 0.01**	**0.40 ± 0.02**	**0.38 ± 0.01**
Murina cyclotis	5	0.45 ± 0.02	0.34 ± 0.02	0.32 ± 0.02	0.51 ± 0.06	0.39 ± 0.02	0.36 ± 0.01	0.49 ± 0.01	0.37 ± 0.02	0.35 ± 0.01
Murina suilla	3	0.36 ± 0.03	0.28 ± 0.04	0.27 ± 0.03	0.44 ± 0.03	0.34 ± 0.04	0.33 ± 0.03	0.37 ± 0.04	0.29 ± 0.04	0.27 ± 0.03
Vespertilioninae										
Myotis ater	2	0.35 ± 0.04	0.27 ± 0.03	0.26 ± 0.02	0.42 ± 0.04	0.33 ± 0.02	0.32 ± 0.01	0.39 ± 0.03	0.30 ± 0.01	0.29 ± 0.01
Myotis ridleyi	5	0.37 ± 0.02	0.29 ± 0.02	0.28 ± 0.02	0.45 ± 0.02	0.36 ± 0.02	0.35 ± 0.02	0.39 ± 0.01	0.31 ± 0.01	0.30 ± 0.01
Scotophilus kuhlii	4	0.45 ± 0.03	0.37 ± 0.04	0.35 ± 0.02	0.41 ± 0.04	0.41 ± 0.04	0.39 ± 0.02	0.47 ± 0.02	0.39 ± 0.01	0.37 ± 0.02

*Cryptic species that were genetically and acoustically divergent and denoted as phonic types based on the mean frequency of their CF component of the call.

Individual with 131 kHz was assigned as *Hipposideros bicolor* 131 kHz and individual with 142 kHz was assigned as *Hipposideros bicolor* 142 kHz

Bite Force Correlates

Across all insectivorous bats studied, we identified strong and positive correlations between maximum bite force and all variables measured for body and head dimensions (Fig. 2.3, see also Table 2.4). At the family level, we obtained similar results for correlations between maximum bite force and all variables measured except in the family Molossidae (Fig. 2.3, see also Table 2.4). Using the stepwise multiple regression analysis across all species (assemblage model), a significant model emerged ($F_{1,33} = 59.804$, $r^2 = 0.644$, $p < 0.0001$) with head length as the only significant predictor of maximum bite force. However, family-level models differed from the assemblage model and among families. For Hipposideridae, the model ($F_{2,6} = 108.587$, $r^2 = 0.973$, $p < 0.0001$) with body mass ($\beta_1 = 2.520$, $p < 0.001$) and forearm length ($\beta_2 = -1.580$, $p < 0.013$) was the best model for predicting maximum bite force and accounted for approximately 97 % of the variance in bite force. However, the squared partial correlation coefficients for this model revealed that body mass was a better predictor of maximum bite force than forearm length ($r^2_{BM} = 0.839$; $r^2_{FA} = 0.672$). This suggests that bite force in the Hipposideridae was primarily predicted by heavier body mass and to lesser extent by smaller length of the forearm. In the Rhinolophidae, the significant model ($F_{1,5} = 82.288$, $r^2 = 0.943$, $p < 0.0001$) included only body mass ($\beta_1 = 0.971$, $p < 0.0001$), and in the Vespertilionidae, the model ($F_{1,10} = 31.975$, $r^2 = 0.762$, $p < 0.0001$) included only head height ($\beta_1 = 0.873$, $p < 0.0001$). None of the morphological variables tested were suitable for creating a model to predict maximum bite force for the family Molossidae.

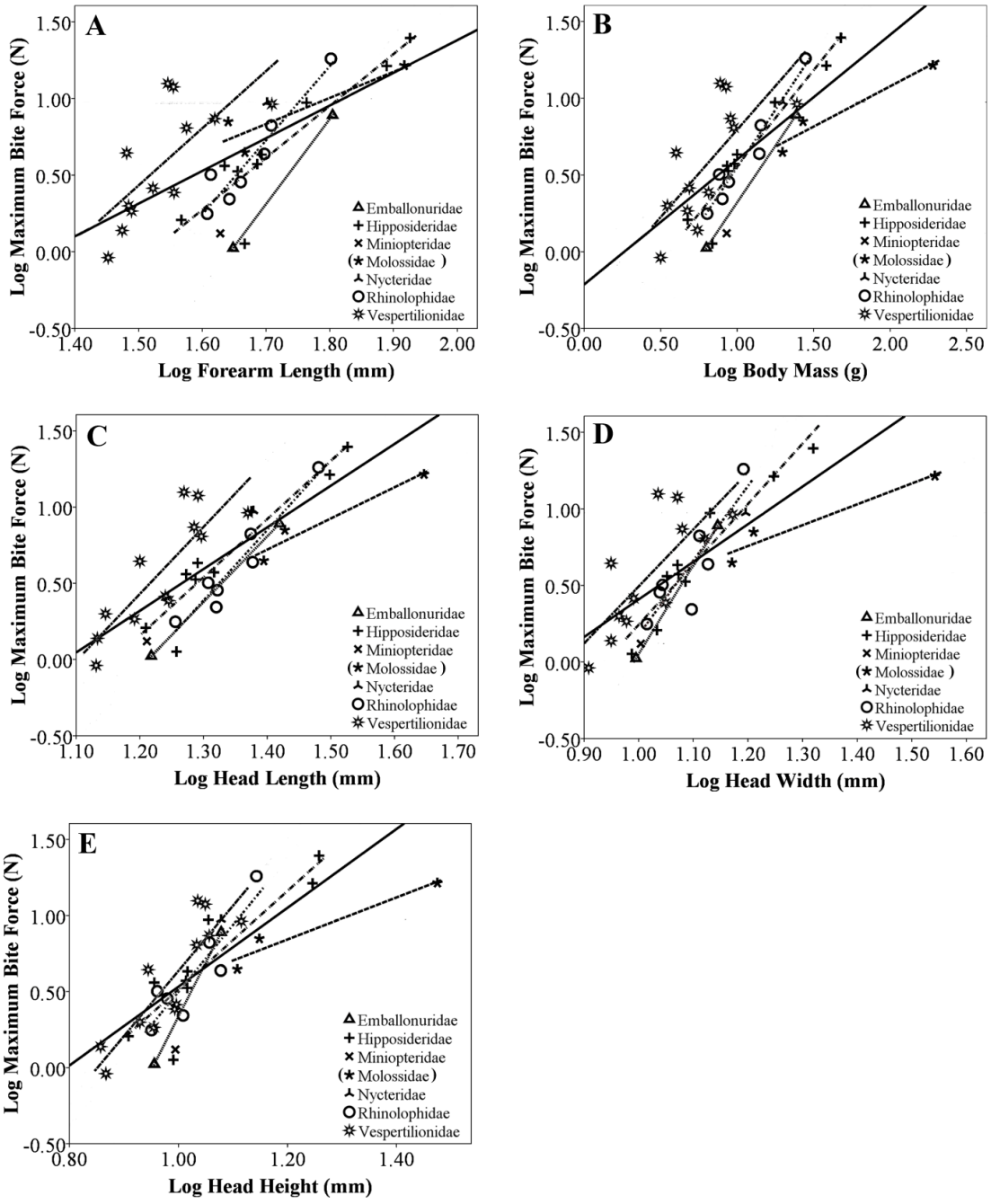

Figure 2.3. The relationship between bite force (N) and five external measures of size across 35 species of insectivorous bats from Krau Wildlife Reserve, Malaysia. A)

forearm length, B) body mass, C) head length, D) head width and E) head height. Solid line describes the relationship across all species, broken lines and symbols describe the relationships within families. Families given in parenthesis if relationship was not significant ($p > 0.05$). Regression equations and results given in Table 2.5.

Table 2.5. The regression equation, r-squared and calculated probability between bite force and five external measures of size across 35 species of insectivorous bats from Krau Wildlife Reserve, Malaysia. A) forearm length, B) body mass, C) head length, D) head width and E) head height.

Family	Regression equation	r^2	p
(A) Log maximum bite force (N) vs. log forearm length (mm)			
Across species	Y = 2.134X – 2.886	0.438	< 0.0001
Hipposideridae	Y = 3.387X – 5.144	0.833	0.001
Molossidae	Y = 1.704X – 2.064	0.817	0.282
Rhinolophidae	Y = 4.840X – 7.501	0.905	0.001
Vespertilionidae	Y = 3.732X – 5.165	0.500	0.010
(**B) Log maximum bite force (N) vs. log body mass (g)**			
Across species	Y = 0.814X – 0.214	0.587	< 0.0001
Hipposideridae	Y = 1.247X – 0.688	0.918	< 0.0001
Molossidae	Y = 0.525X + 0.028	0.948	0.146
Rhinolophidae	Y = 1.496X – 0.943	0.943	< 0.0001
Vespertilionidae	Y = 1.140X – 0.345	0.527	0.008
(C) Log maximum bite force (N) vs. log head length (mm)			
Across species	Y = 2.735X – 2.962	0.644	< 0.0001

Table 2.5. Continued

Family	Regression equation	r^2	p
Hipposideridae	Y = 3.811X – 4.415	0.891	< 0.0001
Molossidae	Y = 2.045X – 2. 142	0.946	0.149
Rhinolophidae	Y = 4.613X – 5.609	0.927	0.001
Vespertilionidae	Y = 4.394X – 4.843	0.728	< 0.0001
(D) Log maximum bite force vs. log head width			
Across species	Y = 2.454X – 2.046	0.584	< 0.0001
Hipposideridae	Y = 3.939X – 3.696	0.913	< 0.0001
Molossidae	Y = 1.362X – 0.877	0.935	0.165
Rhinolophidae	Y = 4.856X – 4.678	0.757	0.011
Vespertilionidae	Y = 3.719X – 3.225	0.587	0.004
(E) Log maximum bite force (N) vs. log head height (mm)			
Across species	Y = 2.593X - 2.060	0.614	< 0.0001
Hipposideridae	Y = 3.233X – 2.718	0.794	0.001
Molossidae	Y = 1.383X – 0.816	0.936	0.162
Rhinolophidae	Y = 4.396X – 3.897	0.810	0.006
Vespertilionidae	Y = 4.285X - 3.649	0.762	0.0001

Mechanistic Link to Bite Performance

We identified a positive, significant correlation between residual maximum bite force (size-independent bite force) and residual mechanical advantage (size-independent mechanical advantage) for all muscle complexes at all three function points tested. However, only the suprazygomatic portion of the temporalis muscle at the molar functional point ($\beta_1 = 0.625$, $p < 0.0001$) was needed to predict maximum bite force across the assemblage (model $F_{1,27} = 75.210$, $r^2 = 0.736$, $p < 0.0001$) (Fig 2.4). At the family level, residual data for Hipposideridae and Rhinolophidae were extracted from the regression of body mass with maximum bite force (size-independent bite force) and the regression of body mass with all mechanical advantage ratios calculated for all muscles complexes at all function points (size-independent mechanical advantage). Size-independent bite force and mechanical advantage were similarly derived for the Vespertilionidae but using the relationship with head height. There were significant, positive correlations between residual maximum bite force and residual mechanical advantage for the superficial portion of the masseter muscle at the molar and incisor function points in Rhinolophidae. When the stepwise method was used, a significant model emerged ($F_{1,4} = 15.670$, $r^2 = 0.797$, $p = 0.017$) with residual mechanical advantage for the superficial portion of the masseter muscle at the incisor function point ($\beta_1 = 0.893$, $p = 0.017$) as the only significant variable (Fig. 2.5). In Vespertilionidae, the residual mechanical advantage of both the superficial portion of the masseter muscle at the molar function point and the suprazygomatic portion of the temporalis muscle at the canine function point correlated with size-independent bite force in linear regressions. However,

only the residual mechanical advantage of the superficial portion of the masseter muscle at the molar function point was retained in the multiple regression ($\beta_1 = 0.635$, $p = 0.036$; model ($F_{1,9} = 6.086$, $r^2 = 0.379$, $p = 0.036$)) (Fig. 2.6). The Hipposideridae returned no statistically significant model for any variable tested.

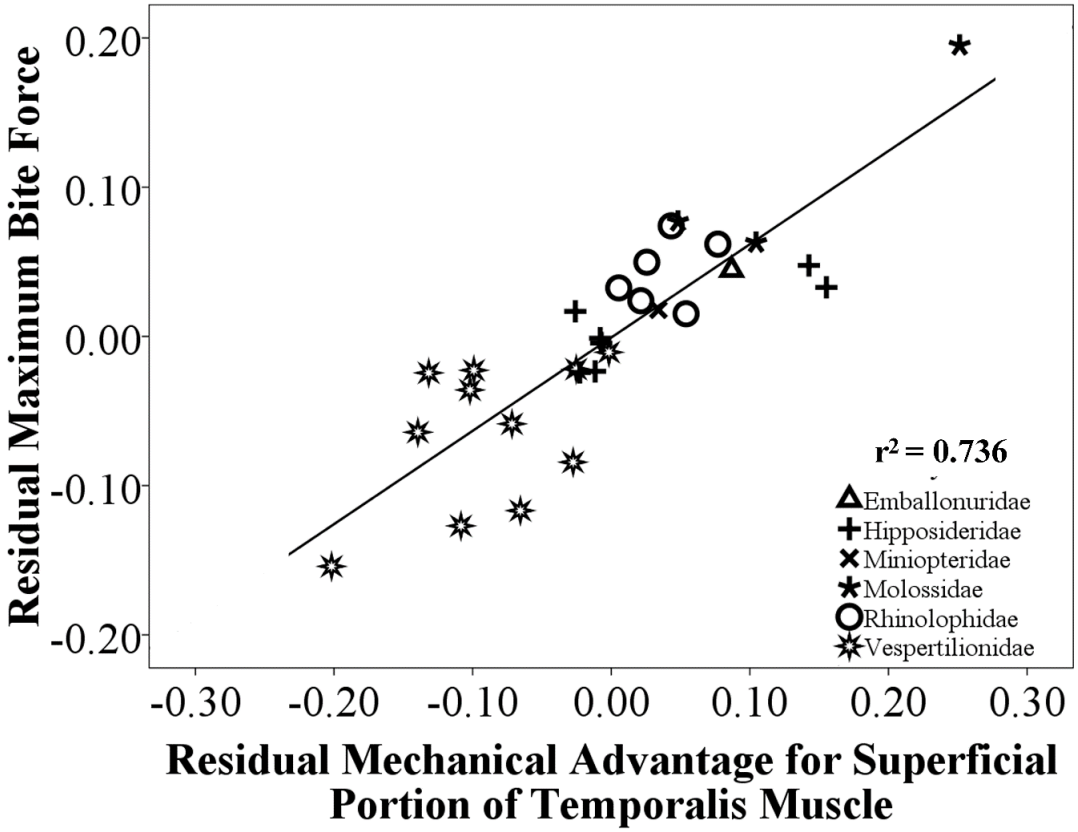

Figure 2.4. Relationship between residual maximum bite force and residual mechanical advantage for suprazygomatic portion of temporalis muscle at molar function point across 29 species of insectivorous bats from Krau Wildlife Reserve, Malaysia; $Y = 0.625X - 0.001$, $p < 0.0001$.

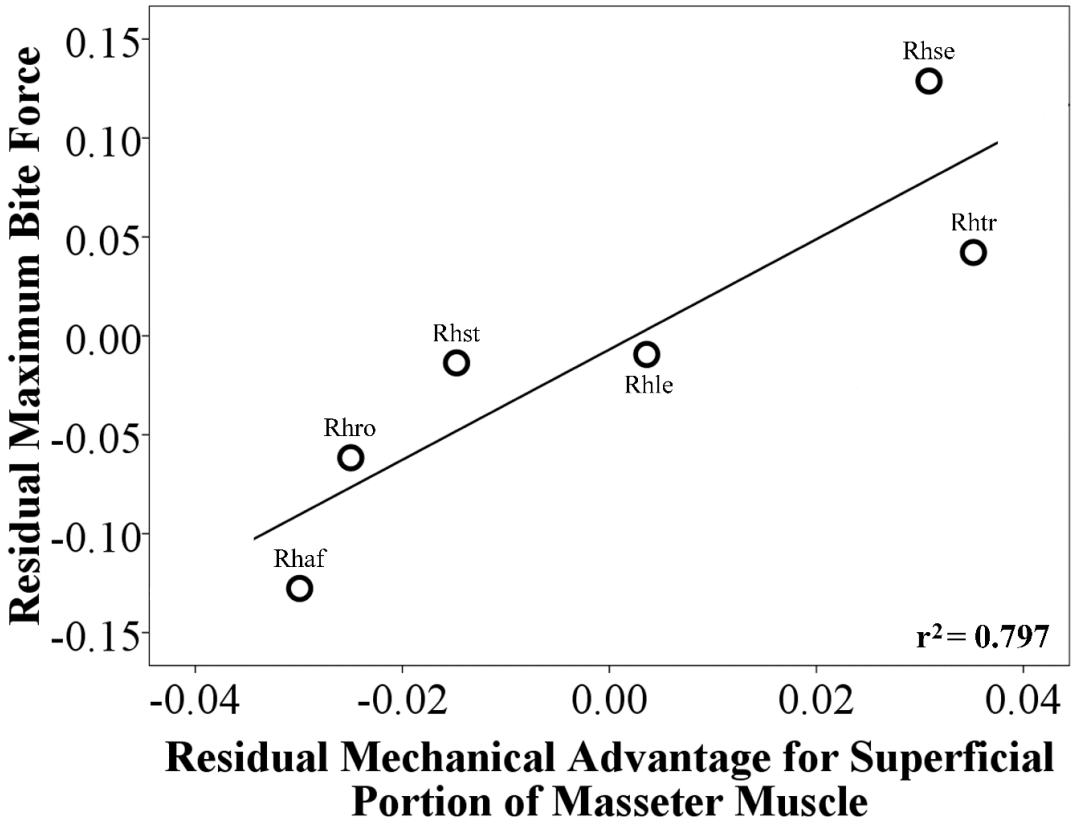

Figure 2.5. Relationship between residual maximum bite force and residual mechanical advantage for superficial portion of masseter muscle at the incisor function point for family Rhinolophidae; Y = 2.788X – 0.007, p = 0.017. Rhaf = *Rhinolophus affinis*, Rhle = *R. lepidus*, Rhro = *R. robinsoni*, Rhse = *R. sedulus*, Rhst = *R. stheno* and Rhtr = *R. trifoliatus.*

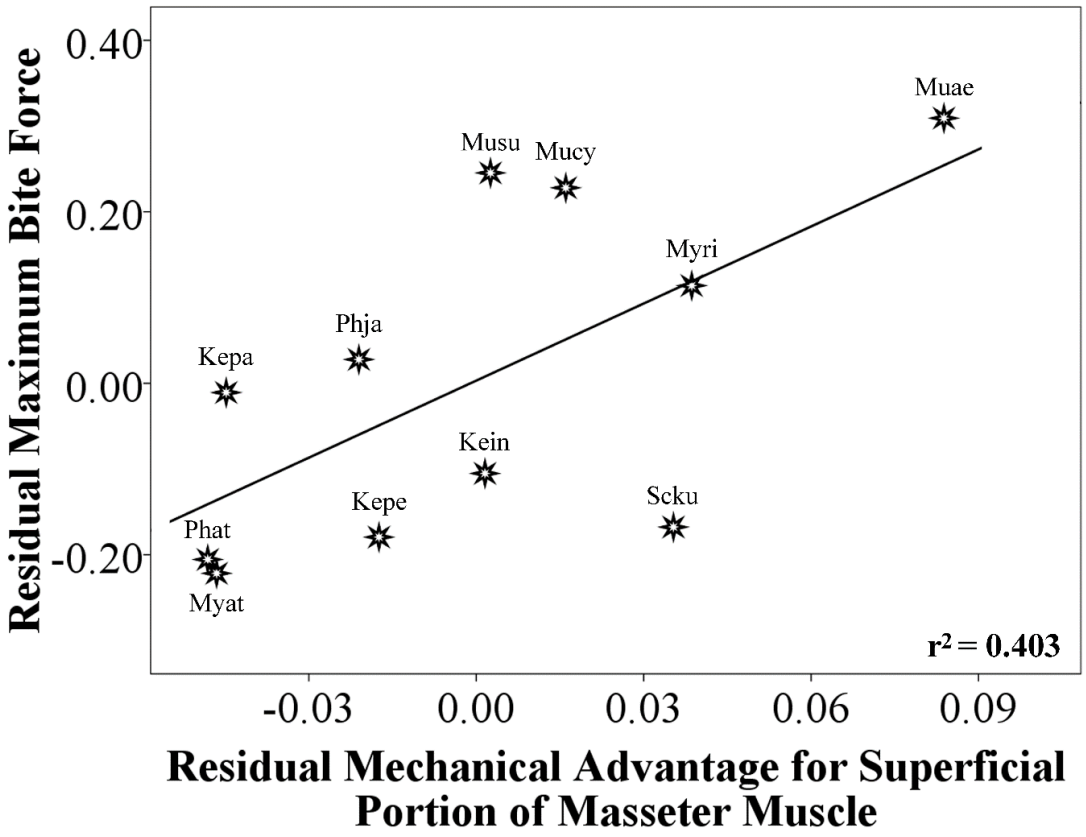

Figure 2.6. Relationship between residual maximum bite force and residual mechanical advantage for superficial portion of masseter muscle at molar function point for family Vespertilionidae; Y = 2.997X + 0.003, p = 0.036. Kein = *Kerivoula intermedia*, Kepa = *K. papillosa*, Kepe = *K. pellucida*, Phat = *Phoniscus atrox*, Phjo = *P. jagorii*, Muae = *Murina aenea*, Mucy = *M. cylotis*, Musu = *M. suilla*, Myat = *Myotis ater*, Myri = *M. ridleyi* and Scku = *Scotophilus kuhlii*.

Discussion

Bite force of insectivorous bats from our studied assemblage is strongly correlated with size. Measures of size in this study included forearm length, body mass and head dimensions, each of which was positively correlated with bite force. In other words, bigger bats can bite harder. However, measures of size only explained 43.8 – 64.4 % of the variance in bite force across the assemblage and our findings suggest both an effect of phylogeny, with more variance explained by size when species were analyzed by family, and size-independent mechanical advantage.

Overall, head length was the best predictor of bite force at the assemblage level (64.4 % of bite force variance), but in the four families tested separately, body mass was the best predictor in the Hipposideridae and Rhinolophidae, head height in the Vespertilionidae, while for Molossidae none of the variables tested could be used to predict maximum bite force. Bite force is strongly correlated with body size in most vertebrates studied, including opossums, felids, canids (Thomason 1991), bats (Aguirre et al. 2002; Herrel et al. 2008) and lizards (Broeckhoven & Mouton 2014) and our study suggests that this relationship holds in the Old World bat families Rhinolophidae, Hipposideridae and Vespertilionidae.

At the assemblage-level, at least 35.6 % of the variance in bite force was unexplained by the main size predictor (head length). The potential role of phylogeny in explaining bite force across species within an assemblage is demonstrated by the much stronger relationships between size variables and bite force when species were grouped by family. For example, variance in bite force explained by size in Rhinolophidae ranged

from 75.7 % (head width) to 94.3 % (body mass) and in the Hipposideridae ranged from 79.4 % (head height) to 91.8 % (body mass). Small hipposiderids and rhinolophids (FA ≤ 45 mm and M ≤ 10 g) were very similar in bite force, but the families diverged at larger sizes, with Rhinolophidae biting slightly harder than same-sized Hipposideridae. As sister taxa, Hipposideridae and Rhinolophidae are expected to exhibit similar relationships between bite force and size because of the phylogeny constrains on the phenotype (Losos 2008; Agnarsson et al. 2011). Unexplained variance in Vespertilionidae remained relatively high (from 23.8 - 50.0 %), likely due to this family being composed of three subfamilies: Kerivoulinae, Murininae and Vespertilioninae. In contrast, the lack of significant linear relationships between bite force and size variables in Molossidae may reflect the limited sample size, with just three species, as well as the unusual size distribution in this family. In this study, Molossidae were represented by two species of very similar size, *Chaerephon johorensis* and *Mops mops* and the largest aerial-hawking bat species in the world, *Cheiromeles torquatus*. Interestingly, whereas bite force in *C. torquatus* and *M. mops* conformed to that predicted by the assemblage relationships of forearm length and bite force, bite force of *C. johorensis* was c. 3 N greater than predicted for its forearm length, suggesting a possible means of ecological separation from *Mops mops.*

Even when limiting the effects of phylogeny by inspecting size relationships within families, 5.7 - 50.0 % of bite force variance remained unexplained by size variables measured. The size-independent mechanical advantage for each of the five mandible lever systems (three delineated by the temporalis muscle and two by the

masseter muscle) operating through three function points (molar, canine, and incisor) were significantly correlated to size-independent bite force. In this study, bats with shorter out-lever arms and hence greater mechanical advantage, can generate greater bite force. Conversely, bats with longer out-lever arms produce a lower bite force because mechanical advantage is reduced. However, following the law of equilibrium as applied to levers, and assuming that other muscle traits were equal among species in this study, the speed at which a load moves (output force applied) increases with the length of the out-lever. This is the speed mechanical advantage, and in biting systems it equates to how fast the tooth is moving at the function point. Speed advantage results in a more rapid movement or rotation of the jaws created by the mandibular lever mechanism during biting. Whereas higher mechanical advantage may facilitate processing a hard food more efficiently, speed advantage may benefit species that need to process their food with faster biting motions. Insectivorous bats of Krau Wildlife Reserve feed on a wide variety of insects ranging from soft-bodied (e.g. Lepidoptera, Isoptera, Diptera) to hard-bodied prey (e.g. Coleoptera) (Kingston at al. 2006). Such prey types require different methods for efficient consumption, thus leading to an ecological trade-off between prey hardness and biting speed. Bat species that consume aerial soft-bodied insects, such as moths, do not require a high bite force, but rapid and repeated biting may help immobilize fluttering prey. On other hand, the exoskeleton of hard-bodied insects requires greater force to process, thus higher bite force is more advantageous than speed when consuming hard-bodied insects, such as beetles. The evidence for this trade-off between mechanical advantage (force) and speed advantage in animal levers has been reported in jaw systems

among species of fish (Westneat 2003, 2004; Wainwright 2004), hindlimb locomotion in frogs (Roberts & Marsh 2003), and crab chelae (Levinton & Allen 2005).

In the Rhinolophidae and Vespertilionidae, lever systems associated with the superficial portion of the masseter muscle played significant roles in generating size-independent bite force in both families. However, in the Vespertilionidae, the molar function point, which corresponds to the shortest out-lever arm of the three function points, provided the best location of the force contrasting with the Rhinolophidae in which it was the incisor function point (longest out-lever arm). Not only might this explain the greater bite force generated by vespertilionids, but it provides insights into possible differences in food processing and diet hardness preferences of these two families. We predict that Vespertilionidae may process their food more efficiently by creating higher bite force, whereas Rhinolophidae may process their food more efficiently by creating rapid biting action.

Among the lever systems, the size-independent mechanical advantage of the suprazygomatic portion of the temporalis muscle at the molar function point was the best predictor, explaining 73.6 % of the 35.6 % variance unexplained by head length for the insectivorous bats assemblage. This indicates the importance of the temporalis muscle in bite force production in bats, as found by Herrel et al. (2008). However, the mechanical advantage levers associated with the masseter muscle were most important in explaining variation in measured bite force when bats were grouped by family. This is similar with Santana et al.'s (2010) findings for muscle contributions to bite force based on the physiological cross-sectional areas of all major cranial muscles. Across phyllostomids,

the moment generated by masseter muscle best predicted bite force at canine and molar function points. However, when phyllostomids were grouped by the mechanical challenge imposed by food (liquid, soft, medium, hard and very hard), the temporalis muscle proved to be most important in generating bite force in bats with hard and very hard diets, and the masseter muscle played the major role in processing of soft diets. Interestingly, there was no correlation between total moment generated at any of the muscles measured (temporalis, masseter, medial pterygoid and lateral pterygoid) and bite force in the insectivorous bats (medium diets) (Santana et al. 2010). In the present study, we found no significant relationship between size-independent mechanical advantage and bite force in Hipposideridae, suggesting a role for other factors such as skull shape and muscle anatomy (see Reduker 1983; Nogueira et al. 2009; Santana et al. 2010).

Previous studies on bats have shown that bite force is associated with food hardness (Dumont 1999; Aguirre et al. 2003). In the diets of both insectivorous and frugivorous phyllostomid bats from the neotropics, there is a strong and positive correlation between food dimensions or mass (size) and maximum force needed to crush the food (Dumont 1999; Aguirre et al. 2003). Coleoptera (beetles) are the hardest arthropods consumed by bats, and beetle hardness increases with their size (Freeman 1979; Aguirre et al. 2003). Aguirre et al. (2003) reported that only larger species of insectivorous bats tested (forearm length: 59.7 - 78.3 mm) included beetles > 15 mm in size in their diet. Similarly, Dumont (1999) demonstrated that hard fruit (e.g. figs) require more force to break down than soft fruit (e.g. papaya). These studies suggest that larger bats are able to process bigger and harder food items (e.g. figs, large beetles). This could

lead to specialization and/or preference for such food in larger bat species, but could also increase overall dietary diversity by expanding the size and hardness range of items that can be processed.

Dietary specialization and preferences may allow for resource partitioning in complex tropical systems. Our study strongly suggests that the phylogentically constrained relationships between bite force, body size and food hardness provide a niche dimension by which food resources can be partitioned within an assemblage. First, within families in the assemblage, bigger bats should be able to take larger and harder prey. Second, species of similar size but from different families will differ in bite force. For example, based on our observed relationships, a bat with forearm length of 45 mm would have a bite force of 7.9 N if it were a vespertilionid, 5.0 N if a molossid, 2.8 N if a rhinolophid, 2.5 N if a hipposiderid and 1.25 N if an emballonurid.

In conclusion, size plays a major role in determining bite force within bat assemblages and provides a mechanism by which complex assemblages may partition food resources. Size is not the only factor however; the mechanical advantage generated by the mandibular lever systems makes a contribution independent of size, and provides insights into the trade-offs between bite force and biting speed that may influence prey selection and manipulation.

Literature Cited

Agnarsson, I., Zambrana-Torrelio, C.M., Flores-Saldana, N.P. & May-Collado, L.J. (2011) A time-calibrated species-level phylogeny of bats (Chiroptera, Mammalia). *PLoS Currents*. doi: 10.1371/currents.RRN1212.

Aguirre, L.F., Herrel, A., Van Damme, R. & Matthysen, E. (2002) Ecomorphological analysis of trophic niche partitioning in a tropical savannah bat community. *Proceeding of the Royal Society of London Series B-Biological Sciences*, **269**, 1271-1278.

Aguirre, L.F., Herrel, A., Van Damme, R. & Matthysen, E. (2003) The implications of food hardness for diet in bats. *Functional Ecology*, **17**, 201-212.

Anderson, R.A., McBrayer, L.D. & Herrel, A. (2008) Bite force in vertebrates: opportunities and caveats for use of a nonpareil whole-animal performance measure. *Biological Journal of the Linnean Society*, **93**, 709-720.

Anwarali Khan, F.A., Solari, S., Swier, V.J., Larsen, P.A., Abdullah, M.T. & Baker, R.J. (2010) Systematics of Malaysian woolly bats (Vespertilionidae: Kerivoula) inferred from mitochondrial, nuclear, karyotypic and morphological data. *Journal of Mammalogy*, **91**, 1058-1072.

Berwaerts, K., Van Dyck, H. & Aerts, P. (2002) Does flight morphology relate to flight performance? An experimental test with the butterfly *Pararge aegeria*. *Functional Ecology*, **16**, 484-491.

Bourke, J., Wroe, S., Moreno, K., McHenry, C. & Clausen, P. (2008) Effects of gape and tooth position on bite force and skull stress in the dingo (*Canis lupus dingo*) using a 3-dimensional finite element approach. *PLoS ONE* **3**(5): e2200.

Broeckhoven, C. & Mouton, P.F.N. (2014) Under pressure: morphological and ecological correlates of bite force in the rock-dwelling lizards *Ouroborus cataphractus* and *Karusasaurus polyzonus* (Squamata: Cordylidae). *Biological Journal of the Linnean Society*, **111**, 823-833.

Cakenberghe, V.V., Herrel, A & Aguirre, L.F. (2002) Evolutionary relationships between cranial shape and diet in bats (Mammalia: Chiroptera). *Topics in functional and ecological vertebrate morphology* (eds P. Aerts, K. D'Août, A. Herrel & R. Van Damme), pp. 205-236. Shaker Publishing, Maastricht.

Currey, J. (1984) *The mechanical adaptations of bones*. Princeton, New Jersey.

Davis, J.L., Santana, S.E., Dumont, E.R. & Grosse, I.R. (2010) Predicting bite force in mammals: two-dimensional versus three-dimensional lever models. *Journal of Experimental Biology*, **213**, 1844-1851.

De Winter, J.C.F. (2013) Using the Student's t-test with extremely small sample sizes. *Practical Assessment, Research & Evolution*, **18**(10). http://pareonline.net/getvn.asp?v=18&n=10.

Dumont, E.R. (1999) The effect of food hardness on feeding behavior in frugivorous bats (Phyllostomidae): an experimental study. *Journal of Zoology*, **248**, 219-229.

Dumont, E.R., Dávalos, L.M., Goldberg, A., Santana, S.E., Rex, K. & Voigt, C.C. (2012) Morphological innovation, diversification and invasion of a new adaptive zone. *Proceedings of the Royal Society*, **279**, 1797-1805.

Dumont, E.R. & Herrel, A. (2003) The effects of gape angle and bite point on bite force in bats. *Journal of Experimental Biology*, **206**, 2117-2123.

Dumont, E.R., Samadevam, K., Grosse, I. Warsi, O.M., Baird, B. & Davalos, L.M. (2014) Selection for mechanical advantage underline multiple cranial optima in New World leaf-nosed bats. *Evolution*, **68**, 1436-1449.

Dumont, E.R & Swartz, S.M. (2009) Biomechanical approaches and ecological research. *Ecology and behavioral methods for the study of bats* (eds T.H. Kunz & S. Parsons) pp. 436-458. The Johns Hopkins University Press. Baltimore.

DWNP-DANCED (2001) *Krau Wildlife Reserve management plan*. Department of Wildlife and National Parks, Kuala Lumpur.

Erickson, G.M., Lappin, A.K. & Van Vliet, K.A. (2003) The ontogeny of bite-force performance in American alligator (*Alligator mississippiensis*). *Journal of Zoology*, **260**, 317-327.

Francis, C.M. (1989) A comparison of mist-nets and two designs of harp-traps for capturing bats. *Journal of Mammalogy*, **70**, 865-870.

Freeman, P.W. (1979) Specialized insectivory: beetle-eating and moth-eating molossid bats. *Journal of Mammalogy*, **60**, 467-479.

Freeman, P.W. (2000) Macroevolution in microchiroptera: Recoupling morphology and ecology with phylogeny. *Evolutionary Ecology Research*, **2**, 317-335.

Greaves, W.S. (2012) *The mammalian jaw: a mechanical analysis*. Cambridge University Press

Hedges, L.V. (1981). Distribution theory for Glass's estimator of effect size and related estimators. *Journal of Educational Statistics*, **6**, 107-128.

Herrel, A., De Smet, A., Aguirre, L.F. & Aerts, P. (2008) Morphological and mechanical determinants of bite force in bats: do muscles matter? *Journal of Experimental Biology*, **211**, 86-91.

Herrel, A. & O'Reilly, J.C. (2006) Ontogenetic scaling of bite force in lizards and turtles. *Physiological and Biochemical Zoology*, **79**, 31-42.

Hodgkison, R., Balding, B.T., Zubaid, A. & Kunz, T.H. (2004) Habitat structure, wing morphology, and the vertical stratification of Malaysian fruit bats (Megachiroptera: Pteropodidae). *Journal of Tropical Ecology*, **20**, 667-673.

Husak, J.F., Lappin, A.K., Fox, S.F., Lemos-Espinal, J.A. (2006) Bite force performance predicts dominance in male venerable collared lizards (*Crotaphytus antiquus*). *Copeia*, 301-306.

Kingston, T., Francis, C.M., Zubaid, A. & Kunz, T.H. (2003) Species richness in an insectivorous bat assemblage from Malaysia. *Journal of Tropical Ecology*, **19**, 67-79.

Kingston, T. Lim, B.L. & Zubaid, A. (2006) *Bats of Krau*. Penerbit Universiti Kebangsaan Malaysia, Bangi.

Koehl, M.A.R. (1996) When does morphology matter? *Annual Review of Ecology, Evolution and Systematic*, **27**, 507-542.

Kunz, T.H., Hodgkison, R. & Weise, C. (2009) Methods of capturing and handling bats. *Ecological and behavioral methods for the study of bats* (eds T.H. Kunz & S. Parsons), pp 3-35. The John Hopkins University Press, Baltimore.

Levinton, J.S. & Allen, B.J. (2005) The paradox of the weakening combatant trade-off between closing force and gripping speed in a sexually selected combat structure. *Functional Ecology*, **19**, 159-165.

Losos, J.B. (1990) The Evolution of form and function: Morphology and locomotor performance in West India *Anolis* lizards. *Evolution*, **44**, 1189-1203.

Losos, J.B. (2008) Phylogenetic niche conservatism, phylogenetic signal and the relationship between phylogenetic relatedness and ecological similarity among species. *Ecology Letters*, **11**, 995-1007.

Nogueira, M.R., Peracchi, A.L. & Monteiro, L.R. (2009) Morphological correlates of bite force and diet in the skull and mandible of phylostomid bats. *Functional Ecology*, **23**, 715-723.

Reduker, R.E. (1983) Functional analysis of the masticatory apparatus in two species of *Myotis*. *Journal of Mammalogy*, **62**, 277-286.

Roberts, T.J. & Marsh, R.L. (2003) Probing the limits to muscle-powered accelerations: lessons from jumping bull-frogs. *Journal of Experimental Biology*, **206**, 2567-2580.

Santana, S.E., Dumont, E.R & Davis, J.L. (2010) Mechanics of bite force production and its relationship to diet in bats. *Functional Ecology*, **24**, 776-784.

Struebig, J.M., Kingston, T., Zubaid, A., Adura, M.A. & Rossiter, J.R. (2008) Conservation value of forest fragments to Palaeotropical bats. *Biological Conservation*, **141**, 2112-2126.

Student. (1908) The probable error of the mean. *Biometrika*, **6**, 1-25.

Swartz, S.M., Freeman, P.W. & Stockwell, E.F. (2003) Ecomorphology of bats: comparative and experimental approaches relating structure design to ecology. *Bat ecology* (eds T.H. Kunz & M.B. Fenton) pp. 257-300. The University of Chicago Press, Chicago.

Thomason, J.J. (1991) Cranial strength in relation to estimated biting forces in some mammals. *Canadian Journal of Zoology*, **69**, 2326-2333.

Verwaijen, D., Van Damme, R. & Herrel, A. (2002) Relationships between head size, bite force, prey handling efficiency and diet in two sympatric lacertid lizards. *Functional Ecology*, **16**, 842-850.

Wainwright, P.C. Bellwood, D.R., Westneat, M.W., Grubich, J.R. & Hoey, A.S. (2004) A functional morphospace for the skull of labrid fishes: patterns of diversity in a complex biomedical system. *Biological Journal of the Linnean Society*, **82**, 1-25.

Wainwright, P.C. & Reilly, S.M. (1994) *Ecological Morphology Integrative Organismal Biology*. The University of Chicago Press, Chicago.

Westneat, M.W. (2003) A biomechanical model for analysis of muscle force, power output and lower jaw motion in fishes. *Journal of Theoretical Biology*, **223**, 269-281.

Westneat, M.W. (2004) Evolution of levers and linkages in the feeding mechanisms of fishes. *Journal of Integrative and Comparative Biology*, **44**, 378-389.

Zani, P.A. (2000) The comparative evolution of lizard claw and toe morphology and clinging performance. *Journal of Evolutionary Biology*, **13**, 316-325.

CHAPTER III

MUSCLE STRESS AND BITE FORCE ESTIMATION IN INSECTIVOROUS BATS

Abstract

Muscle stress is the intrinsic force capacity exerted by muscle fibrils per unit cross-section area of a muscle. It is recognized as a key biomechanical property in the study of animal motion. However, it is impossible to determine *in vivo* stress of mastication muscles of bats without significant ethical implications and serious calibration problems. Current methods to determine muscle stress depend on histochemical and immunocytochemical techniques or large devices that attach directly or indirectly to the muscle of interest. Estimates of bite force in bats calculated from skull parameters (following Thomason 1990) have adopted a masticatory muscle stress value of 250 kPa based on the average value of muscle stress tested on soleus or calf muscle of cats and rats. However, masticatory muscles stress can be estimated by solving the application equation of torque on masticatory muscle when the value of *in vivo* bite force is available. Using a two-dimensional model of the skull we estimated masticatory muscle stress of 29 insectivorous bats species belonging to six families from Krau Wildlife Reserve, Malaysia. The estimation of masticatory muscles stress value of insectivorous bats was determined by rearranging and solving a bite force estimation equation by Thomason 1990. The physiological cross-section areas of temporalis and combined masseter and

medial pterygoid muscles with their lever arms were estimated from images of skulls and used in the equation. The calculated masticatory muscle stress ranged from 71.38 kPa in *Kerivoula intermedia* to 469.74 kPa in *Murina aenea*. There was positive correlation between masticatory muscle stress and mechanical advantage of the mandible lever associated with the temporalis muscles was detected across all species tested. However, relationships between masticatory muscle stress and measures of size (forearm length, body mass, head height, head length, head width, greatest skull length, braincase height and zygomatic breath) were only detected in Hipposideridae, Rhinolophidae and Vespertilionidae. We propose that future calculations of bite force in bats using Thomason's equation and 2D skull models would be improved by adopting masticatory muscle stress values determined from the family regression equations of skull size measures reported in this study.

Key-words: mechanical advantage, palaeotropical bats, physiological cross-section area (PCSA), two-dimensional skull model.

Introduction

Biomechanics, or the application of the principles of mechanics to the study of living organisms, provides insights into the evolutionary patterns and ecological success of animals. For example, the biomechanics of cranial shape and bite force (pressure or force per unit area applied by masticatory muscles during dental occlusion) in bats is linked to their dietary variation (Nogueira et al. 2009), and variability in bite force and morphology suggest mechanisms of resource partitioning and community structure (Bock 1994;

Dumont et al. 2012; Dumont et al. 2014; Juliana et al. 2015). Bats with bigger body size or bigger head size are able to produce higher bite force and factors, and species with higher values for size-independent mechanical advantage of the mandible levers, also bite harder (Juliana et al. 2015).

Bite force capacity of an animal is most often determined directly using a force transducer (e.g. type 9217 Kistler Inc., Switzerland mounted on a purpose-built holder and connected to a charger amplifier type 5995 Kistler Inc., Switzerland). It can also be estimated through a muscle lever system equation. While muscle produces force in a straight line during contraction, when muscles pull the bones, the bones do not move in straight lines, but instead rotate around joints generating force as torque (see Nigg 2007). Torque (τ) is a measure of how much force is acting on an object and causing the object to rotate, and is the product of an exerted force (F) and its lever arm (r). In biological systems, the input torque (τ_{in}) must offset the output torque (τ_{out}) of the muscle to maintain equilibrium:

$$\tau_{in} = \tau_{out}$$

$$or$$

$$F_{in} \times r_{in} = F_{out} \times r_{out} \quad (3.1)$$

Applying this to mastication, the maximum capacity of bite force produced at any bite location (F_{Bite}) is equal to the force given by the related muscle (F_{Muscle}) times the lever arm of the muscle (r_{muscle}) divided by the lever arm of the bite force or bite location (r_{Bite}). The primary muscles for mastication are the temporalis muscle, masseter muscle and

pterygoid muscles. Assuming a bilateral bite, this gives a bite force (F_{Bite}) calculated as follows:

$$F_{Bite} = \frac{(F \times r)_{temporalis} + (F \times r)_{masseter} + (F \times r)_{pterygoid}}{r_{Bite}} \quad (3.2)$$

Muscle force (F) is estimated as the muscle's physiological cross-section area (PCSA) multiplied by muscle stress (Powell et al. 1984).

$$F_{Muscle} = muscle\ stress\ \times PCSA \quad (3.3)$$

PCSA represents a total of the cross sectional areas of all muscle fibers within a given muscle (Taylor et al. 2009), and has been empirically demonstrated to be directly proportional to the maximum force that a muscle can generate (Gans & Bock 1965; Powell et al. 1984). Muscle stress or normalized force is the intrinsic force capacity exerted by muscle fibrils per unit cross-section area of a muscle (Enoka 2008).

PCSA of muscle can be estimated in 2D skull models based on the associated fossa i.e., a depression in the bone associated with the location of muscle attachment (see Davis et al. 2010). For example, the infratemporal fossa from the dorsal view of the skull was used to estimate the PCSA of the temporalis muscle. Length of the muscle lever arms influence the effectiveness with which the contraction force of a given muscle can generate a torque about the temporomandibular joint (TMJ), and can be estimated as the distance from centroid of PCSA to the mandibular fossa (Thomason 1990). However, the

more challenging task is to determine a specific muscle stress. This cannot be measured from the skull models because it requires detailed study of muscle fiber architecture i.e. structural arrangement of muscle fibers and muscle fibers length (Powell et al. 1984). The structural arrangement of muscle fibers and muscle fibers length varies within and between muscles in the same individual and among individuals as well as species (Turnbull 1970; Gans 1982; Roy et al 1991; Anapol & Barry 1996).

Previously, the estimation of muscles stress in animals was determined by the relationship between force and length and force and velocity of skeletal muscular tissues and could only be obtained in isometric conditions with the muscle maximally activated (Herzog 2007). However, because muscle stress is recognized as a key biomechanical property in the study of animal motion, several techniques and devices to measure muscle stress have been developed. Unfortunately, they are designed for humans or large animals. The devices invented typically attach directly to the muscles, e.g buckle transducers and implantable force transducers, or indirectly to the muscles (strain gauge transducers, video dimension analysis, electromyography and Hall Effect transducers (see Nigg 2007). However, none of the devices are applicable to bats, mainly due to the size of the devices in relation to the size of the bats

Values for skeletal muscle stress reported in other mammals using these methods range from 131 kPa in rat tibia muscles (gracilis antiticus muscle) (Close 1972) to 871 kPa in human triceps muscles (Hatze, 1981). Bite force studies have adopted muscle stress values from 250 kPa to 400 kPa (250 kPa in rabbit (Watson et al. 2014); 300 kPa in opossum (Thomason 1990); 370 kPa in carnivores (Christiansen & Wroe 2007); 400 kPa

in human (Hannam et al. 2008)). Previous studies of bats have similarly used a constant muscle stress value of 250 kPa probably because this is the reported average muscle stress values found within soleus or calf muscle of cats and rats (see Herzog 2007).

Torque is the cross product between force and the distance of the force from the central point about which the system turns. Although muscles produce linear forces, motions at joints are all rotary. The rotary torque is the product of the linear force and lever arm or mechanical advantage of the muscle about the joint's center of rotation. In animal body, muscles and bones act together to form levers. During biting, the mechanical advantage of the mandible lever can be determined by the ratio of the length of the lever on the input force side of the fulcrum to the length of the lever on the output force side of the fulcrum (Juliana et al. 2015). The force of the mandible lever was exerted by muscles associated with mastication. Therefore, there will be direct relationship between the mechanical advantage of the muscles and the mechanical advantage of the mandible levers.

Here we determine the masticatory muscle stress value of 29 insectivorous bat species from Krau Wildlife Reserve, Malaysia by solving the equation of Thomason (1990) using the *in vivo* bite force of the species. We hypothesized that there will be a positive relationship between muscle stress and mechanical advantage of the mandible lever that associated with masticatory muscles of the bats tested. This is because masticatory muscle stress is predicted to associate directly with bite force capacity of the bats and bite force is positively correlated with mechanical advantage of the mandible lever system of the bats (Juliana et al. 2015). Therefore species with higher mechanical

advantage or higher bite force will have higher masticatory muscle stress value. Further, we also hypothesized that that masticatory muscles stress will be directly correlated with measures of size. Bats with higher masticatory muscles stress will be bigger in size.

Materials and Methods

Specimens and muscle stress

One thousand three hundred seventy seven ethanol-preserved specimens of 29 insectivorous bats species were used for analyses. The specimens were collected from lowland rainforest of Krau Wildlife Reserve, Peninsular Malaysia, between 2002 and 2012 and were deposited at the Museum of Zoology, Universiti Kebangsaan Malaysia (UKM) (see Juliana (2015) for details of KWR and trapping protocols). Skulls were extracted and cleaned using a colony of dermestid beetles (*Dermestes maculatus*) between August and December 2011 and between June and August 2012. Skulls were photographed at lateral, dorsal and ventral views using Nikon D300 digital camera with macro lens VR105 mm F/2.8G connected to R1C1 wireless close-up speed-light system (Nikon-Malaysia Sdn. Bhd., Petaling Jaya, Selangor, Malaysia).

The estimated muscle area or physiological cross-section area (PCSA) of the temporalis muscle was based on the area of the infratemporal fossa from the dorsal view of the skull, while the PCSA of the combined masseter and medial pterygoid muscle was estimated from the area of the infratemporal fossa from the ventral view of the skull (Fig. 3.1A and 3.1B). The area of the infratemporal fossa was estimated between the posterior and anterior end of the orbital and between the most medial and lateral end of the orbit on

the right side of the skull for both temporalis and combined masseter and medial pterygoid muscles. The infratemporal fossae were outlined and their areas were calculated and the area centroids were determined. The length of the in-lever arm of the temporalis muscle (indicated as *t* in Fig. 3.1B) was determined as the distance from the temporomandibular joint (TMJ) to the estimated infratemporal area centroid of the lateral view when comparing area centroid of infratemporal fossa from dorsal and lateral views of the skull with TMJ is set at 25^{o} gape angle. The gape was set at 25^{o} angle because bats were reported to produce maximum bite force with minimum stress at this angle (Dumont & Herrel 2003; Bourke et al. 2008). The in-lever arm of the combined masseter and medial pterygoid muscles was estimated from the area centroid of the infratemporal fossa of the ventral view of the skull to the mandibular fossa of the skull (indicated as *m* in Fig. 3.1C). The out-lever arm was determined for bite point at second molar measured from the midpoint of the articular condyle to the centre of protoconid on the second lower molar (indicted as *O* in Fig. 3.1D). Estimated PCSAs, PCSAs centroids, in-lever arm and out-lever arm were measured using image processing and analysis in java - Image J version 1.48 (National Institutes of Health, Bethesda, MD, USA).

The masticatory muscles stress; *S* for each species was calculated by rearranging the estimated bite force equation from Thomason (1990);

$$Muscle\ stress; S = \frac{B \times O}{2(T \times t + M \times m)} \tag{3.4}$$

where *B* is the observed or *in vivo* maximum bite force, *T* is PCSA of temporalis muscle, *t* is the in-lever arm of the temporalis muscle, *M* is PCSA of the combined masseter and medial pterygoid muscles, *m* is the in-lever arm of the combined masseter and medial pterygoid muscles and *O* is the out-lever arm to the molar function point measured from the midpoint of the articular condyle to the center of protoconid on the second lower molar (Fig. 3.1D).

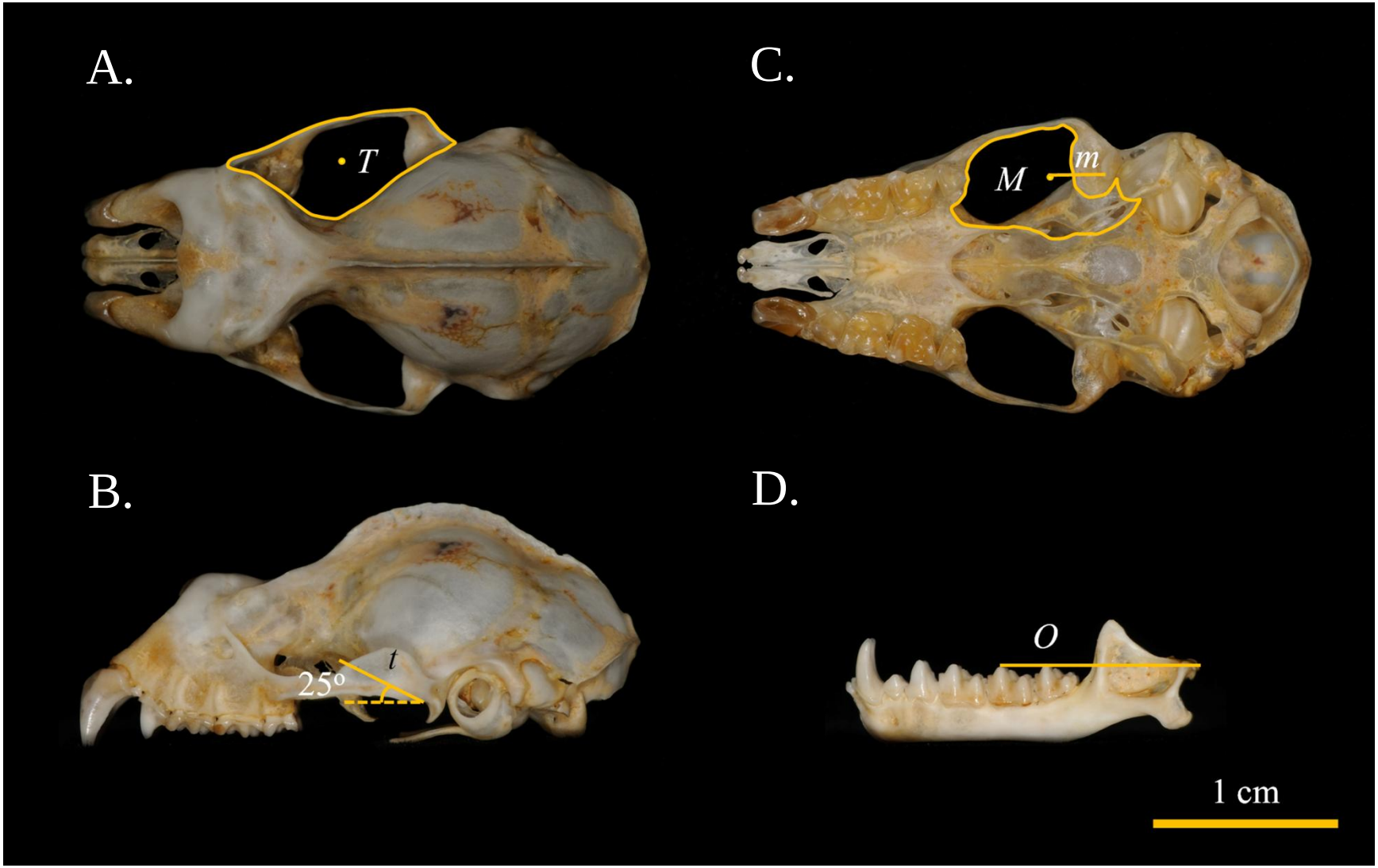
A.
T
C.
M
m
B.
25°
t
D.
O
1 cm

Figure 3.1. Estimated muscle area or physiological cross-section area (PCSA), muscle in-lever arm for both temporalis and combined masseter and medial pterygoid muscles and out-lever arm at molar function point. Centroid location of estimated PCSA for both muscles was indicated by dots. A. Dorsal view of the skull - an outline encloses the area defining the estimated PCSA of the temporalis muscle (indicted as *T*). B. Lateral view of the skull - the length of the in-lever arm of the temporalis muscle estimated at 25^{o} gape angle (indicated as *t*). C. Ventral view of the skull - an outline encloses the area defining the estimated PCSA of the combined masseter and medial pterygoid and muscle (indicted as *M*) and the length of in-lever arm of combined masseter and medial pterygoid muscle (indicted as *m*). D. Lateral view of the mandible - the length of the out-lever arm at the molar function point. Illustrated with reference to the skull of a *Hipposideros lylei.*

Maximum bite force and mechanical advantage of mandible levers

Published data of *in vivo* bite force of all 29 species studied were used for estimating the masticatory muscles stress (Juliana et al. 2015). Data were from independent samples of the same species and location. Bite force was measured using an isometric Kistler force transducer (type 9217, range ± 500N; Kistler Inc., Switzerland) connected to a Kistler charge amplifier (type 5995, Kistler Inc., Switzerland) and was measured at the molar bite point. Bite force was recorded at molars because following the mechanical principle of the lever system the largest bite force is exerted at the most posterior biting position (Greaves 2012). The mandible lever mechanical advantages of all 29 species came from Juliana et al. (2015), and were derived from the same specimens as those used in the present study. Juliana et al. (2015), derived mechanical advantage of three lever systems associated with portions of the temporalis muscle, and two with portions of the masseter muscle, with function points set to reflect output force at the molar, canine and incisor calculated. However, in this study we wanted to match muscles stress estimated from the PCSA of the temporalis, and the PCSA of combined masseter and medial ptergoid muscles and molar function point. Therefore we used the average mechanical advantage of the mandible lever associated with temporalis (suprazygomatic portion, superficial portion and medial and deep potion) and masseter muscles (superficial portion and zygomaticomadibularis portion) at the molar function point.

Masticatory muscle stress and measures of size

For each individual specimen we measured to the nearest 0.1 mm with dial calliper: greatest skull length was measured from the posterior most part of occipital to anteriormost point of the premaxillary bone; zygomatic breadth was measured at the widest point of zygomatic arches; and height of the braincase was measured from the basisphenoid and basioccipital bones to top of braincase on either side of sagittal crest (Fig. 3.2). Measurements were taken following Freeman (1981). Published data from independent sample of the same species from same location of body size (forearm length and body mass) and head dimensions (head length, head height and head with) for all 29 species were used to explore size correlation with masticatory muscle stress (Juliana et al. 2015).

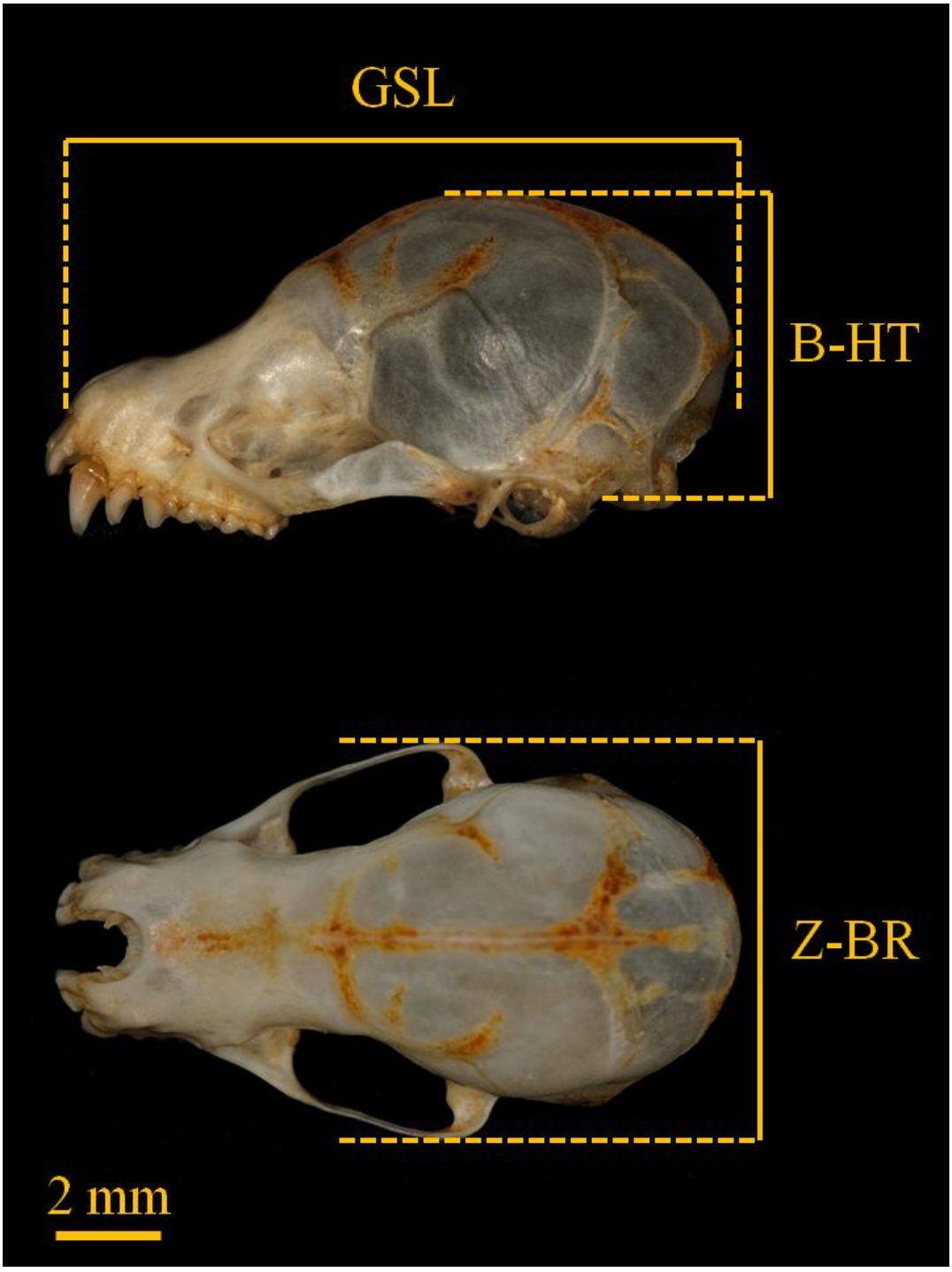

Figure 3.2. The limits of each measurement on the skull. GSL = greatest skull length, B-HT = braincase height and Z-BR = zygomatic breadth. Illustrated with reference to the skull of a *Murina cyclotis.*

Statistical analyses

We calculated species' means of physiological cross-section area (PCSA) and in-lever arms for each measured PCSA for both the temporalis muscle and combined masseter and medial pterygoid muscles before the value was applied to equation 3.4. This is because the *in vivo* bite force used came from different individual bats, so only the average of the *in vivo* bite force for the species could be used. To determine the mechanistic link between mechanical advantage of the mandible levers and masticatory muscles stress, we tested the relationship between calculated masticatory muscle stress and mechanical advantage of the mandible levers using simple linear regression analysis.

To explore which size variables best explained variation in masticatory muscles stress among species, we tested the relationship between masticatory muscle stress and size variables of the skull (skull length, zygomatic breath and height of the braincase) and size variables of the body and head (forearm length, body mass, head length, head height and head width) using simple linear regression analyses. We then ran stepwise multiple regression analysis with masticatory muscle stress as dependent variable and size measurements as independent variables. The stepwise multiple regression analysis chosen was stepwise variable selection or discriminant analysis algorithms in which the variable with the 'best' value for the criterion statistic is entered first. Because of possible correlation between skull and head size, the analyses between masticatory muscles stress and skull size and masticatory muscle stress and body and head size were run separately. Analyses were conducted at both assemblage and family level using SPSS version 17.0

statistical packages for Windows (SPSS Inc., Chicago, Illinois, USA) and all data were log transformed before analysis.

Results

Physiological cross-section area (PCSA) for both the temporalis muscle, combined masseter and medial pterygoid muscles were estimated and masticatory muscles stress were calculated for 29 species of insectivorous bats from Krau Wildlife Reserve (Table 3.1). *Cheiromeles torquatus* has the largest area of PCSA for both temporalis and combined masseter and medial pterygoid muscles with 79.65 ± 6.51 mm^2 and 74.09 ± 10.19 mm^2 (mean ± SD). *C. torquatus* is the largest aerial-hawking bat species in the world with maximum weight recorded from the study site of 190g. Meanwhile, *Miniopterus medius* and *Kerivoula intermedia* had the smallest PCSA of temporalis and PCSA of combined masseter and medial pterygoid muscles with 4.43 ± 0.97 and 6.56 ± 0.98 mm^2 respectively. The calculated masticatory muscle stress range from 71.38 kPa in *K. intermedia* to 469.74 kPa in *Murina aenea*. The family average of masticatory muscle stress f (mean ± SD) were Emballonuridae (1 species) = 159.82 kPa, Hipposideridae (7 species) = 149.70 ± 43.37 kPa, Miniopteridae (1 species) = 113.07 kPa, Molossidae (3 species) = 150.13 ± 37.28 kPa, Rhinolophidae (6 species) = 105.35 ± 23.19 kPa and Vespertilionidae; subfamilies Kerivoulinae (5 species) = 139.54 ± 59.04 kPa, Murininae (3 species) = 370.02 ± 86.91 kPa and Vespertilioninae (3 species) = 154.68 ± 59.52 kPa.

Measurements of skull size variables were completed for 451 specimens of 29 species generated from same specimen used to build a 2D skull model (Table 3.2). *C.*

torquatus had the greatest skull length, braincase height and zygomatic breath with measurements of 35.07 ± 1.76 mm, 11.70 ± 0.36 mm and 24.10 ± 1.21 mm respectively. Meanwhile *K. intermedia* had the shortest skull length, *Myotis ater* had the lowest braincase height and *Hipposideros cineraceus* the smallest zygomatic breath with measurements of 12.31 ± 0.61 mm, 4.75 ± 0.07 mm and 7.40 ± 0.28 mm respectively.

Table 3.1. Summary of the sample sizes and physiological cross-section area (PCSA) of temporalis and combined masseter and medial pterygoid muscles for 29 bat species from Krau Wildlife Reserve, Malaysia (mean ±SD). n is a number of individuals used to determine the PCSAs and lever arm of the muscle. Observed or *in vivo* maximum bite force recorded were from independent samples of the same species but from the same location (Juliana et al. in press). The calculated masticatory muscle stress of each species was determined using the mean of both PCSA muscles and observed maximum bite force of the species.

Species	**n**	**PCSA - temporalis (mm^2)**	**lever arm – temporalis (mm)**	**PCSA - masseter and pterygoid (mm^2)**	**lever arm – masseter (mm)**	**Observed maximum bite force (N)**	**Calculated muscle stress (kPa)**
Emballonuridae							
Taphozous melanopogon	18	22.17 ± 2.57	51.98 ± 4.84	24.90 ± 3.74	32.88 ± 3.42	7.78	159.82
Hipposideridae							
Hipposideros bicolor 131 kHz*	104	11.25 ± 1.36	41.35 ± 4.54	15.32 ± 2.25	25.51 ± 4.65	3.35	128.75
Hipposideros bicolor 142 kHz*	118	11.98 ± 1.40	39.68 ± 5.39	15.69 ± 1.99	24.95 ± 3.91	3.63	132.89

Table 3.1. Continued

Species	**n**	**PCSA - temporalis (mm^2)**	**lever arm – temporalis (mm)**	**PCSA - masseter and pterygoid (mm^2)**	**lever arm – masseter (mm)**	**Observed maximum bite force (N)**	**Calculated muscle stress (kPa)**
Hipposideros cervinus	232	14.16 ± 1.45	43.50 ± 4.82	16.85 ± 3.20	26.08 ± 3.92	4.30	138.48
Hipposideros cineraceus	12	6.60 ± 0.89	32.53 ± 2.19	7.61 ± 0.37	20.12 ± 1.40	1.61	114.60
Hipposideros diadema	72	63.13 ± 10.43	74.33 ± 11.22	61.15 ± 15.23	54.30 ± 7.12	24.81	184.64
Hipposideros lylei	24	39.54 ± 3.54	59.08 ± 6.38	39.59 ± 5.47	43.19 ± 2.79	16.31	232.48
Hipposideros ridleyi	6	13.64 ± 0.56	45.78 ± 3.96	18.15 ± 0.53	29.53 ± 7.66	3.74	116.05
Miniopteridae							
Miniopterus medius	120	4.43 ± 0.97	34.44 ± 5.07	8.02 ± 1.27	18.69 ± 2.10	1.32	113.07

Table 3.1. Continued

Species	**n**	**PCSA - temporalis (mm^2)**	**lever arm – temporalis (mm)**	**PCSA - masseter and pterygoid (mm^2)**	**lever arm – masseter (mm)**	**Observed maximum bite force (N)**	**Calculated muscle stress (kPa)**
Molossidae							
Chaerephon johorensis	16	17.15 ± 1.60	42.94 ± 2.75	18.56 ± 2.28	28.33 ± 2.02	4.45	140.27
Cheiromeles torquatus	8	79.65 ± 6.51	75.54 ± 7.16	74.09 ± 10.19	64.75 ± 7.62	16.41	118.77
Mops mops	18	18.94 ± 1.81	50.49 ± 5.24	20.35 ± 2.97	30.77 ± 2.04	7.06	191.34
Rhinolophidae							
Rhinolophus affinis	118	21.11 ± 2.33	50.85 ± 5.94	19.35 ± 2.39	32.50 ± 3.29	4.35	110.30
Rhinolophus Lepidus	107	10.62 ± 1.13	37.70 ± 4.40	11.28 ± 1.55	24.15 ± 1.79	1.77	81.65
Rhinolophus robinsoni	12	14.21 ± 2.60	35.73 ± 4.57	13.76 ± 1.37	26.53 ± 1.91	2.21	93.59
Rhinolophus sedulus	26	15.37 ± 1.40	38.19 ± 5.63	14.70 ± 1.81	29.00 ± 1.97	3.19	110.61

Table 3.1. Continued

Species	**n**	**PCSA - temporalis (mm^2)**	**lever arm – temporalis (mm)**	**PCSA - masseter and pterygoid (mm^2)**	**lever arm – masseter (mm)**	**Observed maximum bite force (N)**	**Calculated muscle stress (kPa)**
Rhinolophus stheno	32	15.78 ± 1.55	46.13 ± 7.04	14.50 ± 1.73	28.89 ± 1.96	2.85	89.55
Rhinolophus trifoliatus	50	24.32 ± 3.60	52.06 ± 8.66	22.04 ± 3.70	35.39 ± 2.74	6.66	146.42
Vespertilionidae							
Kerivoulinae							
Kerivoula intermedia	48	6.29 ± 0.84	26.91 ± 3.39	6.56 ± 0.98	15.98 ± 0.14	0.91	71.38
Kerivoula papillosa	85	16.45 ± 2.11	44.63 ± 4.82	18.69 ± 2.22	26.04 ± 1.93	7.38	197.92
Kerivoula pellucid	72	6.48 ± 0.83	33.05 ± 5.41	9.94 ± 1.70	18.96 ± 1.97	1.84	114.77
Phoniscus atrox	26	9.05 ± 0.93	36.13 ± 5.60	13.05 ± 2.09	22.78 ± 1.50	2.60	108.46
Phoniscus jagorii	4	12.52 ± 0.62	36.12 ± 3.39	17.87 ± 0.91	25.36 ± 0.74	6.42	205.19

Table 3.1. Continued

Species	n	PCSA - temporalis (mm^2)	lever arm – temporalis (mm)	PCSA - masseter and pterygoid (mm^2)	lever arm – masseter (mm)	Observed maximum bite force (N)	Calculated muscle stress (kPa)
Murininae							
Murina aenea	13	12.79 ± 1.70	39.78 ± 2.25	13.64 ± 0.81	28.25 ± 2.82	12.52	469.74
Murina cyclotis	12	14.17 ± 1.85	50.37 ± 5.59	18.67 ± 2.18	29.93 ± 1.76	11.90	329.97
Murina suilla	12	6.59 ± 0.39	32.11 ± 2.04	8.15 ± 0.95	20.12 ± 1.42	4.41	310.36
Vespertilioninae							
Myotis ater	6	8.76 ± 0.76	28.32 ± 0.02	9.38 ± 0.98	21.67 ± 0.92	2.44	143.95
Myotis ridleyi	12	7.92 ± 0.63	28.93 ± 1.90	8.13 ± 1.13	18.34 ± 1.18	1.38	99.62
Scotophilus kuhlii	12	23.44 ± 1.73	43.92 ± 3.08	23.41 ± 2.46	32.62 ± 3.18	9.18	217.46

*Cryptic species that were genetically and acoustically divergent and denoted as phonic types based on the mean frequency of their CF component of the call. Individual with 131 kHz was assigned as *Hipposideros bicolor* 131 kHz and individual with 142 kHz was assigned as *Hipposideros bicolor* 142 kHz.

Table 3.2. Summary of sample size, skull length, braincase height and zygomatic breath collected from 29 species of insectivorous bats. Specimens used were collected from Krau Wildlife Reserve, Malaysia (mean ±SD).

Species	n	Skull length (mm)	Braincase height (mm)	Zygomatic breath (mm)
Emballonuridae				
Taphozous melanopogon	6	20.60 ± 0.63	8.22 ± 0.55	12.20 ± 0.17
Hipposideridae				
Hipposideros bicolor 131 kHz*	32	19.00 ± 0.29	6.95 ± 0.43	9.11 ± 0.16
Hipposideros bicolor 142 kHz*	37	18.23 ± 0.47	6.78 ± 0.49	9.33 ± 0.21
Hipposideros cervinus	67	18.74 ± 0.47	6.89 ± 0.47	10.02 ± 0.22
Hipposideros cineraceus	2	16.00 ± 0.14	5.90 ± 0.00	7.40 ± 0.28
Hipposideros diadema	35	31.75 ± 0.74	10.16 ± 1.13	18.29 ± 0.64
Hipposideros lylei	8	29.53 ± 0.35	10.14 ± 0.52	15.85 ± 0.19
Hipposideros ridleyi	2	20.50 ± 0.00	7.35 ± 0.35	10.10 ± 0.00

Table 3.2. Continued.

Species	n	Skull length (mm)	Braincase height (mm)	Zygomatic breath (mm)
Miniopteridae				
Miniopterus medius	33	14.54 ± 0.62	6.68 ± 0.48	8.06 ± 0.35
Molossidae				
Chaerephon johorensis	4	19.35 ± 0.80	8.70 ± 0.59	11.43 ± 0.30
Cheiromeles torquatus	3	35.07 ± 1.76	11.70 ± 0.36	24.10 ± 1.21
Mops mops	6	20.92 ± 0.92	8.22 ± 1.13	12.58 ± 0.31
Rhinolophidae				
Rhinolophus affinis	46	22.51 ± 0.76	8.23 ± 0.78	11.71 ± 0.27
Rhinolophus Lepidus	40	17.23 ± 0.93	6.36 ± 0.59	8.46 ± 0.24
Rhinolophus robinsoni	3	21.00 ± 0.17	7.50 ± 1.14	10.00 ± 0.30

Table 3.2. Continued.

Species	n	Skull length (mm)	Braincase height (mm)	Zygomatic breath (mm)
Rhinolophus sedulus	7	19.80 ± 0.56	6.77 ± 0.42	9.74 ± 0.24
Rhinolophus stheno	9	20.43 ± 0.52	6.98 ± 0.35	9.71 ± 0.16
Rhinolophus trifoliatus	18	23.39 ± 0.49	7.64 ± 0.42	11.54 ± 0.67
Vespertilionidae				
Kerivoulinae				
Kerivoula intermedia	18	12.31 ± 0.61	4.67 ± 0.33	7.54 ± 0.46
Kerivoula papillosa	28	16.93 ± 0.98	7.18 ± 0.59	10.70 ± 0.80
Kerivoula pellucid	17	14.39 ± 0.84	6.35 ± 0.43	8.32 ± 0.80
Phoniscus atrox	6	15.10 ± 0.37	6.53 ± 0.27	8.87 ± 0.22
Phoniscus jagorii	2	17.60 ± 0.00	6.90 ± 0.14	10.70 ± 0.14

Table 3.2. Continued.

Species	n	Skull length (mm)	Braincase height (mm)	Zygomatic breath (mm)
Murininae				
Murina aenea	3	17.37 ± 0.06	7.07 ± 0.40	10.10 ± 0.70
Murina cyclotis	5	18.12 ± 0.36	7.90 ± 0.58	10.37 ± 0.13
Murina suilla	3	14.23 ± 0.06	5.97 ± 0.31	8.20 ± 0.00
Vespertilioninae				
Myotis ater	2	13.35 ± 1.34	4.75 ± 0.07	8.55 ± 0.78
Myotis ridleyi	5	12.40 ± 0.10	4.90 ± 0.21	8.26 ± 0.19
Scotophilus kuhlii	4	19.68 ± 0.67	7.00 ± 0.29	13.68 ± 0.10

*Cryptic species that were genetically and acoustically divergent and denoted as phonic types based on the mean frequency of their CF component of the call. Individual with 131 kHz was assigned as *Hipposideros bicolor* 131 kHz and individual with 142 kHz was assigned as *Hipposideros bicolor* 142 kHz.

Masticatory muscle stress and mechanical advantage of the mandible levers

Across all insectivorous bats studied, we indentified positive correlations between masticatory muscle stress and mechanical advantage of the mandible lever associated with the temporalis muscle ($F_{1,28}$ = 17.181, r^2 = 0.399, $p < 0.001$) (Fig. 3.3). This indicated that variation in masticatory muscle stress was explained by mechanical advantage of the mandible lever associated with the temporalis muscles rather than masseter muscles. When species was split into families, this relationship was only retained in the Vespertilionidae ($F_{1,10}$ = 6.011, r^2 = 0.400 , p = 0.037) (Fig 3.4).

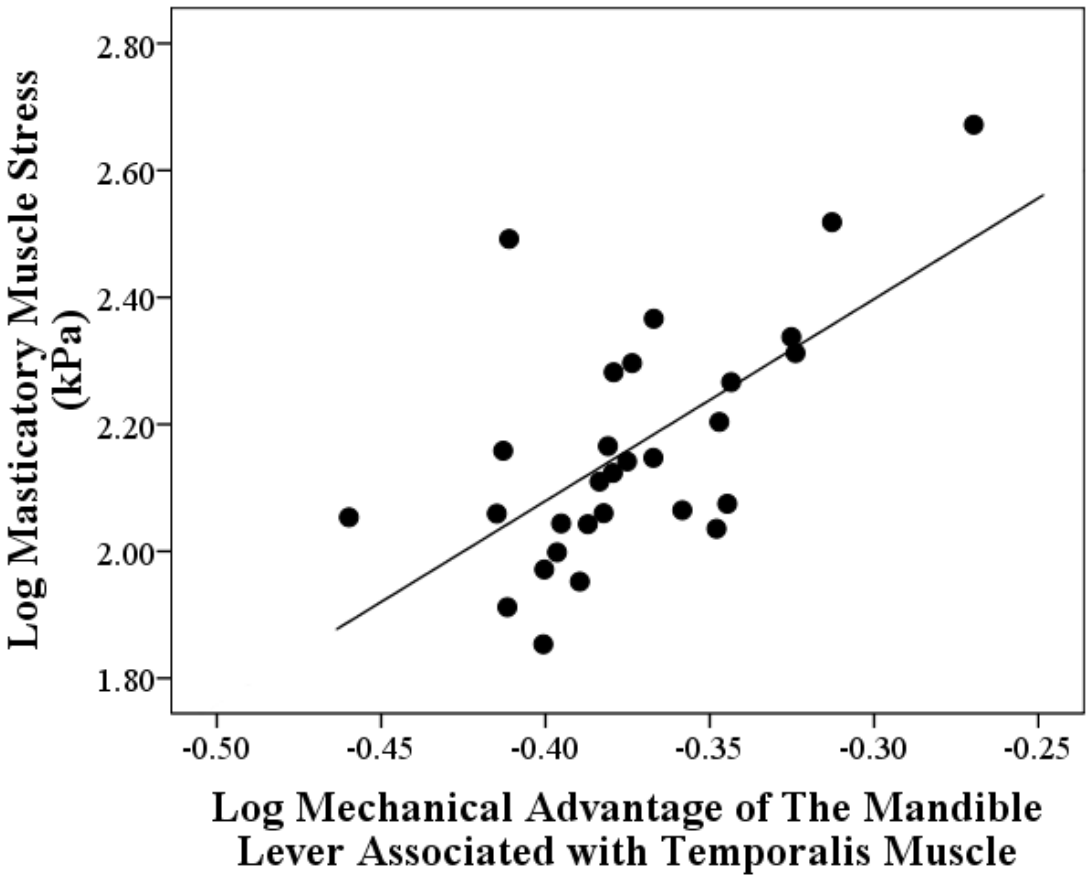

Figure 3.3. Relationship between masticatory muscle stress and mechanical advantage of the mandible lever associated with temporalis muscle across 29 species of insectivorous bats from Krau Wildlife Reserve, Malaysia. $Y = 3.181X + 3.352$, $r^2 = 0.399$.

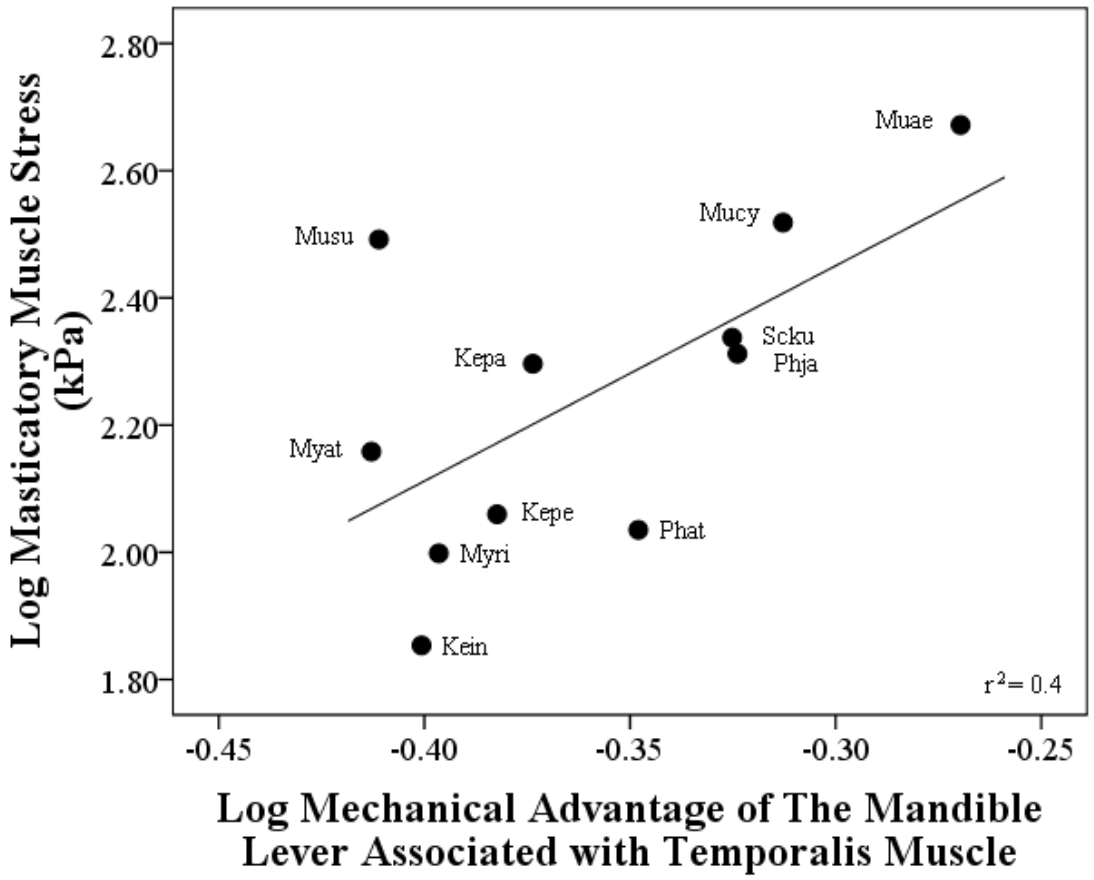

Figure 3.4. Relationship between masticatory muscle stress and mechanical advantage of the mandible lever associated with temporalis muscle for family Vespertilionidae from Krau Wildlife Reserve, Malaysia. Y = 3.386X + 3.466, p = 0.037. Kein = *Kerivoula intermedia,* Kepa = *K. papillosa,* Kepe = *K. pellucida,* Muae = *Murina aenea, M. cyclotis,* Musu = *M. suilla,* Myat = *Myotis ater,* Myri = *Myotis ridleyi,* Phat = *Phoniscus atrox,* Phja = *P. jagorii and* Scku = *Scotophilus kuhlii.*

Masticatory muscle stress and skull size

There was no evidence of correlations between masticatory muscle stress and skull size across the 29 insectivorous bats species in this study. However when the data was analyzed by family the masticatory muscles stress of Hipposideridae was showed a strong and positive correlation with all of the skull size variables tested. Between skull length ($F_{1,6}$ = 17.948, r^2 = 0.782, p = 0.008), braincase height ($F_{1,6}$ = 23.268, r^2 = 0.823, p = 0.005) and zygomatic breath ($F_{1,6}$ = 17.997, r^2 = 0.783, p = 0.008), multiple regression analysis show that the braincase height was the only significant skull size predictor of masticatory muscles stress for this family (Fig. 3.5). There also a strong and positive correlation between masticatory muscle stress and zygomatic breath ($F_{1,5}$ = 10.772, r^2 = 0.729, p = 0.030) for family Rhinolophidae (Fig. 3.6). The masticatory muscle stress in Vespertilionidae was positively correlated with greatest skull length ($F_{1,10}$ = 8.764, r^2 = 0.493, p = 0.016) and braincase height ($F_{1,10}$ = 7.714, r^2 = 0.462, p = 0.021), but greatest skull length was detected to be the best predictor variable of masticatory muscle stress (Fig. 3.7).

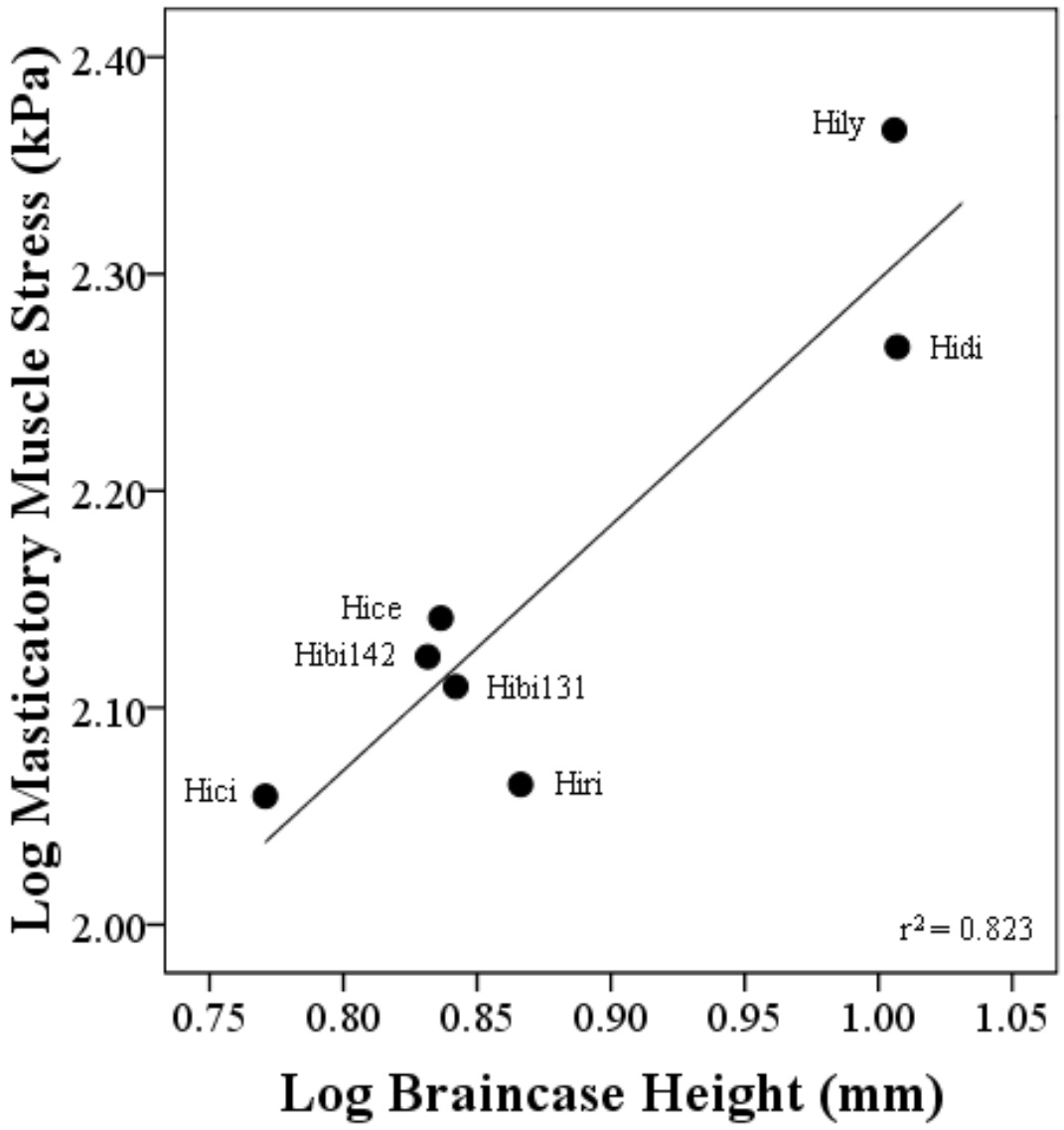

Figure 3.5. Relationship between masticatory muscle stress and braincase height for family Hipposideridae from Krau Wildlife Reserve, Malaysia. Y = 1.131X + 1.166, p = 0.005. Hibi131 = *Hipposideros bicolor* 131 kHz, Hibi142 = *Hipposideros bicolor* 142 kHz, Hice = *Hipposideros cervinus*, Hici = *Hipposideros cineraceus*, Hidi = *Hipposideros diadema*, Hily = *Hipposideros lylei* and Hiri = *Hipposideros ridleyi.*

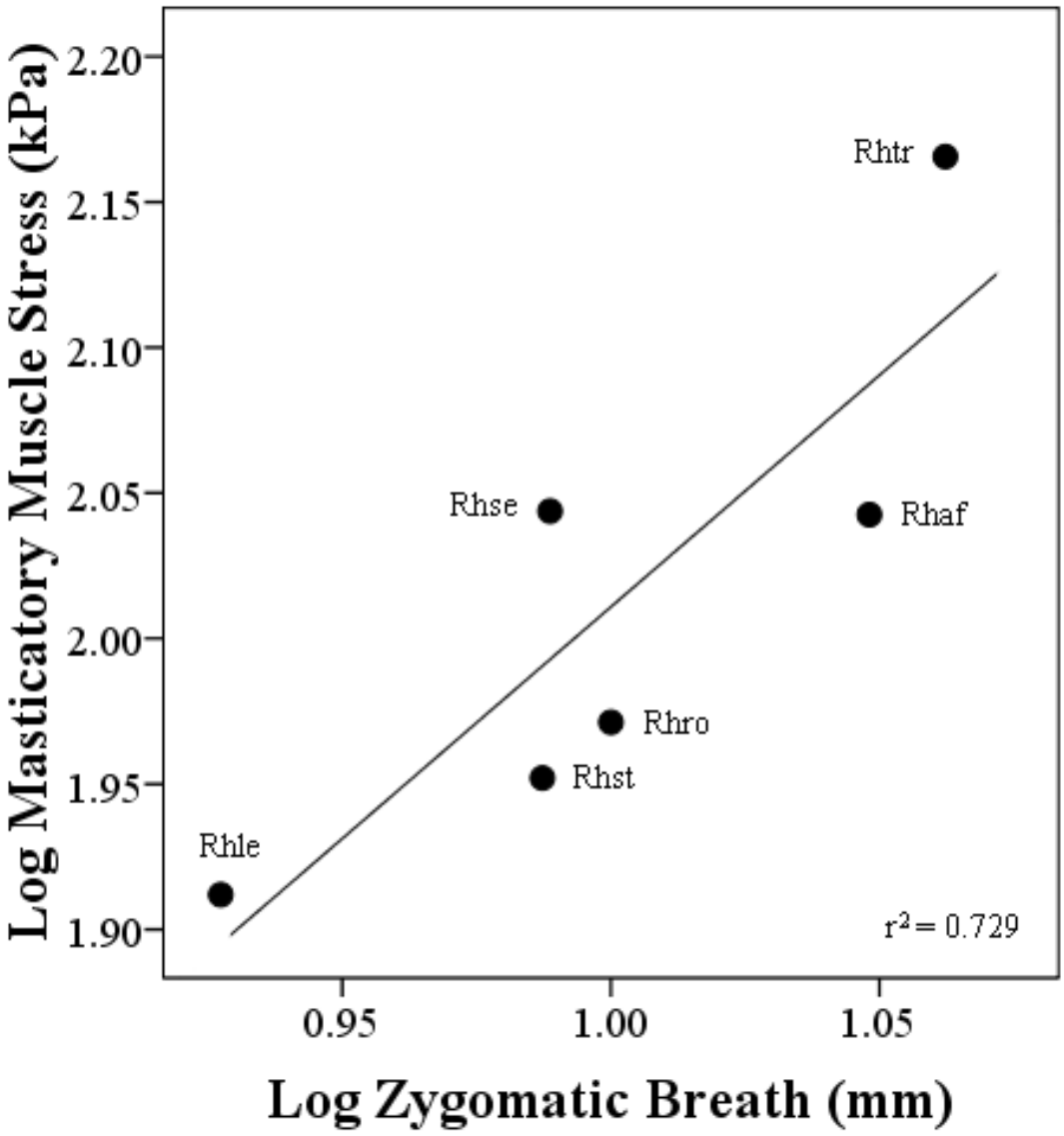

Figure 3.6. Relationship between masticatory muscle stress and braincase height across for family Rhinolophidae from Krau Wildlife Reserve, Malaysia. Y = 1.592X + 0.419, p = 0.03. *Rhaf = Rhinolophus affinis, Rhle = R. lepidus, Rhro = R. robinsoni, Rhse = R. sedulus, Rhst = R. stheno, Rhtr = R. trifoliatus.*

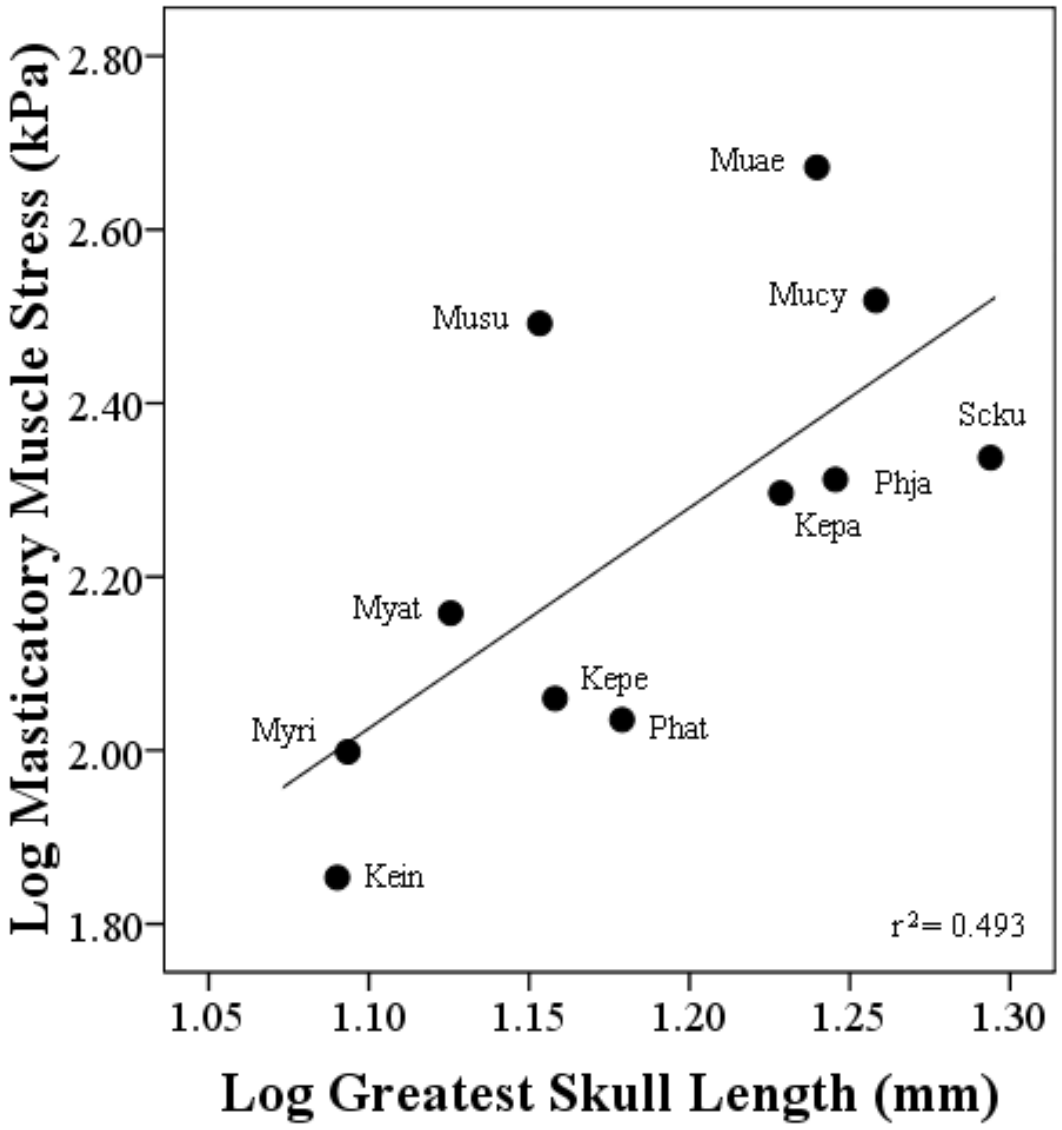

Figure 3.7. Relationship between masticatory muscle stress and braincase height for family Vespertilionidae from Krau Wildlife Reserve, Malaysia. Y = 2.541X - 0.77, p = 0.016. Kein = *Kerivoula intermedia,* Kepa = *K. papillosa,* Kepe = *K. pellucida,* Muae = *Murina aenea, M. cyclotis,* Musu = *M. suilla,* Myat = *Myotis ater,* Myri = *Myotis ridleyi,* Phat = *Phoniscus atrox,* Phja = *P. jagorii and* Scku = *Scotophilus kuhlii.*

Muscles stress, body size and head dimensions

Across all insectivorous bats studied, there was no correlation between masticatory muscle stress and body and head size variables tested. The masticatory muscles stress relationship body and a head dimension in Hipposideridae was strong and positive. Muscle stress correlated with with forearm length ($F_{1,6}$ = 21.802, r^2 = 0.813, p = 0.005), body mass ($F_{1,6}$ = 25.823, r^2 = 0.838, p = 0.004), head length ($F_{1,6}$ = 21.358, r^2 = 0.810, p = 0.006), head height ($F_{1,6}$ = 21.358, r^2 = 0.810, p = 0.006) and head width ($F_{1,6}$ = 15.981, r^2 = 0.762, p = 0.010). Using the stepwise multiple regression analysis across species of Hipposideridae, a head height was detected as the only significant predictor of masticatory muscles stress (Fig. 3.8). None of the body size and head dimensions variables tested were correlated with masticatory muscles stress for family other than Hipposideridae.

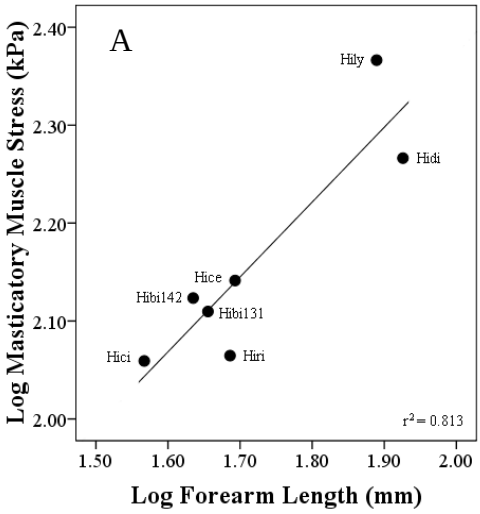
A
Log Masticatory Muscle Stress (kPa)
Log Forearm Length (mm)
Hily
Hidi
Hice
Hibi142
Hibi131
Hici
Hiri
r² = 0.813

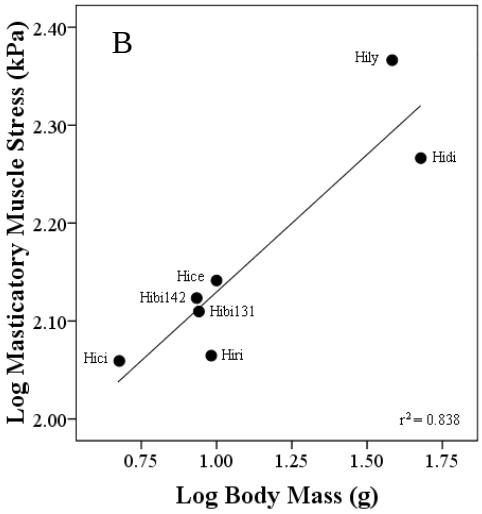
B
Log Masticatory Muscle Stress (kPa)
Log Body Mass (g)
Hily
Hidi
Hice
Hibi142
Hibi131
Hici
Hiri
r² = 0.838

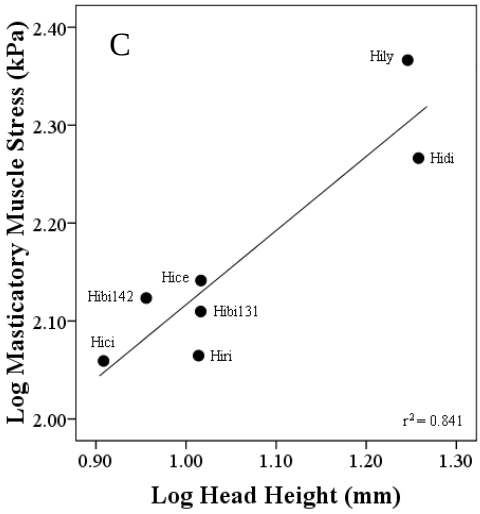
C
Log Masticatory Muscle Stress (kPa)
Log Head Height (mm)
Hily
Hidi
Hice
Hibi142
Hibi131
Hici
Hiri
r² = 0.841

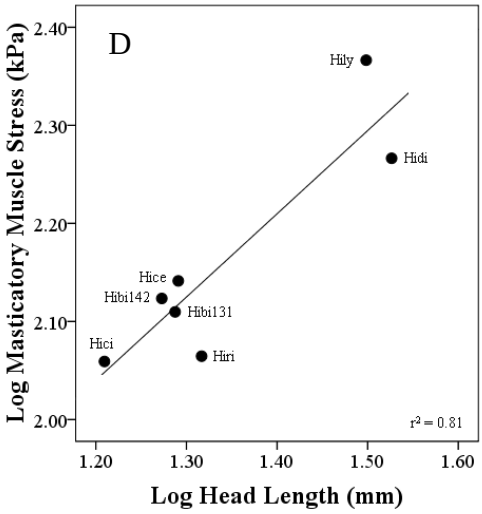
D
Log Masticatory Muscle Stress (kPa)
Log Head Length (mm)
Hily
Hidi
Hice
Hibi142
Hibi131
Hici
Hiri
r² = 0.81

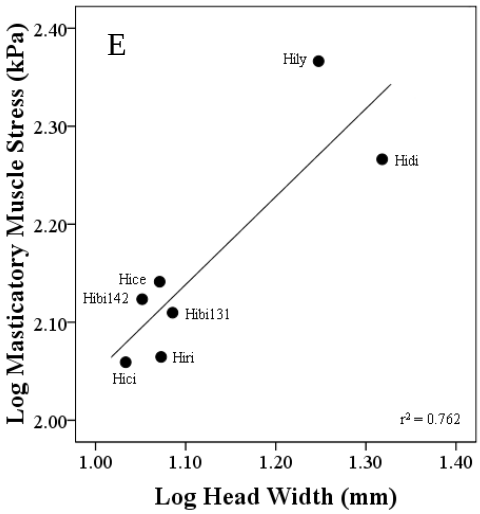
E
Log Masticatory Muscle Stress (kPa)
Log Head Width (mm)
Hily
Hidi
Hice
Hibi142
Hibi131
Hiri
Hici
r² = 0.762

Figure 3.8. The relationship between masticatory muscle stress and five external measures of size for family Hipposideridae. A) Forearm length; Y = 0.764X + 0.846, B) Body mass; Y= 0.281X + 1.849, C) Head height; Y = 0.757X + 1.36, D) Head length; Y = 0.849X + 1.022, E) Head width; Y = 0.897X + 1.152. Hibi131 = *Hipposideros bicolor* 131 kHz, Hibi142 = *Hipposideros bicolor* 142 kHz, Hice = *Hipposideros cervinus*, Hici = *Hipposideros cineraceus*, Hidi = *Hipposideros diadema*, Hily = *Hipposideros lylei* and Hiri = *Hipposideros ridleyi.*

Discussion

Masticatory muscle stress of insectivorous bats from our studied assemblage was correlated with mechanical advantage of the mandible lever associated with temporalis muscle rather than the mechanical advantage of the mandible lever associated with masseter muscle. But when families were tested separately, a similar relationship only emerged for family Vespertilionidae. A previous study of these species reported that mechanical advantage of the mandible lever associated with temporalis muscles was the best predictor variable of bite force across species with positive and significant correlations (Juliana et al. 2015). This may suggest that the masticatory muscle stress of temporalis muscle was positively corrected with the bite force. Furthermore, Herrel et al. (2008) reported that fiber length of the temporalis muscle in bats was one of the best predictor variables of bite force. Thus we conclude that muscle force contributed by the temporalis muscle is an important factor in bite force production across species.

Although there was no evidence that measures of size from skull, body and head dimensions correlated with masticatory muscle stress across the assemblage, at the family level (Hipposideridae, Rhinolophidae and Vespertilionidae) size parameters were predictive.

Studies of bite force that have directly compared *in vivo* measurements with those calculated from theoretical models, for example in reptile skulls (Curtis et al. 2013), phyllostomid bats (Davis et al. 2010), and humans (Rohrle & Pullan 2007) caution that the value of the masticatory muscles stress used was a possible source of error. Masticatory muscle stress values used in bite force estimation in bats is 250 kPa (Herrel

et al. 2008; Davis et al. 2010). Here we have shown that masticatory muscle stress in insectivorous bats from our study were range between 71.38 kPa and 469.74 kPa. Estimating the bite force using a value of 250 kPa would overestimate the bite force capacity of all families and subfamilies of insectivorous bats in this study, with the exception of the subfamily Murininae. Because of the substantial variation between 250 kPa and our calculated masticatory muscle stresses, we propose that future estimates of bite force using 2D models of the skull of paleotropical insectivorous bats use masticatory muscle stress values determined from the regression equations of skull size measures (i.e., regression equation of the braincase height for Hipposideridae, regression equation of the zygomatic breath for the Rhinolophidae and regression equation of the greatest skull length for Vespertilionidae). This provides a quick solution to improve the accuracy of estimated bite force among species within these families that has no information of *in vivo* bite force.

Calculated masticatory muscles stress value from our 2D models are only applicable when the same 2D model is used to estimate bite force. This is because different theoretical models, such as 3D or multi-body dimensions models, have different calculation restrictions and limitations. However, 2D models of the bat skulls have generated reasonable estimates of bite force in comparison to 3D models of the skull (Davis et al 2010). Prior to this study, the biggest constraint on bite force estimation through theoretical models was actual masticatory muscle stress values produce by a muscle. Here we provided a quick solution to overcome this problem; however, future efforts could focus on improving methods for direct measures of forces generated by specific muscles.

Literature Cited

Anapo, I.F. & Barry, K. (1996) Fiber architecture of the extensors of the hindlimb in semiterrestrial and arboreal guenons. *American Journal of Physical Anthropology*, **99**, 429-447.

Bock, W.J. (1994) Concepts and methods in ecomorphology. *Journal of Biosciences*, **19**, 403-413.

Bourke, J., Wroe, S., Moreno, K., McHenry, C. & Clausen, P. (2008) Effects of gape and tooth position on bite force and skull stress in the dingo (*Canis lupus dingo*) using a 3-dimensional finite element approach. *PLoS ONE,* **3**(5), e2200.

Christiansen, P. & Wroe, S. (2007) Bite forces and evolutionary adaptations to ecology in carnivores. *Ecology,* **88,** 347-358.

Close, R.I. (1972) Dynamic properties of mammalian skeletal muscle. *Physiological Review*, **52**, 129-197.

Curtis, N., Jones, M.E.H., Lappin, A.K., Higgins, P.O., Evans, S.E. & Fagan, M.J. (2010) Comparison between in vivo and theoretical bite force: using multi-body modeling to predict muscle and bite forces in a reptile skull. *Journal of Biomechanics*, **43**, 2804-2809.

Davis, J.L., Santana, S.E., Dumont ER & Grosse I.R. (2010) Predicting bite force in mammals: two-dimensional verses three-dimensional lever models. *The Journal of Experimental Biology*, **213**, 1844-1851.

Dumont, E.R., Dávalos, L.M., Goldberg, A., Santana, S.E., Rex, K. & Voigt, C.C. (2012) Morphological innovation, diversification and invasion of a new adaptive zone. *Proceedings of the Royal Society*, **279**, 1797-1805.

Dumont, E.R. & Herrel, A. (2003) The effects of gape angle and bite point on bite force in bats. *Journal of Experimental Biology*, **206**, 2117-2123.

Dumont, E.R., Samadevam, K., Grosse, I. Warsi, O.M., Baird, B. & Davalos, L.M. (2014) Selection for mechanical advantage underline multiple cranial optima in New World leaf-nosed bats. *Evolution*, **68**, 1436-1449.

Freeman, P. W. (1981) A multivariate study to a family Molossidae (Mammalia, Chiroptera): morphology, ecology, evolution. *Fieldiana (Zoology),* **7**, 1-173.

Gans, C. (1982) Fiber architecture and muscle function. *Exercise and Sport Sciences Reviews*, **10**, 160-207.

Gans, C. & Bock, W.J. (1965) The functional significance of muscle architecture - a theoretical analysis. *Advances in Anatomy, Embryology and Cell Biology*, **38**, 115-142.

Greaves, W.S. (2012) *The mammalian jaw: a mechanical analysis*. Cambridge University Press.

Hannam, A. G., Stavness, I., Lloyd, J.E., Fels, S. (2008). A dynamic model of jaw and hyoid biomechanics during chewing. *Journal of Biomechanics*, **41**, 1069 - 1076.

Hatze, H. (1981) Estimation of myodynamics parameter values from observations on isometrically contracting muscle groups. *European Journal of Applied Physiology and Occupational Physiology*, **46**, 325-338.

Herzog,W. (2007) Muscle. *Biomechanics of the musculo-skeletal system* (eds. B.M. Nigg & W. Herzog) pp 169 -217. John Wiley & Son Canada Ltd, Ontario, Canada.

Juliana, S., Schmieder, D., Siemers, B., & Kingston, T. (2015) Beyond size - morphological predictors of bite force in a diverse insectivorous bat assemblage from Malaysia. *Functional Ecology,* http://doi:10.1111/1365-2435.12447.

Nigg B.M. (2007) Force System Analysis. *Biomechanics of the musculo-skeletal system* (eds. B.M. Nigg & W. Herzog) pp 311 -342. John Wiley & Son Canada Ltd, Ontario, Canada.

Nogueira, M.R., Peracchi, A.L. & Monteiro, L.R. (2009) Morphological correlates of bite force and diet in the skull and mandible of phyllostomid bats. *Functional Ecology,* **23**, 715-723.

Powell, P.L., Roy, R.R., Kanim, P., Bello, M.A., & Edgerton, V.R. (1984). Predictability of skeletal muscle tension from architectural determinations in guinea pig hindlimbs. *Journal of Applied Physiology,* **57**, 1715-1721.

Rohrle, O. & Pullan, A.J. (2007) Three-dimensional finite element modeling of muscle forces during mastication. *Journal of Biomechanics*, **40**, 3363-3372.

Roy, R.R., Bodine-Flower, S.C., Kim, J., Haque, N., De Leon, D., Rudolph, W. & Edgerton, V.R. (1991) Architectural and fiber type distribution properties of selected rhesus leg muscle: feasibility of multiple independent biopsies. *Acta Anatomica,* **140**, 350-356.

Thomason, J.J. (1990) Cranial strength in relation to estimated bite forces in some mammals. *Canadian Journal of Zoology*, **69**, 2326-2333.

Turnbull, W.D. (1970) Mammalian masticatory apparatus. *Fieldiana Geology*, **18**, 1-356.

Tylor, A.B., Eng, C.M., Anapol, F.C. & Vinyard, C.J. (2009) The functional correlates of jaw-muscle fiber architecture in tree-gouging and non-gouging callitrichid monkeys. *American Journal of Physical Anthropology*, **139**, 353-367.

Watson, P.J., Gröning, F., Curtis, N., Fitton, L.C., Herrel, A., McCormac, S.W. & Fagan, M.J. (2014). Masticatory biomechanics in the rabbit: a multi-body dynamic analysis. *Journal of The Royal Society Interface,* 11, 20140564. http://dx.doi.org/10.1098/rsif.2014.0564

CHAPTER IV

COLLISION-AVOIDANCE IN CLUTTERED ENVIRONMENTS: DO THE RESPONSES TO OBSTACLES ALIGN WITH WING MORPHOLOGY IN INSECTIVOROUS BATS OF MALAYSIA?

Abstract

It is predicted that differences in wing morphology will reflect differences in foraging strategies of bats. Several studies have experimentally tested this prediction, typically assessing the relationship between aspects of wing morphology and maneuverability through an obstacle course. However, studies have lacked measures of flight ability true scores and this may confound the interpretation of ability across the range of tasks presented to the subjects. Here, we used a collision-avoidance experiment to determine the relationships among flight performance, wing morphology and foraging strategy in 15 syntopic bat species from Malaysia. The bats were all members of the same foraging ensemble of forest interior insectivores. Foraging in the densely cluttered environment of the forest interior requires that these bats be able to quickly alter their flight direction and speed, so maneuverability is important. In this study, flight performance scores were quantified based on individual responses of 15 species to 11 different obstacle arrangements (four banks of vertical strings 10 - 60 cm apart). Both species ability and task difficulty (inter-string distance) appear along the same scale and all inter-string distances (ISDs) fit to define a unidimensional variable with sequence of

ISD difficulty in the expected order from easiest (largest ISD) to hardest (smallest ISD). The tasks employed for the collision-avoidance experiment were reliable and valid even though a Rasch analysis suggested that overall the experiment was too easy to discriminate among the 15 species completely. We tested the relationship between flight ability and morphological parameters related to flight (body mass, wing parameters) and found a negative correlation between wing loading and ability ($r^2 = 0.79$), confirming the importance of this parameter in determining the habitat use and foraging space of bats tested. Rasch analysis of data subsets and connection identified five clusters of species based on ability, suggesting that maneuverability provides a mechanism for further division of the forest interior ensemble and partitioning of foraging space.

Key words: flight performance, maneuverability, obstacles course, paleotropical bats, Rasch analysis.

Introduction

In insectivorous bat assemblages, partitioning of food resources is effected largely by physical and sensory access to the insect prey base. Differences in wing morphology influence access to particular foraging habitats and the prey capture strategy deployed within them (Norberg & Rayner 1987; Fenton 1990; Norberg 1994, 1998). The functional relationship between foraging habitat and wing morphology in bats is expressed by differences in wing aspect ratio (the square of the bat's wingspan divided by the wing area), wing loading (the body mass of the bat divided by wing area) and wingtip shape (the wingtip area ratio divided by portion of wingtip length ratio minus the wingtip area

ratio) (Norberg & Rayner 1987). These parameters influence the energetic cost of flight, flight speed and maneuverability, in which maneuverability refers to the space required by a bat to alter the flight path (Aldridge 1987; Norberg & Rayner 1987; Aldridge & Brigham 1988). High aspect ratios are associated with low energetic costs of flight but low maneuverability (Norberg & Rayner 1987; Norberg 1990; Swartz et al. 2012). High wing loading facilitates fast flight, but energetic costs are high and maneuverability is low (Norberg & Rayner 1987; Norberg 1990; Swartz et al. 2012). Conversely, bats with low wing loading are capable of slow, maneuverable flight. As a result, flight morphology (especially wing loading and aspect ratio) is often used to infer three main foraging ensembles of insectivorous bat species, based primarily on how these parameters influence their ability to fly in cluttered environments. First, species that forage in highly cluttered environments, such as the interior of a rainforest, must maximize maneuverability so usually have low aspect ratio and low wing loading. Second, bats that forage in uncluttered environments, for example above the forest canopy or in open tree-less habitats, must maximize their agility (the rapidity of change in speed and direction (Dudley 2002)) rather than maneuverability. The need for fast, efficient flight and aerial hawking ability is usually met with high aspect ratios and high wing loadings. Third, bats that forage in semi-cluttered environments, such as tree fall gaps and forest edges, have intermediate maneuverability and agility. Typically, semi-cluttered foragers combine high wing loading and low aspect ratio or low wing loading and high aspect ratio (Norberg & Rayner 1987).

Studies have experimentally tested predictions about the relationship between bat morphology and flight performance by measuring maneuverability through obstacle

courses. The courses require bats to fly through sets of vertical rods or strings, and the degree of clutter is manipulated by increasing or decreasing the distance between the rods/strings. Performance is then scored based on collision avoidance. From the experimental design perspective, the distance between the rods/strings represents a task and collectively the tasks make up an experiment that describes the performance of the bats. Performance scores are then correlated with aspects of flight morphology (e.g. Aldridge 1986; Aldridge & Rautenbach 1987, Jones et al. 1993; Stockwell 2001).

To date, performance scores have been quantified directly from observed scores of tasks from the experiment. This may compromise interpretations of performance because true score theory states that our observed score is equal to the sum of our true score or true underlying ability plus the measurement error associated with estimating our observed score or

$$X = T + e_x \tag{4.1}$$

where X is a observed score, T is a true ability and e_x is a measurement error (Allen & Yen 2002). A score that has no measurement error (i.e. true score) is perfectly reliable whereas a measure that has no true score (i.e. all variability is attributable to measurement error) has zero reliability. Thus, reliability describes the consistency or reproducibility of the test score (Trochim 2006; DeVon et al. 2007), which indicates the quality of the test. Therefore, the observed scores of a flight performance experiment are not synonymous with the ability score because observed scores will always depend on the selection of flight performance tasks that comprise the experiment over which their

ability score is defined; i.e. the number, range and values of the inter-string distances. An experiment of five tasks with inter-string distances increasing from 5 to 25 cm (5 cm intervals) is not the same as one of 5 tasks from 10 to 50 cm. Conceptually, observed scores are test dependent but ability is test-independent (Lord 1953; Hambleton & Jones 1993). In practice, bats are more likely to have lower true scores on difficult tasks and higher true scores on easier tasks, but their ability remains constant over any task that might be built to measure the ability (Wright & Stone 1979). Ability scores or estimated ability scores that are independent of the particular flight performance tasks would be of value because they would allow an unbiased comparison among species. Validity provides another indication of test quality, referring to whether or not the experiment (or individual tasks) measures what it claims to measure (Messick 1995; Borsboom et al. 2004).

Rasch analysis is a scaling approach widely used to measure performance, attitudes and perceptions in human sciences (see Bond & Fox 2001). It provides a mechanism for estimating the reliability and validity of observed scores and determining the true score (ability score) of subjects in experiments comprising multiple tasks. Scaling is the branch of measurement that involves procedures that are independent of the subject so that a numerical value of the subject's performance is generated. In other words, scaling provides an option to calculate values that represent the true score for each subject tested. Rasch analysis is built around a statistical logistic response model and specifies that each task response is taken as an outcome of the linear probabilistic interaction of a subject's ability and a task's difficulty such that the scale is a unidimensional measure of ability (Wright & Masters 1982; Andrich 1988).

Unidimensionality of a scale indicates that tasks used for the scale reflect a single construct of function. Under this construct, tasks vary from easy to difficult, and test subjects can be ranked based on ability from less to more able on the same scale. For example, the scale of the tasks in a collision-avoidance experiment should be able to assess the maneuverability of each insectivorous bat species in within a specified environment. Easy tasks can be performed by bats with almost all ability levels, whereas only more able bats are more likely to successfully perform the difficult tasks. A set of tasks that focuses too heavily on the most difficult tasks, representing the most cluttered environments, may not be a good measure of a bat's ability to express their maneuverability because the task may overlook the bat's maneuverability in the least cluttered environments and vice-versa.

In order to understand the relationships among flight performance, wing morphology and foraging ecology within a foraging group, we tested the flight ability of 15 insectivorous bat species from Malaysia with a collision-avoidance experiment. We used Rasch analysis to generate true ability scores and assess the reliability and validity of the experiment. Bat species were of three families, but belonged to the same ensemble – forest interior insectivores that forage in the cluttered environments of the rainforest understory. Here, two specific questions were addressed: 1. Are collision-avoidance experiments reliable and a valid test of flight ability? 2. If so, what is the relationship between flight ability and wing morphology within the forest interior foraging ensemble? We hypothesized that there will be positive relationship between flight ability and task difficulty and predicted that bats with high flight ability will clear the largest inter-string distance set for the collision-avoidance experiment with no difficulty. We further

hypothesized that flight ability would be influenced by wing morphology and predicted a negative relationship between ability and wing loading and aspect ratio, and a positive relationship with the roundness of the wing tip. Thus bats with low wing loading, aspect ratio and rounded wing tips should be more maneuverable than those with higher values for these parameters.

Materials and Methods

Study site and species

The study was conducted in Krau Wildlife Reserve, an area of 62,395 ha of continuous old-growth forest, located in the state of Pahang, Malaysia (DWNP-DANCED 2001). The reserve supports at least 55 insectivorous bat species of seven families with about 30 of these species foraging in the forest interior (cluttered environment) (Kingston et al. 2006). However, this study focused on the most common insectivorous bats species caught in the forest interior habitat in a 300 ha area around Kuala Lompat Research Station (KLRS) ($3^{o}43$'N, $102^{o}17$'E) on the eastern edge of the reserve. The elevation at KLRS is approximately 50 m a.s.l with vegetation classified as lowland evergreen mixed dipterocarp forest (Hodgkison et al. 2004). Insectivorous bats were captured in the forest understory using four-bank harp traps (Francis 1989) positioned across trails. Harp-traps were attended at 21:00 and captured bats were held individually in cloth bags and identified from morphological characters following Kingston et al. (2006). Only adult and non-pregnant individuals were used in this study. All captured individuals were banded and released at the point of capture within 12 hours

after all essential measurements and experiments were completed. Trapping and flight performance experiments were conducted between May and July 2010 and July and September 2011. All procedures were approved by Department of Wildlife and National Park Peninsular Malaysia and Texas Tech University, Lubbock (IACUC 10014-04).

Morphological measurements

For each captured individual we measured the length of the forearm (FA) from the outside of the elbow to the outside of the wrist in the bent wing with a dial caliper to the nearest 0.1 mm. We also measured the body mass (M) using Pesola scales (Pesola AG, Baar, Switzerland) to the nearest 0.25 g. Photographs of the wings were taken for each individual captured with both wings fully extended using a Canon PowerShot G10 digital camera (Canon USA Inc., Melville, New York, USA) mounted on a quadra-pod (Forensic Imaging Inc., Victor, New York, USA). The bat was placed on a drafting mat and adhesive packaging tape was applied to restrain the bat's extended wings and wing tail membrane while the photograph was taken (see McKenzie et al. 1995, Saunders & Barclay 1992). Using image processing and analysis in java - Image J version 1.48 (National Institutes of Health, Bethesda, Maryland, USA), wing length and wing area (Fig. 4.1) were measured for each individual. From these measurements, we calculated the following additional wing parameters for each bat (after Norberg & Rayner 1987);

$$Wingspan, B = 2 \times \frac{1}{2}B \tag{4.2}$$

Wing span is the distance between wingtips when the wings are fully extended. The $\frac{1}{2}B$ is half wingspan of the bat determined from wing photographs (Fig. 4.1).

$$Wing\ area, S = 2\ \times \frac{1}{2}S \tag{4.3}$$

Wing area is that of both wings and the body surface area, excluding the head, when the bat's wings are fully extended. The $\frac{1}{2}S$ is a half wing area of the bat determined from wing photograph (Fig. 4.1).

$$Aspect\ ratio, AR = \frac{B^2}{S} \tag{4.4}$$

where *B* is a wing span and *S* is a wing area.

$$Wing\ loading, WL = \frac{Mg}{S} \tag{4.5}$$

where *M* is a body mass, *S* is a wing area and g is acceleration due to gravity estimated at 9.8 ms^{-2}.

$$Wingtip\ length\ ratio, TL = \frac{L_{HW}}{L_{AW}} \tag{4.6}$$

where L_{HW} is a hand-wing length and L_{AW} is a arm-wing length in which both values were determined from the wing photograph (Fig. 4.1). Hand-wing length is measured

from the proximal end of the carpus to the distal end of the third finger. Arm-wing length is measured from proximal end of the propatagium to the distal end of the carpus in fully extended wings.

$$Wingtip\ area\ ratio, TS = \frac{A_{HW}}{A_{AW}} \tag{4.7}$$

where A_{HW} is hand-wing area and A_{AW} is arm-wing area in which both values were determined from wing photographs (Fig. 4.1). Hand-wing area is a surface area of the hand-wing measured between midline of fifth finger and wing-tip meanwhile arm-wing area is a surface area of the arm wing measured between line from proximal end of propatagium to proximal end of the wing membrane near the foot and midline of fifth finger (Fig. 4.1).

$$Wingtip\ shape\ index, I = \frac{TS}{TL-TS} \tag{4.8}$$

where *TS* is a wingtip area ratio and *TL* is wingtip length ratio.

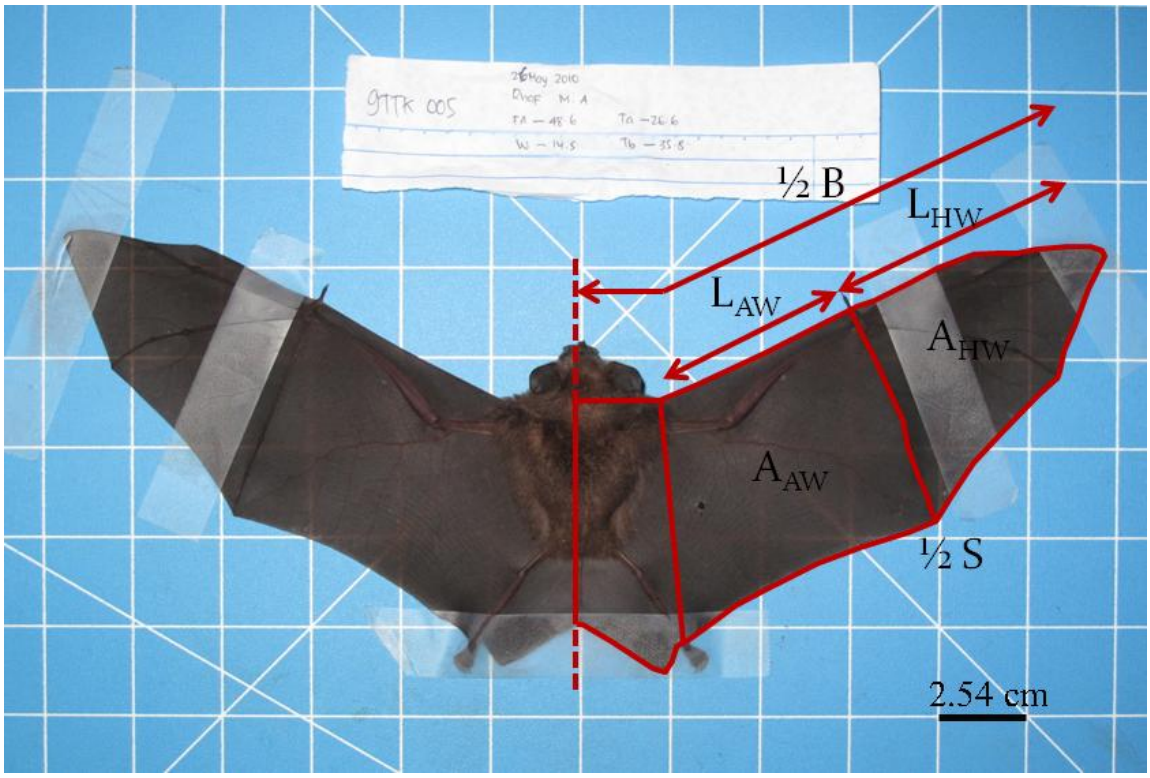

Figure 4.1. Photograph of bat wing with indication of wing dimensions that were measured using Image J. 1/2 B; half wingspan, L_{AW}; arm-wing length, L_{HW}; hand-wing length, A_{AW}; arm-wing area, A_{HW}; hand-wing area and 1/2 S; half wing area (A_{AW} + A_{HW} + area between the midline of the body and the proximal edge of the A_{AW}). Illustrated with reference to the wing of a *Rhinolophus affinis*.

Experimental setup

Collision-avoidance experiments were conducted in a flight cage located at the forest edge. The cage was 3 m wide x 3 m tall x 10 m long and the walls made of ½ inch steel hexagonal twist chicken wire. Experiments were conducted between 22:00 and 06:00 hrs. Flight performance was evaluated using an obstacle course of four banks of vertical strings that were suspended in the centre of the flight cage (Fig. 4.2). The distance

between strings could be set at 10 cm, 15 cm, 20 cm, 25 cm, 30 cm, 35 cm, 40 cm, 45 cm, 50 cm, 55 cm, or 60 cm and each bank was set to the same inter-string distance for a given test but off-set one bank to another (Fig. 4.2). Resetting the distances took several hours, so a different inter-string distance (ISD) was tested each night, with ISDs progressing from 10 cm to 60 cm, then reversing the order back to 10 cm. This rotation was continued for 16 sets (176 nights). These distances were considered representative of the range of clutter encountered by the insectivorous bat species tested when foraging in the forest understory around KLRS.

The banks were made from curtain rails to make it easier to change the inter-string distances. Each vertical string consisted of a mason line twisted nylon string (diameter; ø = 1.5 mm), secured to the top and bottom rails by curtain hooks. The line was cut between 5 and 20 cm from the bottom rail and the descending and ascending pieces of line attached to a magnet and thumbtack respectively to provide a magnetic attraction that held the string in place vertically. Hitting the string hard enough to break might reflect the physical consequences for the bat in the wild. In this experiment, strong contact with the string broke the attraction, leaving the long descending piece of string hanging, while the small ascending piece dropped to the ground. When the contact was not strong enough, touches were indicated by a movement of the string while the magnetic attraction stays attached. This mechanism gave an easy indication that a bat had hit the string as fast flying bats were expected and the experiments were conducted in natural darkness. Captured bats were presented with an inter-string distance set for that night and had to negotiate the obstacle course for ten passes (counted as one test). At the start of the test, the bat was left undisturbed, hanging at the perch station (Fig. 4.2), until

it flew through the obstacle course. A bat's observed score was quantified after each pass by observation of obstacles touched and manual counting of broken magnetic connections (which were reset between passes). Two observers were present for this experiment, one designated for recording the score and another one restoring the magnetic connections as needed. Both of the observers used a headlamp equipped with a red filter to avoid disturbing the bats, which were free to continue with the pass attempts, or rest between them.

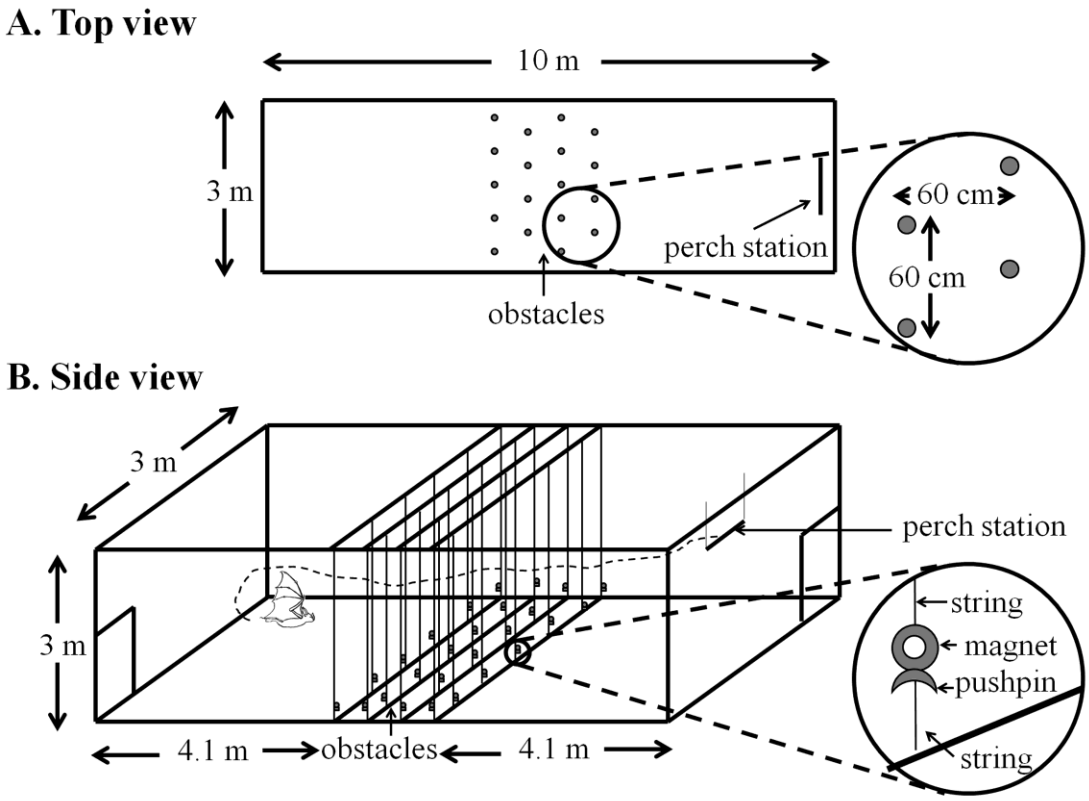

Figure 4.2. Experimental set-up. Each bat was presented with four rows of obstacles with evenly spaced inter-string distance but off-set setting from one row to another. The bat began the trial on a perch station and negotiated obstacle course for 10 times to complete one test (10 passes per test).

At each bank of strings, the bat's observed score could be classified as: refusal (bat refused to negotiate the bank within an hour); break (magnetic connection between strings broken); touch (any part of the bat body touching the strings but no break in the magnetic connection of the string) and clear (flew through the obstacle without breaking or touching any of the strings) on four banks of vertical strings. These scoring classification give the range scored from 0 – 15 points, with zero point = refusal and 15 points = cleared all banks without touching or breaking any strings and scores in between depended on the combination of breaks, touches, and clears across the four banks (Table 4.1). The gradation in the scoring system gives us a better understanding of the degree of bats performance ability in which may reflect to their foraging success.

Table 4.1. Classification of the observed scores of the collision-avoidance experiment. B = break, T = touch and C = clear.

Response	Score point	Definition
Refusal	0	bat refused to enter the course, turned back or circled in front of the first row
BBBB	1	bat broke at least one of the string in all four banks
BBBT	2	bat broke at least one of the strings in three of the banks and touched at least one of the strings in the remaining row
BBTT	3	bat broke at least one of the strings in two of the banks and touched at least one of the strings in the remaining two banks
BTTT	4	bat broke at least one of the strings in one of the bank and touched at least one of the strings in the remaining three banks
TTTT	5	bat touched at least one of the strings in all four banks
BBBC	6	bat broke at least one of the strings in three of the banks and cleared the strings in the remaining bank
BBTC	7	bat broke at least one of the strings in two of the banks, touched at least one of the strings in one of the bank and cleared the strings in the remaining bank
BTTC	8	bat broke at least one of the strings in one of the bank, touched at least one of the strings in two of the banks and cleared the strings in the remaining bank

Table 4.1. Continued

Response	Score point	Definition
TTTC	9	bat touched at least one of the strings in three of the banks and cleared all the strings in the remaining bank
BBCC	10	bat broke at least one strings in two of the banks and cleared the obstacles in the remaining two banks
BTCC	11	bat broke at least one of the strings in one of the banks, touched at least one of the strings in one of the banks and cleared the strings in the remaining two banks
TTCC	12	bat touched at least one of the strings in two of the banks and cleared all of the obstacles in the remaining two banks
BCCC	13	bat broke at least one of the strings in one of the bank and cleared all the obstacles in the remaining banks
TCCC	14	bat touched at least one of the obstacles in one of the row and cleared all the obstacles in three of the rows
CCCC	15	bat cleared all of the obstacles in all four rows.

Rasch analysis – Modeling ability score from observed collision-avoidance score

To convert the observed scores from individual tests at set ISDs to species ability scores, we first assumed that individuals of the same species have similar flight performance ability. Then, we determined the mode of the observed score for the test of each individual (ten passes per test). The mode was chosen as the measure of central tendency in order to avoid the potential influence of low scores from passes at the beginning of the test when the bats were familiarizing themselves with the course, or at the end if they began to tire. If multiple individuals of the same species were tested at the same ISD, we took the mode of the observed scores across individuals. The output going into the Rasch analysis was therefore a single observed score for each species at each ISD.

Rasch analysis was used to convert the observed ISD scores to overall flight ability scores for each species and to score the ISDs for difficulty. First, a scale of the ISDs was constructed by comparing the response patterns of species from the entire sample, creating a flight performance scale for the collision-avoidance experiment conducted. In this study, the scale is a linear transformation of the Rasch logit scale to fit a -10 to 10 scale (we standardized the measures to have zero mean and standard deviation of one with USCALE = 0.3170; UMEAN = -0.2894). Then, species were placed on the scale according to their flight ability score (true score) derived from all tasks in the experiment. The length of the flight performance scale determines the range of flight ability for all the species tested and the range of task difficulties was expected to be in order of ISD, with the easiest task (ISD of 60 cm) at the base of the scale and the hardest

task (ISD 10 cm) at the top of the scale. Disordering would indicate that the flight performance scale does not work as intended for the sample of species tested.

Finally, the quality of the flight performance scale was determined with goodness-of-fit statistics. Specifically, we examined whether the flight performance scale constructed met the criteria for unidimensionality and a hierarchical structure of ISD difficulty. The assessment of goodness-of-fit statistics was based on the mean-square (MNSQ) value (size of randomness i.e. amount of distortion of the measurement system) of outfit and infit statistics. Outfit or outlier-sensitive fit statistics are more sensitive to unexpected scores of species on ISDs that are relatively very easy or very hard for them. Infit or inlier-pattern-sensitive fit statistics are more sensitive to unexpected patterns of species's on the ISDs. The expected pattern is that in which the order of scores follows the order of task difficulty (i.e. higher score on easier tasks). The MNSQ values > 1.5 indicate possible misfits between a specific item (bat ability score or ISD difficulty score) and the rest of items in the scale (Linacre 2014). To reduce the possibility of misinterpreting the MNSQ statistics caused by the relatively small sample size of this study, the significance of MNSQ values were determined by the standardized fit statistic (ZSTD). ZSTD > 2.0 indicates that the corresponding MNSQ value is significant at an alpha level of 0.05 (Linacre 2014). Therefore, the misfit criteria in this study were determined by significant infit or outfit MNSQ values > 1.5 and the ZSTD values for that infit or outfit MNSQ > 2.0).

Previous studies have suggested that a scale built using Rash analysis is considered to be unidimensional when < 5% of the tasks used in the test or experiment

fail to fit into the scale (Wright & Masters 1982; Wright & Mok 2000). For scales with < 20 tasks (ISDs), however, as is the case with our collision-avoidance experiment, a single misfit task would exceed this 5% criterion (see Hwang & Davies 2009). Therefore, in this study, we set the criterion for unidimensionality as no more than one misfit ISD within the scale. Finally, the task difficulties were expressed as logit (the natural logarithm of the odds of a bat being able to negotiate a particular ISD). As the scoring in our experiment is based on an ordinal dependent variable (i.e. refusal, break, touch and clear), the logit is an ordered logit and is computed automatically using Rasch analysis. The logit of task difficulty was then used to determine whether the hierarchy of task difficulty was consistent with the expected difficulty of the ISDs i.e. the smaller the ISD, the more difficult the task. Rasch analysis was performed using MINISTEPS version 3.81.0 (www.winsteps.com/ministep.htm).

Reliability and validity of the collision-avoidance experiment

Reliability in Rasch analysis was reported as Cronbach's alpha (Cronbach's α) which is a coefficient of internal consistency that explains interrelatedness or inter-task correlations within the generated scale and indicates how well the tasks fit together as a scale (DeVon et al. 2007). The value of Cronbach's α ranges from 0 to 1 in which the higher values indicate a more reliable scale (DeVon et al. 2007). The sample separation ratio, which indicates how well the dataset is spread out along the performance scale of the experiment, was also reported. In our analysis, the species separation ratio was used to classify the bats' ability and the tasks separation ratio verified the hierarchy. Species

separation ratio values less than 2 with Cronbach's α less than 0.8 are considered low, suggesting that the performance scale generated may not be sensitive enough to distinguish between high and low performers (Linacre 2014). However for task separation, ratio values less than 3 with Cronbach's α less than 0.9 are consider low, suggesting that the species sample is not large enough to confirm the task difficulty hierarchy. Therefore, a high separation ratio is able to explain the validity of the performance scale generated for this experiment in which the validity refers to whether or not the experiment measures what it claims to measures (Messick 1995, Borsboom et al. 2004).

Relationships between wing morphology and flight ability

We calculated species' means for body mass (M), wing dimensions (B; wing span, S; wing area, TL; wingtip length ratio and TS; wingtip area ratio) and wing parameters (WL; wing loading, AR; wing aspect ratio and I; wingtip shape index) for all 15 species. The body mass and wing dimensions (M, B, S, TL and TS) are primary measures in the study of animal flight morphology (Norberg & Rayner 1987). The value of the wing aspect ratio and wing loading that describe respectively the size and shape of the wings were derived from body mass and the wing dimensions measures B and S (equation 4 and 5). Meanwhile, the ratio of the wing-tip length (equation 6) and wing-tip area (equation 7) were derived from wing dimension measures of TL and TS, in which these ratio than were used to determine the wing-tip shape index (I) of an animal (equation 8). Analyses of body mass and wing dimensions variables (M, B, S, TL and TS) were run separately

from those of wing parameters variables (WL, AR and I). We tested the relationship between flight ability and body mass and wing dimensions using simple linear regression. We then ran stepwise multiple regressions with flight ability score (in logit unit scale) as the dependent variable and body mass and wing dimensions to determine which variables best explained variation in flight ability among species. Next, we investigated the relationships between ability and wing parameters following the same procedure - simple linear regressions and stepwise multiple regressions. The stepwise multiple regression analysis was based on stepwise variable selection or discriminant analysis algorithms in which the variable with the 'best' value for the criterion statistic is entered first. Analyses were performed in SPSS version 17.0 statistical packages for Windows (SPSS Inc., Chicago, Illinois, USA) and all data were log transformed before analysis.

Results

426 individuals of the 15 bat species that forage in the forest interior of KLRS completed all tasks in the experiment (Table 4.2). The individuals belong to three families: the Hipposideridae (*Hipposideros bicolor* 131 kHz, *H. bicolor* 142 kHz, *H. cervinus*, *H. diadema* and *H. ridleyi*); Rhinolophidae (*Rhinolophus affinis*, *R. lepidus*, *R. stheno* and *R. trifoliatus*); and Vespertilionidae (*Kerivoula intermedia*, *K. papillosa*, *K. pellucida*, *Murina cyclotis*, *M. suilla* and *Myotis ridleyi*). Morphological measurements were taken from the 426 individuals and an additional 335 individuals from the same 15 species that were not flown through the obstacle course (Table 4.3).

Table 4.2. Observe scores recorded in mode for each species tested and number of individual used for each inter-string distances were recorded in parentheses.

Species	Inter-string distances score / number of individual tested										
	10 cm (n)	**15 cm (n)**	**20 cm (n)**	**25 cm (n)**	**30 cm (n)**	**35 cm (n)**	**40 cm (n)**	**45 cm (n)**	**50 cm (n)**	**55 cm (n)**	**60 cm (n)**
Hipposideros bicolor 131 kHz*	13 (2)	15 (2)	15 (1)	15 (9)	15 (3)	15 (2)	15 (2)	15 (1)	15 (2)	15 (1)	15 (3)
Hipposideros bicolor 142 kHz*	13 (2)	15 (1)	15 (2)	15 (9)	15 (11)	15 (3)	15 (2)	15 (2)	15 (2)	15 (2)	15 (4)
Hipposideros cervinus	12 (1)	12 (2)	12 (2)	15 (7)	15 (2)	15 (3)	15 (3)	15 (3)	15 (2)	15 (2)	15 (2)
Hipposideros diadema	0 (3)	1 (4)	1 (2)	1 (4)	1 (1)	2 (2)	3 (1)	7 (2)	10 (1)	10 (2)	15 (4)
Hipposideros ridleyi	2 (2)	14 (2)	12 (3)	12 (2)	15 (2)	15 (1)	15 (1)	15 (1)	15 (1)	15 (1)	15 (2)
Kerivoula intermedia	15 (6)	15 (7)	15 (8)	15 (6)	15 (3)	15 (3)	15 (4)	15 (8)	15 (3)	15 (5)	15 (4)
Kerivoula papillosa	3 (2)	14 (5)	15 (3)	15 (5)	15 (4)	15 (1)	15 (2)	15 (4)	15 (2)	15 (3)	15 (3)
Kerivoula pellucida	15 (2)	15 (2)	15 (1)	15 (1)	15 (3)	15 (1)	15 (2)	15 (2)	15 (2)	15 (1)	15 (2)
Murina cyclotis	5 (3)	11 (1)	12 (1)	15 (2)	15 (2)	15 (1)	15 (1)	15 (1)	15 (2)	15 (2)	15 (1)
Murina suilla	15 (2)	15 (2)	15 (2)	15 (1)	15 (1)	15 (2)	15 (1)	15 (2)	15 (2)	15 (1)	15 (3)
Myotis ridleyi	9 (1)	12 (3)	12 (1)	15 (1)	15 (1)	15 (1)	15 (1)	15 (1)	15 (1)	15 (2)	15 (1)
Rhinolophus affinis	3 (2)	3 (2)	5 (1)	12 (1)	14 (2)	15 (2)	15 (2)	15 (2)	15 (1)	15 (2)	15 (4)
Rhinolophus lepidus	13 (2)	14 (2)	15 (4)	15 (6)	15 (4)	15 (1)	15 (2)	15 (3)	15 (5)	15 (2)	15 (3)

Table 4.2. Continued.

Species	Inter-string distances score / number of individual tested										
	10 cm (n)	**15 cm (n)**	**20 cm (n)**	**25 cm (n)**	**30 cm (n)**	**35 cm (n)**	**40 cm (n)**	**45 cm (n)**	**50 cm (n)**	**55 cm (n)**	**60 cm (n)**
Rhinolophus stheno	4 (6)	10 (2)	13 (4)	15 (9)	15 (2)	15 (5)	15 (3)	15 (2)	15 (3)	15 (4)	15 (3)
Rhinolophus trifoliatus	0 (2)	0 (2)	3 (3)	4 (2)	4 (6)	14 (1)	14 (1)	15 (2)	15 (2)	15 (3)	15 (3)

*Cryptic species that were genetically and acoustically divergent and denoted as phonic types based on the mean frequency of their CF component of the call. Individual with 131 kHz was assigned as *Hipposideros bicolor* 131 kHz and individual with 142 kHz was assigned as *Hipposideros bicolor* 142 kHz.

Table 4.3. Summary of the sample sizes, body mass, wing dimensions and wing parameter collected for 15 bat species from Krau Wildlife Reserve, Malaysia (mean ±SD).

Species	**n**	**Body Mass (Kg)**	**Wing Area (m^2)**	**Wing Span (m)**	**Ratio Wing-tip Length**	**Ratio Wing-tip Area**	**Wing Loading (Nm^{-2})**	**Wing Aspect Ratio**	**Wing-tip Index**
Hipposideros	34	0.008 ±	0.014 ±	0.278 ±	1.163 ±	0.704 ±	5.646 ±	5.369 ±	1.545 ±
bicolor 131 kHz*		0.001	0.001	0.008	0.046	0.021	0.476	0.384	0.140
Hipposideros	56	0.008 ±	0.014 ±	0.274 ±	1.188 ±	0.694 ±	5.750 ±	5.558 ±	1.418 ±
bicolor 142 kHz*		0.001	0.001	0.012	0.043	0.033	0.557	0.264	0.173
Hipposideros	88	0.010 ±	0.015 ±	0.303 ±	1.080 ±	0.610 ±	6.647 ±	6.098 ±	1.317 ±
cervinus		0.001	0.001	0.008	0.050	0.031	0.669	0.301	0.205
Hipposideros	66	0.047 ±	0.043 ±	0.499 ±	1.080 ±	0.576 ±	10.824 ±	5.822 ±	1.165 ±
diadema		0.006	0.003	0.020	0.057	0.031	1.327	0.292	0.207
Hipposideros	18	0.009 ±	0.016 ±	0.302 ±	1.182 ±	0.714 ±	5.819 ±	5.809 ±	1.546 ±
ridleyi		0.001	0.001	0.010	0.051	0.029	0.609	0.411	0.216

Table 4.3. Continued

Species	**n**	**Body Mass (Kg)**	**Wing Area (m^2)**	**Wing Span (m)**	**Ratio Wing-tip Length**	**Ratio Wing-tip Area**	**Wing Loading (Nm^{-2})**	**Wing Aspect Ratio**	**Wing-tip Index**
Kerivoula intermedia	103	0.003 ± 0.000	0.008 ± 0.000	0.215 ± 0.006	1.753 ± 1.503	0.891 ± 0.046	3.928 ± 0.539	5.621 ± 0.266	1.245 ± 0.250
Kerivoula papillosa	48	0.009 ± 0.001	0.018 ± 0.002	0.313 ± 0.017	1.665 ± 0.080	0.964 ± 0.059	5.082 ± 0.514	5.551 ± 0.290	1.366 ± 0.289
Kerivoula pellucida	26	0.005 ± 0.005	0.011 ± 0.011	0.233 ± 0.009	1.765 ± 0.109	0.947 ± 0.072	3.963 ± 0.446	4.870 ± 0.241	1.186 ± 0.221
Murina cyclotis	18	0.008 ± 0.001	0.013 ± 0.001	0.259 ± 0.011	1.444 ± 0.076	0.778 ± 0.042	6.128 ± 0.541	5.130 ± 0.265	1.189 ± 0.185
Murina suilla	22	0.004 ± 0.000	0.008 ± 0.001	0.210 ± 0.015	1.421 ± 0.068	0.808 ± 0.063	4.830 ± 0.333	5.372 ± 0.386	1.335 ± 0.205
Myotis ridleyi	20	0.004 ± 0.000	0.007 ± 0.001	0.205 ± 0.013	1.503 ± 0.081	0.767 ± 0.023	5.609 ± 0.344	5.651 ± 0.275	1.051 ± 0.107

Table 4.3. Continued.

Species	**(n)**	**Body Mass (Kg)**	**Wing Area (m^2)**	**Wing Span (m)**	**Ratio Wing-tip Length**	**Ratio Wing-tip Area**	**Wing Loading (Nm^{-2})**	**Wing Aspect Ratio**	**Wing-tip Index**
Rhinolophus affinis	35	0.015 ± 0.001	0.018 ± 0.001	0.311 ± 0.010	1.198 ± 0.047	0.665 ± 0.032	8.134 ± 0.498	5.489 ± 0.244	1.263 ± 0.157
Rhinolophus lepidus	58	0.006 ± 0.001	0.011 ± 0.001	0.242 ± 0.009	1.103 ± 0.057	0.685 ± 0.036	5.704 ± 0.533	5.557 ± 0.318	1.671 ± 0.256
Rhinolophus stheno	98	0.009 ± 0.001	0.014 ± 0.001	0.287 ± 0.008	1.180 ± 0.048	0.694 ± 0.052	6.030 ± 0.489	5.940 ± 0.321	1.455 ± 0.236
Rhinolophus trifoliatus	71	0.014 ± 0.002	0.020 ± 0.001	0.329 ± 0.014	1.307 ± 0.058	0.717 ± 0.047	6.810 ± 0.668	5.338 ± 0.270	1.237 ± 0.208

*Cryptic species that were genetically and acoustically divergent and denoted as phonic types based on the mean frequency of their CF component of the call. Individual with 131 kHz was assigned as *Hipposideros bicolor* 131 kHz and individual with 142 kHz was assigned as *Hipposideros bicolor* 142 kHz.

Flight performance scale

Both species' ability and task difficulty appear along the same scale in the species ability and task difficulty map determined by Rasch analysis (Fig. 4.3). Species appear in increasing order of ability with species with poor performances on the collision-avoidance experiment at the bottom of the scale and species of greater ability at the top of the scale (the left-hand side of Fig. 4.3). In contrast, the task difficulty (i.e. ISD) appears in an inverse order compared to the species ability scale with more difficult ISDs at the top and easier ISDs at the bottom of the scale (the right-hand side of Fig. 4.3). The sequence of the ISD difficulty was in the expected order, with the smallest ISD (10 cm) at the top of the scale and biggest ISD (60 cm) at the bottom of the scale. Theoretically, the species ability and task difficulty are comparable when species and tasks are aligned to each other on the map. Species that aligned with a specific task (ISD) have a 50% probability of clearing that ISD (i.e. achieving a perfect score by flying through the task without breaking or touching any of the strings on all four banks of vertical strings). Five species aligned with specific ISDs in this study. For example, *Rhinolophus trifoliatus* aligned with the 30 cm ISD, indicating a 50% probability that *R. trifoliatus* would clear that ISD. By extension, *R. trifoliatus* has less than 50% chance of clearing ISDs located above the 30 cm task on the flight performance scale, but >50% of clearing ISDs below it. Similarly, *Hipposideros diadema* aligned with 45 cm, *R. affinis* aligned with 20 cm and both *Kerivoula papillosa* and *Myotis ridleyi* were aligned with 10 cm ISD.

The mean (M) and two standard deviation points from the mean (S = one standard deviation and T = two standard deviation) are shown for both species ability (left hand

side of the map) and task difficulty (right) (Fig. 4.3). From the map, the mean (M) of species ability is approximately one and a half standard deviations above the mean (M) of task difficulty. This suggests that bats with average flight ability were able to perform tasks about 1.5 SD above the mean task difficulty, indicating that overall the test was easy to perform. The logit measures corresponding to both species ability and ISD difficulty depicted in Fig. 4.3 are reported in Table 4.4 and Table 4.5. The measurement range and coverage of the flight performance scale is illustrated on the left in Fig. 4.3, and covers 4.96 logits (between 1.16 and -3.80 logits).

When we compared the distribution of species ability to that of task difficulty, seven species (*Kerivoula intermedia, K. pellucida, Murina suilla, Hipposideros bicolor* 131 kHz, *H. bicolor* 142 kHz, *Rhinolophus lepidus* and *H. cervinus*) were scaled above the most difficult ISD (10 cm ISD), suggesting that these species were able to clear the most difficult task in the experiment with probability above 50%. Indeed, three of these species (*K. intermedia, K. pellucida, Murina suilla*) cleared all tasks and shared the maximum measure of ability at 1.1578 logits (Table 4.5). Thus the most difficult ISD set for the experiment was not able to differentiate among the abilities of these three species, suggesting that smaller ISDs were needed to fully characterize their ability and maybe improve discrimination. At the easy end of the ISD scale, there were three ISDs (ISD 50 cm, ISD 55 cm and ISD 60 cm) that had above 50% chance of being cleared by the poorest performer (*Hipposideros diadema*) with ISD 60 cm has minimum measure that indicated all species tested clear the ISD 60 (Table 4.4). This suggests that all these three ISDs were very easy tasks to perform with ISD 60 cm not contributing to the

discrimination among species at all. In general, the comparison between species ability and task difficulty suggests that this collision-avoidance experiment was very easy to perform for most of the bats tested.

We detected no misfits in the dataset, supporting unidimensionality of the flight performance scale used in this study. Separation and reliability statistics for both species and tasks were high with species separation of 3.60 and species reliability (Cronbach α) of 0.93, and ISD separation for the dataset of 5.48 with a reliability value of Cronbach α = 0.97. The high separation ratios and reliability statistics of our dataset demonstrated that the performance scale generated was valid.

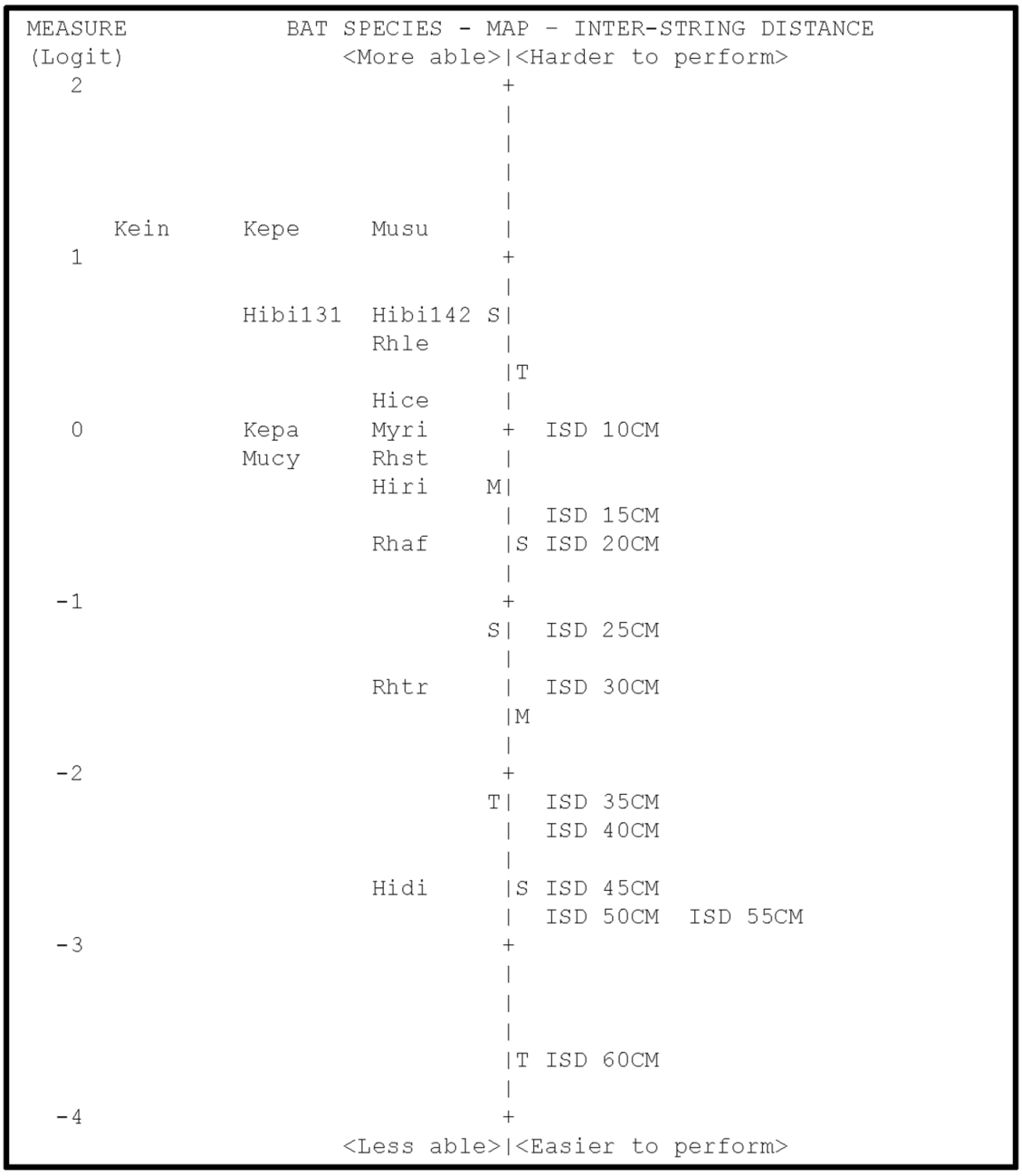

Figure 4.3. Hierarchal order of species ability and inter-string distance difficulty with logit values given on the left. Species' ability level are represented as abbreviated names and aligned to the left of the corresponding measure. Inter-string distances are aligned to the right of the corresponding values. M = mean of species ability or inter-string distance

difficulty distribution, S = one standard deviation from species ability or inter-string distances distribution mean and T = two standard deviation from the species ability or inter-string distance distribution mean. Hibi131 = *Hipposideros bicolor* 131, Hibi142 = *H. bicolor* 141, Hice = *H. cervinus*, Hidi = *H. diadema*, Hiri = *H. ridleyi*, Kein = *Kerivoula intermedia*, Kepa = *K. papillosa*, Kepe = *K. pellucida*, Mucy = *Murina cyclotis*, Musu = *Murina suilla*, Myri = *Myotis ridleyi*, Rhaf = *Rhinolophus affinis,* Rhle = *R. lepidus*, Rhst = *R. stheno* and Rhtr = *R. trifoliatus*.

Table 4.4. Inter-string distances (obstacles) statistics in measure order.

Total Score	Total Count	Measure	Model S.E	Infit		Outfit		Inter-string Distance
				MNSQ	ZSTD	MNSQ	ZSTD	
122	15	-0.0518	0.0532	0.69	-0.6	0.56	-0.5	10 cm
167	15	-0.5476	0.0817	1.38	0.7	1.56	1.0	15 cm
175	15	-0.7164	0.0768	0.67	-0.4	1.03	0.3	20 cm
194	15	-1.2171	0.1303	1.05	0.3	0.59	0.0	25 cm
198	15	-1.4318	0.1164	0.24	-0.5	0.23	-0.4	30 cm
211	15	-2.1811	0.1992	0.41	-0.6	0.10	-0.7	35 cm
212	15	-2.3144	0.2134	0.01	-1.9	0.01	-1.2	40 cm
217	15	-2.7232	0.1034	0.01	-2.9	0.02	-1.1	45 cm
220	15	-2.8462	0.1396	0.00	-1.3	0.01	-1.2	50 cm
220	15	-2.8462	0.1396	0.00	-1.3	0.01	-1.2	55 cm
225	15	-3.7975	0.5049	Minimum Measure				60 cm

Table 4.5. Bats statistics in measure order. Hibi131 = *Hipposideros bicolor* 131, Hibi142 = *H. bicolor* 141, Hice = *H. cervinus*, Hidi = *H. diadema*, Hiri = *H. ridleyi*, Kein = *Kerivoula intermedia*, Kepa = *K. papillosa*, Kepe = *K. pellucida*, Mucy = *Murina cyclotis*, Musu = *Murina suilla*, Myri = *Myotis ridleyi*, Rhaf = *Rhinolophus affinis*, Rhle = *R. lepidus*, Rhst = *R. stheno* and Rhtr = *R. trifoliatus*.

Total Score	Total Count	Measure	Model S.E	Infit MNSQ	Infit ZSTD	Outfit MNSQ	Outfit ZSTD	Bat Species	Subset
165	11	1.1578	0.5211	Maximum Measure				Kein	1
165	11	1.1578	0.5211	Maximum Measure				Kepe	1
165	11	1.1578	0.5211	Maximum Measure				Musu	1
163	11	0.6629	0.2239	0.11	-1.3	0.04	-0.9	Hibi142	2
163	11	0.6629	0.2239	0.11	-1.3	0.04	-0.9	Hibi131	2
162	11	0.5191	0.2037	0.20	-0.7	0.09	-0.7	Rhle	3
156	11	0.1033	0.0992	1.19	-0.5	0.46	0.0	Hice	4
154	11	0.0478	0.0899	0.33	-1.2	0.22	-0.4	Myri	4
152	11	-0.0032	0.0919	1.35	-0.7	0.47	0.0	Kepa	4
148	11	-0.1462	0.1249	0.33	-0.4	0.15	-0.5	Mucy	4
147	11	-0.1973	0.1288	0.50	-0.2	0.20	-0.4	Rhst	4
145	11	-0.2952	0.1168	2.33	1.2	1.03	0.5	Hiri	4
127	11	-0.7093	0.0917	0.14	-1.3	0.14	-0.5	Rhaf	4
99	11	-1.4707	0.0976	0.47	-0.5	0.61	-0.3	Rhtr	5
50	11	-2.6470	0.0676	0.14	-1.9	1.43	0.7	Hidi	5

Species clustering on the flight performance scale

Examination of estimated true scores of species ability and ISD difficulty revealed breaks in connectivity within the dataset. Rasch analysis of data subsets and connection reported that the species fit into the flight performance scale in five different subsets or clusters (Table 4.5). The first cluster comprised species that had the highest flight ability scores in negotiating all the ISDs (*K. intermedia, K. pellucida* and *M. suilla*). They were placed at the top of the flight performance scale with 1.16 logits. The second cluster contained *H. bicolor* 131 kHz and *H. bicolor* 142 kHz at 0.66 logits. The third cluster was represented by a single species, *R. lepidus,* at 0.52 logits. Seven species made up the fourth cluster: *H. cervinus, H. ridleyi, Myotis ridleyi, Kerivoula papillosa, Murina cyclotis, Rhinolophus stheno* and *R. affinis* at 0.10, 0.05, 0.00, -0.15, -0.20, -0.30 and -0.71 logits respectively. The fifth cluster was represented by two species of bats; *H. diadema* and *R. trifoliatus* at -1.47 and -2.65 logits, respectively.

Associations between flight ability and wing morphology

There was a negative correlation between flight ability and body mass (M), wing area (S) and wing span (B) but a positive correlation between flight ability and wingtip length ratio (TL) and wingtip area ratio (TS). The correlations between flight ability and M, S, B, TS were significant (M: $r^2 = 0.829$, $p < 0.000$; S: $r^2 = 0.730$, $p < 0.0001$; B: $r^2 = 0.744$, $p < 0.0001$; TS: $r^2 = 0.350$, $p = 0.020$), but between flight ability and TL was not significant ($r^2 = 0.206$, $p = 0.089$). This indicates that species with smaller body mass, smaller wing area and smaller wing span but large wing-tip areas performed better in our

collision-avoidance experiment. However, using the stepwise multiple regression analysis, a significant model emerged ($F_{1,14} = 63.075$, $r^2 = 0.829$, $p < 0.0001$) with body mass as the only significant predictor for flight ability. This suggests that flight ability in the bats tested was primarily predicted by lighter body mass rather than the wing dimensions measured (Fig. 4.4).

The role of wing morphology was clearer when the wing parameters known to influence the use of cluttered space were tested directly. Flight ability correlated negatively with wing loading (WL) and aspect ratio (AR), and positively with wingtip shape index (I). However, only the correlation between flight ability and WL was significant ($r^2 = 0.790$, $p < 0.0001$) (Fig. 4.5) and suggests that wing loading is able to predict flight ability in insectivorous bats tested.

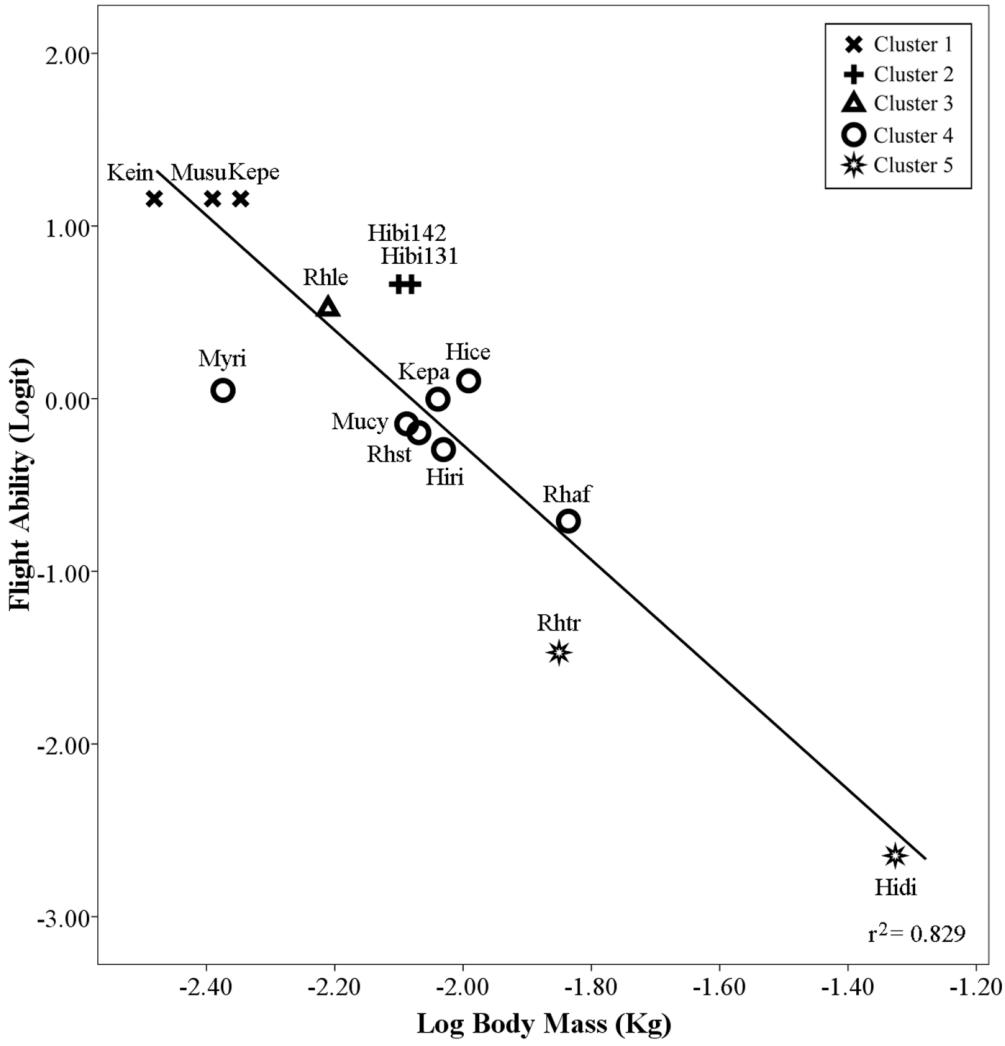

Figure 4.4. Relationship between fight ability and body mass across 15 species of insectivorous bats from Krau Wildlife Reserve, Malaysia with indication of their performance clusters; Y = -3.325X – 6.919, $p < 0.0001$. Hibi131 = *Hipposideros bicolour* 131 kHz, Hibi142 = *H. bicolour* 142 kHz, Hice = *H. cervinus*, Hidi = *H. diadema*, Hiri = *H. ridleyi*, Kein = *Kerivoula intermedia*, Kepa = *K. papillosa*, Kepe = *K. pellucida*, Mucy = *Murina cyclotis*, Musu = *M. suilla*, Myri = *Myotis ridleyi*, Rhaf = *Rhinolophus affinis*, Rhle = *R. lepidus*, Rhst = *R. stheno* and Rhtr = *R. trifoliatus.*

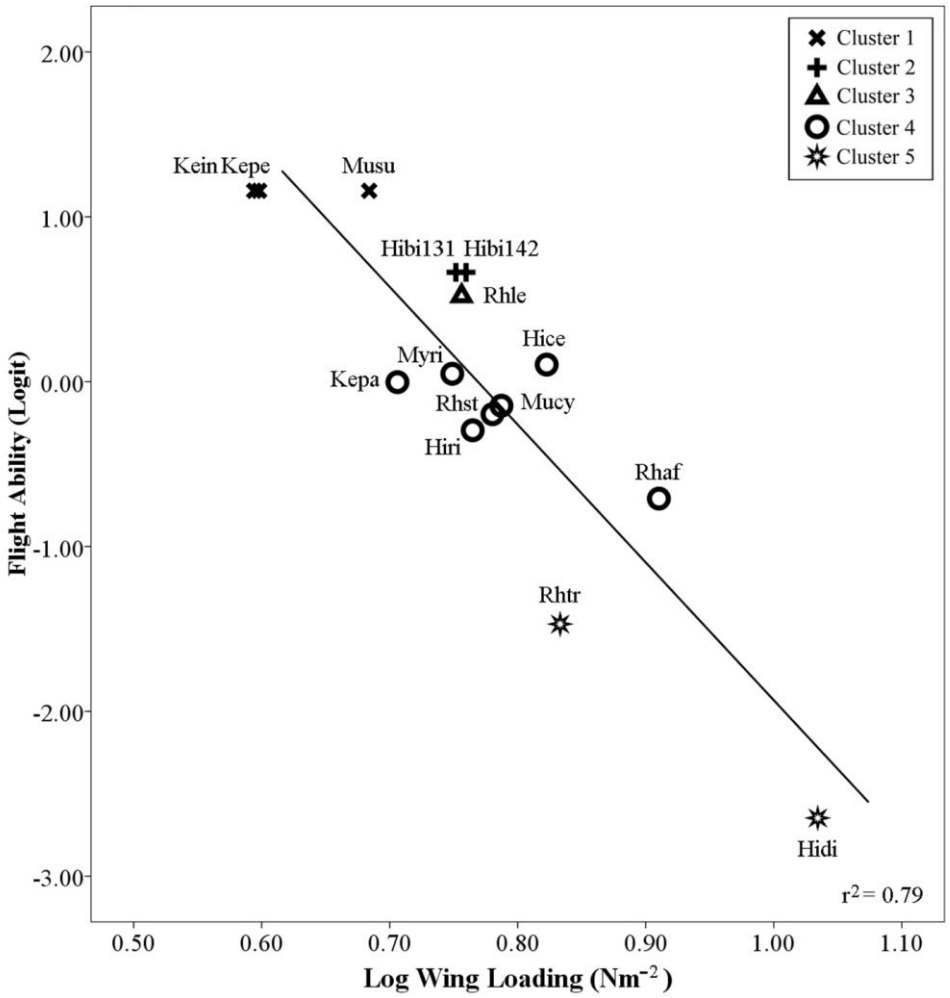

Figure 4.5. Relationship between fight ability and wing loading across 15 species of insectivorous bats from Krau Wildlife Reserve, Malaysia with indication of their performance clusters; Y = -8.357X – 6.425, $p < 0.0001$. Hibi131 = *Hipposideros bicolour* 131 kHz, Hibi142 = *H. bicolour* 142 kHz, Hice = *H. cervinus*, Hidi = *H. diadema*, Hiri = *H. ridleyi*, Kein = *Kerivoula intermedia*, Kepa = *K. papillosa*, Kepe = *K. pellucida*, Mucy = *Murina cyclotis*, Musu = *M. suilla*, Myri = *Myotis ridleyi*, Rhaf = *Rhinolophus affinis*, Rhle = *R. lepidus*, Rhst = *R. stheno* and Rhtr = *R. trifoliatus.*

Discussion

The scaling method used to analyze our dataset provided a true score estimation of flight performance of bats in a collision-avoidance experiment that enabled us to evaluate the bat's flight ability directly. Because of our approach, we were able to determine the reliability and validity of the experimental design and identify tasks that could be modified in future experiments. In this study, the linear scale constructed by Rasch analysis allowed an easy comparison of ISD difficulty and species ability along the same scale, and indicated thresholds of performance, based on 50% probability of clearing a specific task, that allow discrimination among species. This is a unique approach in which the relationship between bat's flight ability and task difficulty can be evaluated simultaneously.

The flight performance scale discrimination for species with maximum measures of ability beyond the most difficult ISD (10 cm) was less informative. Although we know that the species were able to clear the most difficult ISD, we do not know the limits of their ability. This illustrates poor targeting of ISD difficulty to species ability and the only conclusion that we can made was many of the ISDs are too easy for species listed beyond 10 cm ISD (*Kerivoula intermedia*, *K. pellucida* and *Murina suilla*). However, this suggests that adding the more challenging ISDs e.g. 8 cm, 6 cm, 4 cm and 2 cm might able to improve the targeting of ISD difficulty to species ability. In previous studies, the most challenging inter-string distance was set at half the wingspan of the smallest bat species tested. Stockwell (2001) tested five species of bats with obstacles spaced at multiples of 0.5, 0.75 or 1 of the bats' wing span. For example, the obstacle distances for

Carollia castanea with a 30 cm wingspan (smallest wingspan among species tested) were set at 15 cm, 22.5 cm and 30 cm. However, Aldridge (1986) set the smallest inter-string at absolute distance of 11 cm for *Myotis lucifugus* and *M. yumanensis* with wingspans of 25 cm and 24 cm, respectively. In both cases, the bats were highly successful in negotiating the smallest inter-string distance for the obstacle course (Aldridge 1986; Stockwell 2001), suggesting that they too failed to target ISD difficulty to species ability.

In this study, the wingspan of the three species that had the maximum measures of flight ability (*Kerivoula intermedia, K. pellucida and Murina suilla*) were 21.5 cm, 23.3 cm and 21.0 cm, respectively, close to the 0.5 ratio of other studies. The bat with the shortest wingspan in this study is *Myotis ridleyi* with 20.5 cm, a species that was not one of the highest performers, although it still was estimated to have 50 % chance of clearing the 10 cm ISD. Interestingly, *Kerivoula papillosa*, with 30 cm wingspan was also estimated to have 50 % chance of clearing the 10 cm ISD. This suggesting that the length of the wingspan is not reliable for scaling the ISDs in flight performance experiments, as it is not a reliable determinant of ability. As our morphological analyses illustrated, wing loading, not wingspan, was the best predictor of performance in this study. Whereas wing loading for *M. ridleyi* and *K. papillosa* was 5.609 Nm^{-2} and 5.082 Nm^{-2}, respectively, the three most able species, *Kerivoula intermedia, K. pellucida* and *Murina suilla* were characterized by extremely low wing loadings of 3.928 Nm^{-2}, 3.963 Nm^{-2} and 4.830 Nm^{-2}, respectively. Future collision-avoidance experiments should thus based on manipulation of wing loading rather than wing span of the bats. However, to be more practical with field situation, the inter-strings distances maybe manipulated based on combined body mass and estimated of wing area.

Although flight ability correlated with body mass, wingspan, wing area, wingtip shape, wing loading and aspect ratio in our study, body mass and wing loading were the only significant predictors in the stepwise regressions. The importance of wing loading has been reported in other collision-avoidance experiments, although typically in combination with other parameters. A comparison of two *Myotis* species (Aldridge 1986) found that both wing loading and wingspan played a significant role, and wing loading and wing tip shape explained performance differences between *Phoniscus papuensis* and *Nyctophilus bifax* (Rhodes 1995). Jones et al. (1993) attributed differences in performance between *Hipposideros ruber* and *Asellia tridens* to differences in wing span, wing loading and aspect ratio. Interestingly Stockwell (2001) reported that bat's overall size seemed to be a more important maneuverability criterion than specific wing morphology parameters for five phyllostomid bats. Regardless of this variability in results, lower wing loading was almost always reported as one of the main predictors of greater maneuverability of bats in collision-avoidance experiments.

The discrimination information from our flight performance scale grouped the insectivorous bats' abilities into five different clusters. In most human sciences studies using Rasch analysis, researchers try to avoid clusters in their dataset because it suggests that subjects are not drawn from a population with a normal distribution of ability across the distribution of task difficulties (Linacre 2014). Clusters indicate that subjects are coming from populations with different abilities so cannot be compared based on their performance on the same test. In this study, however, clusters may have ecological meaning, suggesting the presence of groups (sub-ensembles) within the forest interior

ensemble characterized by differential use of space within the habitat. Information regarding foraging strategies of insectivorous bats from the paleotropical region is rare, limiting the interpretation of our findings. However, based on our observations, the two members of the least able cluster, *Hipposideros diadema* and *Rhinolophus trifoliatus*, are perch hunters. Typically, these species hang from a perch and acoustically scan the airspace of small gaps in the forest understory and midstory for insects. Upon detection of prey, they sally forth to catch it and return to the perch. Although the overall structure of the forest understory or midstory in which the bats live may be cluttered, the degree of clutter in the actual foraging space is low. Other species do not use perches, but hunt continuously on the wing (hawking). Hawking insects near or within vegetation requires both high maneuverability (Norberg 1994) and clutter-tolerant echolocation (Siemers & Schnitzler 2004). In tests of the sensory constraints on prey detection in an uncluttered environment, four of the more able species in our study (*Kerivoula intermedia, K. papillosa, Murina cyclotis* and *M. suilla*) were able to detect and catch insects less than 6 cm away from the high echo-reflecting background with best performance as close as 2.5 cm away from the background (Schmieder et al. 2012). Moreover, detection performance was related to signal bandwidth – the greater the bandwidth, the closer the prey could be to a background and still be detected. In combination with Schmieder et al. (2012), our findings provide empirical support for the correlation or co-adaption between wing morphology and echolocation signal design to particular foraging niches (Norberg 1994).

Although 30 species of insectivorous bats in Krau Wildlife Reserve are considered to be forest interior species (Kingston et al. 2006), only 15 completed all tasks in our collision-avoidance experiment due to limited time and resources. Several species

occurred too rarely to complete all tasks, particularly because resetting the ISDs took all day, so ISD could not be adjusted to capitalize on rare captures. However, with the exception of *Nycteris tragata* (family Nycteridae) and *Megaderma spasma* (Megadermatidae), the missing species were members of the same subfamily or genus of those tested and most fell within the range of morphological parameters represented. The general pattern of the flight ability distribution of generated flight performance scale was relatively consistent with the distribution of wing loading, so inclusion of missing species would be unlikely to change the dynamics of the performance scale by much. By adding smaller inter-string distances and adding more species/genera, the performance scale can be fully tested. At this point, we believe generating a performance scale is a useful way to quantity flight ability of bats. However, the explanation of the species distribution on the performance scale could be improved with knowledge of foraging strategy and echolocation structure of the species.

Even with the 15 species, our experiment identified five flight performance clusters that might reflect differential use of the forest interior habitat. Several niche dimensions that might facilitate resource partitioning in this species-rich ensemble from Krau Wildlife Reserve have been explored. Kingston et al. (1999) and Schmieder et al. (2012) focused on echolocation signal design in species of Kerivoulinae and Murininae. Interspecific differences in call parameters and bandwidth suggest a role for sensory niche partitioning among species. A recent study by Juliana et al. (2015) demonstrated that differences in bite force among species provide a mechanism by which food resources may be partitioned. Furthermore, Kingston et al. (2000) tested the distribution of echolocation calls, body mass and wing dimensions of 15 species from the families

Hipposideridae and Rhinolophidae. Although they found no evidence of deterministic separation of echolocation call frequency alone, overdispersion suggestive of niche differentiation was detected in multivariate space derived from both echolocation and wing parameters. In this study, we demonstrated that wing loading relates to flight performance in cluttered environments, clarifying the importance of maneuverability as an additional niche dimension (expressed morphologically by wing loading) facilitating ecological separation of species in this diverse ensemble.

Transformation of qualitative scales to allow quantitative analyses is widely used in assessments of human performance and ability. Rasch analysis belongs to a family of approaches based on Item Response Theory (IRT) that emphasize how individual responses to a particular test item is influenced by qualities of the individual and qualities of tests. IRT was originally developed by Lord (1953) and was first used to assess ability in the field of psychometrics. IRT is widely used to calibrate and evaluate items in tests or questionnaires to score subjects on their abilities, attitudes or other latent traits. For example, all major educational tests in the USA, such as the Graduate Record Examination (GRE) and Scholastic Aptitude Test (SAT), are developed and assessed using IRT-based techniques. This is because IRT-based techniques can significantly improve measurement accuracy and reliability while providing potentially significant reductions in assessment time and effort (Kingston & Dorans 1984). In recent years, IRT-based models have also become increasingly popular in health outcomes research (Hays et al. 2000; Duncan et al. 2003), quality-of-life research (Edelen & Reeve 2007), and clinical research (Holman et al. 2003; Reise & Waller 2009).

Assessments of animal ability or performance have relied heavily on quantitative measures because these lend themselves to conventional statistical approaches e.g. determining sprint speed of reptiles using treadmills (Losos & Irschick 1995) or hi-speed video recordings (Irschick 2000), maximum bite force capacity of vertebrates using force transducers (Herrel et al. 2005; Santana et al. 2010; Erickson et al. 2012; Juliana et al. 2015). Constraints in performance studies in animals may occur when there is no measurement instrument (such as a treadmill or transducer) available to measure the performance or when dealing with more descriptive performances (qualitative data). For example, no measurement instrument exists to quantify the quality of courtship behavior in studies of mating success or aggression levels in dominance hierarchies. Instead, scales derived from observer evaluations might be more applicable and IRT may be the best way to analyze those responses. Rasch analysis in aggression studies, for example, could integrate the rank order of focal individuals with that of their opponents to create a single scale. To the best of our knowledge, however, item response theory has never been applied in animal performance studies, but as, we have demonstrated, has the potential to expand our statistical horizon in exploring and understanding animal performance and its relationship to morphology.

Literature Cited

Aldridge, H. (1986) Manoeuvrability and ecological segregation in the little brown (*Myotis lucifugus*) and Yuma (*M. yumanensis*) bats (Chiroptera: Vespertilionidae). *Canadian Journal of Zoology*, **64**, 1878-1882.

Aldridge, H.D.J.N. (1987) Turning flight of bats. *Journal of Experimental Biology*, **128**: 419-425.

Aldridge, H.D.J.N. & Brigham, R. M. (1988) Load carrying and maneuverability in an insectivorous bat: a test of 5% "rule" of radio-telemetry. *Journal of Mammalogy*, **69**: 380-382.

Aldridge, H.D.J.N. & Rautenbach, I.L. (1987) Morphology, echolocation and resource partitioning in insectivorous bats. *Journal of Animal Ecology*, **56**, 763-778.

Allen, M.J. & Yen, W.M. (2002) *Introduction to measurement theory*. Waveland Press: Illinois.

Andrich, D. (1988) *Rasch model for measurement*. SAGE Publications Inc., Newbury Park, California.

Bond, T.G. & Fox, C.M. (2001) *Applying the Rasch model: fundamental measurement in the human sciences*. Lawrence Erlbaum Associates, Mahwah, New Jersey.

Borsboom, D., Mellenbergh, G.J. & Van Heerden, J. (2004) The concept of validity. *Psychological review*, **111**, 1061-1071.

DeVon, H.A., Block, M.E., Moyle-Wright, P., Ernst, D.M., Hayden, S.J. & Lazzara, D.J. (2007). A psychometric toolbox for testing validity and reliability. *Journal of Nursing scholarship*, **39**, 155-164.

Dudley, R. (2002). Mechanisms and implications of animal flight maneuverability. *Integrative and Comparative Biology*, **42**, 135-140.

Duncan, P.W., Bode, R.K., Lai, S.M., Perera, S. (2003). Rash analysis of a new stroke-specific outcome scale: the stroke impact scale. *Archives of Physical Medicine and Rehabilitation,* **84**, 950-963.

DWNP-DANCED (2001) *Krau Wildlife Reserve management plan*. Department of Wildlife and National Parks, Kuala Lumpur.

Edelen, M.O. & Reeve, B.B. (2007) Applying Item Response Theory (IRT) modeling to questionnaire development, evaluation and refinement. *Quality of Life Research*, **16**, 5-18.

Erickson, G.M., Gignac, P.M., Steppan, S.J., Lappin, K.A., Vliet, K.A., Brueggen, J.D., Inouye, B.D., Kledzik, D. & Webb, G.J.W. (2012) Insights into the ecology and evolutionary success of crocodilians revealed through bite-force and tooth-pressure experimentation. *PLoS One* DOI:10.1371/journal.pone.0031781

Fenton, M.B. (1990) The foraging ecology and behavior of animal-eating bats. *Canadian Journal of Zoology*, **68**, 411-422.

Francis, C.M. (1989) A comparison of mist-nets and two designs of harp-traps for capturing bats. *Journal of Mammalogy,* **70**, 865-870.

Hambleton, R.K. & Jones, R.W. (1993) An NCME instructional module on comparison of classical test theory and item response theory and their applications to test development. *Educational Measurement: Issues and Practice*, **12**, 38-47.

Hays, R.D., Morales, L.S., & Reise, S.P. (2000) Item response theory and health outcomes measurement in the twenty-first century. *Medical Care*, **38**, Suppl. 9, 1128–1142.

Herrel, A., Podos, J., Huber, S.K. & Hendry, A.P. (2005) Evolution of bite force in Darwin's finches: a key role for head width. *Journal of Evolutionary Biology*, **18**: 669-675.

Hodgkison, R., B. T. Balding, A. Zubaid and T. H. Kunz. 2004. Habitat structure, wing morphology, and the vertical stratification of Malaysian fruit bats (Megachiroptera: Pteropodidae). *Journal of Tropical Ecology* **20**, 667 – 673.

Holman, R., Glas, C.A.W. & De Haan, R.J. (2003) Power analysis in randomized clinical trials based on item response theory. *Controlled Clinical Trials*, **24**, 390-410.

Hwang, J-L. & Davies, P.L. (2009) Brief report - Rash analysis of the school function assessment provides additional evidence for the internal validity of the activity performance Scales. *American Journal of Occupational Therapy*, **63**, 369-373.

Irschick, D.J. (2000) Comparative and behavioral analyses of preferred speed: *Anolis* lizards as a model system. *Physiological and Biochemical Zoology*, **73**, 428-437.

Jones, G., Morton, M., Hughes, P.M. & Budden, R.M. (1993) Echolocation, flight morphology and foraging strategies of some West African hipposiderid bats. *Journal of Zoology*, **230**, 385-400.

Juliana, S., Schmieder, D., Siemers, B. & Kington, T. (2015). Beyond size - morphological predictors of bite force in a diverse insectivorous bat assemblage from Malaysia. *Functional Ecology*, http://doi:10.1111/1365-2435.12447.

Kingston, N.M. & Dorans N.J. (1984) Item location effects and their implications for IRT equating and adaptive testing. *Applied Psychological Measurement*, **8**, 147-154.

Kingston, T., Jones, G., Akbar, Z. & Kunz, T.H. (1999) Echolocation signal design in Kerivoulinae and Murininae (Chiroptera: Vespertilionidae) from Malaysia. *Journal of Zoology*, **249**, 359-374.

Kingston, T., Jones, G., Zubaid, A. & Kunz, T.H. (2000) Resource partitioning in rhinolophoid bats revisited. *Oecologia*, **124**, 332-342.

Kingston, T., B. L. Lim, and A. Zubaid. (2006) *Bats of Krau Wildlife Reserve*. Penerbit Universiti Kebangsaan Malaysia, Bangi, Malaysia.

Linacre, J. M. (2014) Winsteps® Rasch measurement computer program User's Guide. Beaverton, Oregon: Winsteps.com

Lord, F.M. (1953) The relation of test score to the trait underlying the test. *Educational and Psychological Measurement*, **13**, 517-548.

Losos, J.B. & Irschick, D.J. (1996) The effect of perch diameter on escape behaviour of *Anolis* lizards: laboratory predictions and field tests. *Animal Behaviour*, **51**, 593–602.

McKenzie, N.L., Gunnell, A.C., Yani, M. & Williams, M.R. (1995) Correspondence between flight morphology and foraging ecology in some Palaeotropical bats. *Australian Journal of Zoology*, 43, 241-257.

Messick, S. (1995) Validity of psychological assessment: validation of inferences from persons responses and performances as scientific inquiry into score meaning. *American Psychologist*, **50**, 741-749.

Norberg, U.M. (1990) *Vertebrate Flight: Flight Mechanics, Physiology, Morphology, Ecology and Evolution*. Springer-Verlag, Berlin:

Norberg, U.M. (1994) Wing design, flight performance and habitat use in bats. *Ecological morphology: integrative organismal biology* (eds P.C. Wainright and M Reilly) pp. 205-239. University of Chicago Press, Chicago, Illinois.

Norberg, U.M. (1998) Morphological adaptations for flight in bats. *Bat biology and conservation*, (eds. T. H. Kunz and P. A. Racey) pp. 93-108. Smithsonian Institute Press, Washington DC.

Norberg, U.M. & Rayner, J.M.V. (1987) Ecological morphology and flight in bats (Mammalia; Chiroptera): wing adaptations, flight performance, foraging strategy and echolocation. *Philosophical Transactions of the Royal Society of London. Series B, Biological Sciences* **316**, 335-427.

Reise, S.P. & Waller, N.G. (2009) Item Response Theory and Clinical Measurement. *Annual Review of Clinical Psychology*, **5**, 27–48.

Rhodes, M.P. 1995. Wing morphology and flight behaviour of the golden-tipped bat, Phoniscus papuensis (Dobson) (Chiroptera: Vespertilionidae). *Australian Journal of Zoology*, **43**: 657-663.

Santana, S.E., Dumont, E.R & Davis, J.L. (2010) Mechanics of bite force production and its relationship to diet in bats. *Functional Ecology*, **24**, 776-784.

Saunders, M.B. & Barclay, R.M.R. (1992) Ecomorphology of insectivorous bats: a test of predictions using two morphologically similar species. *Ecology*, **73**, 1335-1345.

Schmieder, D.A., Kingston, T., Hashim, R. & Siemers, B.M. (2012) Sensory constraints on prey detection performance in an ensemble of vespertilionid understorey rain forest bats. *Functional Ecology*, **26**, 1043–1053.

Siemers, B.M. & Schnitzler, H.U. (2004) Echolocation signals reflect niche differentiation in five sympatric congeneric bat species. *Nature*, **429**, 657-661.

Stockwell, E.F. (2001) Morphology and flight manoeuvrability in New World leaf-nosed bats (Chiroptera: Phyllostomidae). *The Zoological Society of London*, **254**, 505 – 514.

Swartz, S.M, Iriarte-Díaz, J., Riskin, D.K. & Breuer, K.S. (2012) A bird? A plane? No, it's a bat: an introduction to the biomechanics of bat flight. *Evolutionary history of bats: fossils, molecules and morphology* (eds. G.F. Gunnell & N.B. Simmons) pp. 317-352. Cambridge University Press.

Trochim, W. (2006) *The research method knowledge base*. Atomic Dog Publishing, Cincinnati, Ohio.

Wright, B.D. & Masters, G.N. (1982) *Rating scale analysis*. MESA Press, Chicago.

Wright, B.D. & Mok, M. (2000) Rash model overview. *Journal of Applied Measurement*, **1**, 83-106.

Wright, B. D. & Stone, M.H. (1979) *Best test design*. MESA Press: Chicago.